Microbially influenced corrosion of stainless steel 304 under halogenated fluids
by Vivek Agrawal

A thesis submitted in partial fulfillment of the requirements for the degree of Master of Science in Environmental Engineering
Montana State University

Abstract:
The focus of the research was significant pitting corrosion which occurred under biofilm deposits on the cooling water side of 304 (16 ga) stainless steel heat exchanger tubing in an open, recirculating, cooling tower system (RCT) in a methanol plant. The corrosion morphology was characterized by pitting of two types: (1) large, round surface pits, and (2) small surface pits leading to subsurface caverns and tunnels.

The main objectives of this study were to simulate these corrosion phenomena in the laboratory and to observe the effect of operating variables on corrosion. The make-up water from the RCT system was used as nutrient feed in the laboratory experiments. RotoTorque reactors were fed continuously with make-up water at different dilution rates which influences biofilm accumulation. The make-up water was enriched with biodegradable carbon (methanol) to recirculating water strength to simulate the effect of cycles of concentration in the Methanol plant RCT system. Chlorine was added as a biocide once a day.

A computer model of the RCT system was developed to mathematically simulate the general system behavior under different operating conditions. The computer simulations were used to "numerically experiment" with the recirculating cooling water as opposed to the make-up water which was the only reasonable choice for laboratory experimentation for two reasons: (1) the source water for cooling at the plant was modified between the times of the corrosion episodes and the laboratory experiment and (2) the recirculating water at the plant during this laboratory study was receiving high dosages of biocide which altered its quality considerably.

Field experiments were also conducted in the Methanol plant RCT system make-up water line.

No conclusive evidence of MIC was observed of any kind from the laboratory or field experiments. No significant corrosion was observed in the laboratory experiments. The stainless steel 304 coupons installed in the industrial RCT system experienced no corrosion. The cooling source water has changed since the failures occurred. The new source water is of higher quality. In addition, biocide is dosed at relatively high levels to the RCT. No failures have been observed with these new conditions. However, from the experimental results, we conclude that poor water quality alone was not the cause of failure of stainless steel heat exchanger tubing in the RCT system.

MICROBIALLY INFLUENCED CORROSION OF STAINLESS STEEL 304 UNDER HALOGENATED FLUIDS

by

Vivek Agrawal

A thesis submitted in partial fulfillment
of the requirements for the degree

of

Master of Science

in

Environmental Engineering

MONTANA STATE UNIVERSITY
Bozeman, Montana

April 1991

APPROVAL

of a thesis submitted by

Vivek Agrawal

This thesis has been read by each member of the thesis committee and has been found to be satisfactory regarding content, English usage, format, citations, bibliographic style, and consistency, and is ready for submission to the College of Graduate Studies.

8 May 1991
Date

Chairperson, Graduate Committee

Approved for the Major Department

8 May '91
Date

Head, Major Department

Approved for the College of Graduate Studies

June 14, 1991
Date

Graduate Dean

STATEMENT OF PERMISSION TO USE

In presenting this thesis in partial fulfillment of the requirements for a master's degree at Montana State University, I agree that the Library shall make it available to borrowers under rules of the Library. Brief quotations from this thesis are allowable without special permission, provided that accurate acknowledgement of source is made.

Permission for extensive quotation from or reproduction of this thesis may be granted by my major professor, or in his/her absence, by the Dean of Libraries when, in the opinion of either, the proposed use of the material is for scholarly purposes. Any copying or use of the material in this thesis for financial gain shall not be allowed without my written permission.

Signature 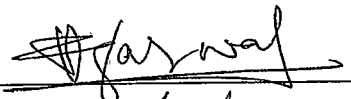

Date 05/30/01.

ACKNOWLEDGEMENTS

I wish to express my appreciation to the following:

Bill Characklis for providing advice, support, and research environment which made my graduate experience a particularly productive and enjoyable period of my life.

Dick Cahoon for providing advice and support on my research work and thesis report.

Whonchee Lee for being my mentor and his contribution to my research work.

Ron Larsen for helping me develop the computer model.

Warren Jones and Zbigniew Lewandowski for serving on my thesis committee.

Anne Camper and Paul Stoodley for providing help in the laboratory work.

Gordon Williams, John Rompel, Andy Blixt, and Vern Griffiths for technical and analytical assistance.

Diane, Lynda, Jamie, Al, Frank, Ewout, Brent, Feisal, Bill, Robert, Gabi, Bryan, Mike, Wendy, Satoshi, Narayan, and Dave for their cooperation.

The staff of Civil and Chemical Engineering who have contributed generously to my education.

E.I. DuPont De Nemours & Co. (Chemical & Pigments Department), Beaumont, Texas and IPA Industrial Associates for financial support.

And the people of Bozeman who taught me skiing and were always there to accompany me to bars.

TABLE OF CONTENTS

LIST OF TABLES viii

LIST OF FIGURES ix

ABSTRACT xiii

INTRODUCTION 1
Problem Characterization 1
Problem 2
Research Goal and Objectives 3

LITERATURE REVIEW 4
Biofilm Formation: A Process Analysis 4
Control of Biofilm Accumulation 5
SS 304: Metal Structure and Corrosion Resistance . . . 7
Corrosion of SS 304 in Absence of Bacteria 7
Corrosion of SS 304 in Presence of Bacteria 9
Filamentous Iron Bacteria (Fe/Mn-oxidizers) . . 10
Acid Producing Bacteria 10
Sulfate Reducers (SRB) 11

DESCRIPTION OF THE INDUSTRIAL SYSTEM 12
Macroscale: RCT System 12
Material Balance 16
Conserved Species. 17
Suspended Cells 18
Substrate. 19
Water. 20
Mesoscale: Condensers 21
Microscale: Condenser Tubing Wall and Biofilm 22
Differential Material Balances in the Biofilm . 22
Substrate. 22
Biofilm Thickness. 22

EXPERIMENTAL APPARATUS AND METHODS 24
Annular Reactor 24
Coupons 25
Bulk Media 26
Experimental Start-Up 26
Coupons 27
Reactor 27
Experimental Procedure 28
Laboratory Experiments 28
Methanol Plant Experiments 30
Water Quality 31
Analytical Methods 32
General Sample Processing 32
Sample Processing for Chemical Analyses 32
Total solids 32
Volatile solids 33
Total organic carbon 33
Sample Processing for Microbial Analyses 33
Heterotrophic plate count 34
Sulfate reducing bacteria 34

TABLE OF CONTENTS - Continued

General anaerobic bacteria 35
Total cell count 35
Microscopic examination for Mn/Fe oxidizing bacteria 36
Surface Analysis of Biofilm and Corrosion Products 36
Metallurgical Analyses 37
Analyses of New SS 304 Heat Exchanger Tubing and Laboratory Corrosion Coupons 37
General surface morphology 37
General surface chemistry 37
General Metal Structure 38
Electrochemical Cleaning Procedure 38
Sample Processing for Corrosion Analysis 39
Corrosion Analyses 39

RESULTS 40
Make-up Water Analysis 40
Analysis of 304 SS Laboratory coupons 41
Laboratory Experiment Results 42
Make-up Water 42
Recirculating Water Experiment 47
Chemical Analysis 47
Microbial Analyses 49
SEM/EDAX Analyses 49
Corrosion Analysis 51
Field Experiment Results 51
Chemical Analysis 53
Microbial Analyses 56
SEM/EDAX Analysis 56
Corrosion Analyses 58
Analysis of RCT system 304 SS Heat Exchanger Tubing . 58
Statistical Analyses of Results 64
RCT System Modelling Results 67
Effect of Operating Variables on RCT System . . 70
Cycles of Concentration 70
Biocide Concentration 70
Inlet Substrate Concentration 70

DISCUSSION OF RESULTS 76
Water Quality Results 76
Laboratory Experiment Results 77
Chemical and Microbial Analyses 77
SEM/EDAX Analysis 78
Field Experiment Results 79
RCT System Modelling Results 81
Analyses of Coupon and Tubing Metal Surface 82

SUMMARY 86
Recommendations for Further Work. 87

LITERATURE CITED 89

TABLE OF CONTENTS - Continued

APPENDICES 93
Appendix A: RCT System Make-up Water Quality Analysis 94
Appendix B: Experimental Data 97
Appendix C: Media For Growth of Bacteria Culture . . 102
Appendix D: RCT System Make-up Water Historical Data 104
Appendix E: RCT System Recirculating Water Data . . . 108
Appendix F: SEM/EDAX Analysis of Failed Tubing by DuPont 111
Appendix G: Data Generated from Computer Simulation . 113
Appendix H: Observation by Plant Personnel 116

LIST OF TABLES

Table

1. Elemental composition of the SS 304 coupons 26
2. Average Composition of Experimental Reactor Feed as well as make-up water for RCT (Tables 3, 4, and 5, Appendix A) 27
3. Raw water quality data: Sample description and physical analyses. 95
4. Raw water quality data: chemical analyses 95
5. Raw water quality data: microbial analyses. 96
6. Coupon biofilm chemical analysis: Laboratory system with recirculating water strength bulk reactor media. . . 98
7. Coupon biofilm microbial analysis: Laboratory System with recirculating water strength bulk reactor media. . . 99
8. Biofilm chemical analysis: RCT system 100
9. Biofilm microbial analysis: RCT system. 101
10. Postgate's B media for SRB. 103
11. Fluid Thioglycollate media for HPC. 103
12. Raw data: LNVA water quality. 105
13. RCT system make-up water quality. 106
14. RCT system recirculating water data 109
15. Raw data: Deposit analysis on failed Dupont tubing. . . .112
16. Effect of cycles of concentration 114
17. Effect of biocide concentration 114
18. Effect of inlet substrate concentration 115
19. Effect of inlet substrate concentration 115

LIST OF FIGURES

Figure

1. Scanning Electron Micrograph (SEM) of a corrosion pit from a section of 304 stainless steel heat exchanger tubing (x43) from a plant which has suffered similar problems (photograph provided by Tatnall, Dupont, Delaware) 2

2. The relationship of engineering scale to interfacial microbial processes 13

3. Schematic of RCT system at Methanol plant 15

4. Detail design of laboratory reactor used for simulation of corrosion problem 25

5. Experimental plan for laboratory experiment with RCT system make-up water as nutrient. One coupon was pulled from each reactor at the end of 3, 6, 9, 12 weeks respectively. 29

6. Experimental plan for laboratory experiment with RCT make-up water as nutrient. One coupon was pulled from each reactor at the end of week 3, and the rest at the end of week 12. 30

7. Results of chemical analyses performed on Methanol plant make-up water. (x10) indicates that the values shown in Figure have been magnified ten times 41

8. SEM of blank (unused) laboratory coupon surface (x100) after ultrasonic cleaning. EDAX, performed on region marked by arrow in SEM, is typical of SS 304. 43

9. X-ray dot map of a blank coupon surface (x980), shown on right, after ultrasonic cleaning. The results are typical of SS 304 44

10. SEM of coupon surface (x97). The coupon was in laboratory reactor with make-up water for 7 weeks. The reactor was chlorinated for 3 weeks. EDAX highlights the inorganic nature of deposits as well as absence of highly localized chloride deposits. 45

11. SEM of coupon surface (x97). The coupon was in laboratory reactor for 7 weeks, receiving no treatment during that time. 46

12. TOC/dry mass/volatile mass distribution on deposits at low dilution rate. No chlorine treatment was provided. 48

LIST OF FIGURES - Continued

13. TOC/dry mass/volatile mass distribution on deposits at high dilution rate. No chlorine treatment was provided. 48

14. TOC/dry mass/volatile mass distribution on deposits at different dilution rates at the end of 12 weeks. No chlorine treatment was provided 50

15. TOC/dry mass/volatile mass distribution on deposits at different dilution rates with chlorine treatment. The coupons were in the reactor for 12 weeks. 50

16. GAB/SRB/HPC distribution on deposits at different substrate loading rates with chlorine treatment 51

17. SEM of coupon surface (x600) exposed to recirculating water strength bulk reactor media at high dilution rate. No treatment was provided. Comparison with Figure 20 indicates differences in deposit characteristics, presumbly due to absence of biocide treatment 52

18. SEM of coupon surface (x600) exposed to recirculating water strength bulk reactor media at low dilution rate. No chlorine treatment was provided during that time. 53

19. SEM of coupon surface (x870) exposed to recirculating water strength bulk reactor media at high dilution rate with chlorine treatment EDAX, performed on area shown by arrow in SEM highlights the inorganic nature of deposits. Visual observation did not indicated the presence of microbial organisms in deposits. Comparison with Figure 10 shows deposit's physical similarity with make-up water and recirculating water simulations. 54

20. SEM of coupon surface (x600) exposed to recirculating water strength bulk reactor media at low dilution rate, receiving chlorine treatment during that time . . . 55

21. SEM of coupon surface (x390) beneath the deposit after ultrasonic cleaning. Note the scratch lines on the surface, indicating absence of corrosion phenomenon. 57

22. TOC/dry mass/volatile mass distribution on deposits from field experiment 57

LIST OF FIGURES - Continued

23. SEM of surface (x40) of a coupon which was in the RCT system make-up water system for 8 weeks. EDAX, performed on the whole surface shown in the micrograph, indicates the inorganic nature of deposits. See Figures 20 and 23 for physical and chemical similarity of results obtained from laboratory and field experiments. 59

24. SEM of surface (x530) of a coupon which was in the RCT system make-up water system for 8 weeks 60

25. X-ray dot map of surface (x530) of a coupon which was in RCT system make-up water for 8 weeks. X-ray analysis, performed on the whole surface shown in Figure 26, highlights the absence of Fe/Mn, hypothesized to associated with corrosion phenomenon. 61

26. SEM of surface (x2000) of a coupon which was in the RCT system make-up water system for 8 weeks. The micrograph shows physical characteristics of a cell in biofilm on the coupon surface. Cell identification was not performed. 62

27. Photograph of a coupon surface (x100) after ultrasonic cleaning. The coupon which was in RCT system make-up water for 8 weeks. The photograph highlights the scratch lines on the surface, indicating absence of corrosion phenomenon. 62

28. X-ray digitized image of non-conductive deposits on surface (x490) 63

29. SEM of sulfide inclusions (x550) in the RCT system heat exchanger tubing. See Figure 32 for x-ray dot map of the region 64

30. Energy Dispersive X-ray Analysis (EDAX) of sulfide inclusion (x550) in Methanol plant heat exchanger tubing. 65

31. X-ray dot map of a sulfide inclusions (x2000) in RCT system heat exchanger tubing. 66

32. Prediction of suspended cell population, biofilm thickness and substrate consumption in the Methanol plant RCT system by computer simulation technique with make-up water as feed. 68

33. Computer simulation results for biofilm thickness versus time for different substrate concentrations. . . . 69

LIST OF FIGURES - Continued

34. Computer simulation results for suspended cell concentration versus time for different substrate concentrations. 71

35. Computer simulation results for biofilm thickness versus time for different biocide concentrations. 72

36. Computer simulation results for suspended cell concentration versus time for different biocide concentrations. 73

37. Computer simulation results for biofilm thickness versus time for different cycles of concentration 74

38. Computer simulation results for suspended cell concentration versus time for different cycles of concentration 75

39. Schematic illustration of MnS inclusion in SS, showing dimensions. Preferential adsorption of chloride ions occurs on the sulfide inclusion due to its higher electron conductivity, giving stronger electrostatic image forces than on the surrounding oxide film. 83

40. First stage of initiation of piting on SS: dissolution of the sulfide inclusion under the seperation of elementary sulfur and the exposure of active, not oxide-coated steel along the periphery 83

41. Continued anodic attack on sulfide inclusion in SS under oxidation to H_2SO_3 and H_2SO_4, which cause chemical dissolution of the sulfide. Incipient attack on the metal close to the inclusion. 83

ABSTRACT

The focus of the research was significant pitting corrosion which occurred under biofilm deposits on the cooling water side of 304 (16 ga) stainless steel heat exchanger tubing in an open, recirculating, cooling tower system (RCT) in a methanol plant. The corrosion morphology was characterized by pitting of two types: (1) large, round surface pits, and (2) small surface pits leading to subsurface caverns and tunnels.

The main objectives of this study were to simulate these corrosion phenomena in the laboratory and to observe the effect of operating variables on corrosion. The make-up water from the RCT system was used as nutrient feed in the laboratory experiments. RotoTorque reactors were fed continuously with make-up water at different dilution rates which influences biofilm accumulation. The make-up water was enriched with biodegradable carbon (methanol) to recirculating water strength to simulate the effect of cycles of concentration in the Methanol plant RCT system. Chlorine was added as a biocide once a day.

A computer model of the RCT system was developed to mathematically simulate the general system behavior under different operating conditions. The computer simulations were used to "numerically experiment" with the recirculating cooling water as opposed to the make-up water which was the only reasonable choice for laboratory experimentation for two reasons: (1) the source water for cooling at the plant was modified between the times of the corrosion episodes and the laboratory experiment and (2) the recirculating water at the plant during this laboratory study was receiving high dosages of biocide which altered its quality considerably.

Field experiments were also conducted in the Methanol plant RCT system make-up water line.

No conclusive evidence of MIC was observed of any kind from the laboratory or field experiments. No significant corrosion was observed in the laboratory experiments. The stainless steel 304 coupons installed in the industrial RCT system experienced no corrosion. The cooling source water has changed since the failures occurred. The new source water is of higher quality. In addition, biocide is dosed at relatively high levels to the RCT. No failures have been observed with these new conditions. However, from the experimental results, we conclude that poor water quality alone was not the cause of failure of stainless steel heat exchanger tubing in the RCT system.

INTRODUCTION

Problem Characterization

Microorganisms exhibit a tendency for adsorbing to and colonizing surfaces which are submerged in aquatic environments. The immobilized cells grow, reproduce, and produce extracellular polymeric substance (EPS). The EPS frequently extends from the cell, forming a tangled mass of fibers lending structure to the entire assemblage known as biofilm. Biofilms tend to grow on almost any surface including teeth, concrete, plastic, and metal surfaces.

Biofilms serve beneficial purposes in natural environments and in some modulated systems (e.g., removal of contaminants from natural flowing streams, trickling filters and rotating biological contactors). Biofilms can, however, impair the performance of process equipment. They can impede the flow of heat across the surface, increase fluid frictional resistance at the surface, and enhance corrosion rate at the surface.

Significant, costly, localized corrosion of the cooling water side surfaces of stainless steel (SS) heat exchanger tubing has occurred repeatedly (Puckorius, 1983) in condensers in open, recirculating, cooling tower systems (Figure 1). The problem is faced by industries including the chemical, petroleum, and power industry. Repeated and frequent failures of condensers have cost several billion dollars in inspection, repairs, interim, and final replacement (Tatnall, 1981).

Figure 1. Scanning Electron Micrograph (SEM) of a corrosion pit from a section of 304 stainless steel heat exchanger tubing (x43) from a plant which has suffered similar problems (photograph provided by Tatnall, Dupont, Delaware).

Problem

The focus of this study was pitting corrosion under biofilm deposits on the cooling water side of a SS 304 heat exchanger tubing in an open, recirculating, cooling tower/condenser system of a Methanol plant (RCT system). The corrosion failures were very costly and occurred in 1982. Since then, the source of cooling water has changed as well as RCT operation and the failures have not occurred again.

Research Goal and Objectives

The goal of the research was to determine the controlling mechanism and factors influencing pitting corrosion on SS 304 heat exchanger tubing in the RCT system at the Methanol plant during the failures of 1982. The specific objectives were as follows:

1. Develop a laboratory system for simulating the corrosion phenomenon observed in the RCT system heat exchanger tubing.
2. Evaluate the effect of operating variables (biocide, cycles of concentration, and substrate loading rate) on the observed corrosion phenomenon in the laboratory.
3. Develop a RCT model for performing computer simulations to integrate laboratory results with observations in the RCT system.

LITERATURE REVIEW

The durability, versatility, and economics of SS 304 have made it one of the most widely used alloys in the chemical, petroleum, and power industries. However during the last few decades, it has become apparent that SS 304 is susceptible to MIC phenomena. Although the exact mechanism of MIC is still not fully understood, corrosion influenced by bacteria is a widely accepted and costly phenomenon.

The literature review focuses on surface morphology and physical characteristics of SS 304, properties of biofilms and treatments for their control, and the possible role of biofilms in the corrosion of SS 304.

Biofilm Formation: A Process Analysis

The adsorption of bacteria is a general phenomenon encountered in natural environments with important ecological implications. Bacterial adsorption to surfaces offers survival advantages because of increased nutrient availability, particularly in fast flowing and nutrient-deficient habitats. The adsorbed cells reproduce and form extracellular polymers leading to the formation of biofilm. Accumulation of biofilm at the surface is the net result of the following fundamental processes (Characklis, 1981):

1. Adsorption of organic molecules to the surface forming a conditioned surface.
2. Transport of microbial cells to the conditioned surface.
3. Microbial transformation (growth, reproduction) at the

surface.

4. Partial detachment of biofilm due to fluid shear stress.

Biofilm formation is not a sequence of the above rate processes occurring individually but rather the net result of these processes occurring simultaneously. At specific times in the overall development, certain rate processes contribute more to biofilm accumulation and activity than the others.

Control of Biofilm Accumulation

Biological fouling in cooling water systems is the result of excessive growth and development of different members of the lower life forms, namely algae, bacteria, and fungi.

Many different types of chemical agents are employed for microorganism control in recirculating cooling water systems. The primary purpose of the chemical agent is to kill and/or inhibit the growth and accumulation of organisms. If a given toxicant or biocide is present in sufficient quantity the microorganisms will be killed. Biocides also cause the detachment of biofilm from the surface thus keeping the system surfaces relatively free of microbial populations and minimizing biofouling and other related phenomena. The scope of this literature review is restricted to one biocide, chlorine.

Chlorine is one of the most widely employed agents for control of microbiological deposits in recirculating cooling water systems and is frequently the most economical treatment method. Chlorine is highly toxic and has traditionally been employed in RCTs on an intermittent (shock fashion) basis. However in recent years, continuous low dosage treatment has also been widely practiced.

Unfortunately, chlorine has also been found to be one of the most damaging materials to both metal and non-metal parts of the cooling tower system (Cooling Water Treatment Manual, NACE, 1971). Widely accepted practice suggests that the free chlorine residual be less than 1E-3 kg/m^3 in the hot return line to the tower.

The effectiveness of chlorine is decreased by the presence of organic matter including biomass, reducing agents such as hydrogen sulfide, and chemicals containing reactive nitrogen, e.g., ammonia:

$$Cl_2 + NH_3 = NH_2Cl + H^+ + Cl^-$$

An ammonia plant located near the RCT system at the Methanol plant can produce similar effects in the system under study. Thus, when the wind is from the direction of the ammonia plant, much of the chlorine is in the form of chloramines. Chloramines do not disinfect suspended cells as effectively as free chlorine. However, there are indications that chloramines are more effective against biofilms.

The rate of chlorine transport to the biofilm through the bulk water depends on the concentration of chlorine in the bulk water, the concentration of chlorine-demanding compounds, and the intensity of the turbulence in the system. The chlorine concentration in the bulk water is the net result of the chlorine addition rate minus the chlorine demand rate of the water. Sufficient chlorine must be added to the water to satisfy all these reactions, collectively known as "chlorine demand", and to allow a suitable concentration of residual chlorine to persist in the water.

SS 304: Metal Structure and Corrosion Resistance

Stainless steel is an iron-base alloy containing more chromium than the 12 per cent necessary to produce passivity but less than 30 per cent. SS 304 belongs to the class of austenitic steels. Austenitic steel exhibits a wide range of mechanical properties, making it one of the most widely used alloys. Austenitic steel is manufactured by annealing at elevated temperatures high enough to avoid carbide precipitation, usually above 1850°F. The steel is cooled rapidly from the annealing temperature to avoid austenitic transformation. Chromium-containing SS are generally made austenitic by the addition of nickel, a strong austenite stabilizing agent. Manganese and nickel are added to retain the austenite at room temperature.

Pitting and crevice corrosion occurs in SS resulting from a highly localized breakdown in the passive oxide film protecting the surface and followed by electrochemical action. The presence of chlorides has been hypothesized to be a major cause of pitting and crevice corrosion. Collection or accumulation of solids on surfaces is also conducive to pitting (Source Handbook of Stainless Steels, American Society for Metals Publications, 1977).

Corrosion of SS 304 in Absence of Bacteria

Most metals in their pure form are unstable in many environments and tend to revert to corresponding oxides or other stable combinations from which they were derived, i.e., they corrode.

Electrochemical theory indicates that a difference in potential must exist between two or more points and current must flow for corrosion to occur. A difference in potential can be caused by several factors including difference in concentration of dissolved oxygen at one point compared with another, difference in composition, and slag inclusions.

When corrosion occurs, metals go into solution at anodic areas as metal hydroxide. This is an oxidation reaction. One or more reactions occur at cathodic areas (reduction reactions). Hydrogen ions are reduced to atomic hydrogen by taking on the available electrons. The atomic hydrogen combines to form hydrogen gas at cathodic areas. If this monomolecular layer of hydrogen gas is not disturbed, polarization will occur and the corrosion reaction will be suppressed. The hydrogen layer can be destroyed by either mechanical or chemical means, or both.

SS 304 does not corrode in neutral pH water free of oxygen. However cooling water is usually saturated with dissolved oxygen and is high in concentration of dissolved and particulate materials. These factors tend to enhance corrosion. Other factors influencing the corrosion of SS are temperature, rate of water flow, pH, chloride concentration and carbon dioxide concentration.

If the metal hydroxide is relatively soluble, as in the case of ferrous hydroxide, it will remain in solution until the solution becomes saturated, and then separate out. More ferrous ions can diffuse through the precipitated ferrous hydroxide ($Fe(OH)_3$), and can be oxidized and precipitated as it reaches the oxide-water interface. An active anode continually produces ferrous ions which diffuse and electrochemically migrate toward the water-$Fe(OH)_3$

interface at much greater rates than oxygen can diffuse through the deposit towards the corroding metal surface. Thus, the cell continues to function as a differential aeration cell. The result is that a small pit is formed at the anodic area, covered with a canopy of deposited material called a tubercle.

Corrosion may also occur as a result of differences in oxygen concentration in contact with a metal surface due to the presence of insoluble deposits. The covered metal surface is reached by a solution containing smaller amounts of dissolved oxygen and continues to corrode, while the adjacent metal surface in contact with oxygen-rich solution, acting as a cathode, is protected.

Corrosion of SS 304 in Presence of Bacteria

The corrosion resistance of SS 304 in industrial water systems can be greatly influenced by biological factors. Corrosion of SS 304 induced by bacteria is a widely recognized phenomenon in the pulp and paper industry and in cooling systems among others.

Several theories have been proposed to explain the mechanism of microbially influenced corrosion (MIC) of SS 304. MIC is believed to be initiated at sites of inclusions on the metal surface resulting in concentrated metal chloride formation. Mollica et al. (1987) and others reported aerobic bacteria settlement on the stainless steel surfaces leading to an increased oxygen reduction rate causing enhanced localized corrosion propagation rate. Some of the bacteria identified with MIC of SS 304 surfaces are described below.

Filamentous Iron Bacteria (Fe/Mn-oxidizers)

Filamentous iron bacteria, typified by Sphaerotilus, oxidize dissolved ferrous iron to insoluble ferric hydrate, which forms a common sheath for several cells and produces a characteristic stalk-like, filamentous form. Some species can oxidize and concentrate even manganese. Filamentous iron bacteria have been hypothesized to be responsible for the common hollow, tubercles seen at the site of corrosion. They are aerobic and create oxygen depletion under the tubercles (Tatnall, 1981).

Gallionella, another "iron bacterium" tends to concentrate chlorides, with the result that deposits are rich in ferric and manganic chlorides which act like dilute HCl causing pitting corrosion of stainless steel.

Ghiorse (1984) has pointed out that metal oxidation has not been demonstrated in some cases and that certain microorganisms can catalyze the oxidation of metals. Other microorganisms accumulate abiotically oxidized metal precipitates. Metal oxidizing organisms create environments for the accumulation of chloride ions (to maintain charge neutrality) and form acidic ferric chloride and manganic chloride, which are highly corrosive to SS 304. Further pit development is enhanced as an oxygen concentration cell develops. Also, metal-oxidizing organisms efficiently scavenge oxygen and, therefore, provide conditions for the growth of obligate, anaerobic bacteria.

Acid Producing Bacteria

Acid producers, typified by Clostridia, produce short-chain organic acids by either fermentation or acidogenesis. The localized

acidic attack can create a localized low pH environment, initiating the corrosion of metal surface at those sites.

Sulfate Reducers (SRB)

Von Wolzogen Kuhr and van der Vlugt (1934) proposed the cathodic depolarization theory for SRB corrosion. The theory suggests that hydrogenase catalyzed the hydrogen reduction reaction on the iron surface. King and Miller (1973) supported the hydrogenase theory but proposed that the cathodic depolarization occurred on the iron sulfide instead of the iron surface. Costello (1974) reports that Desulfovibrio desulfuricans produces H_2S which directly depolarizes the cathode. In summary, H_2S corrosion is under kinetic control and the sulfide film seems to play an important role in the anaerobic corrosion process both in biotic and abiotic systems.

DESCRIPTION OF THE INDUSTRIAL SYSTEM

The RCT system was analyzed on a continuum of scales ranging from the microscale to the macroscale (Figure 2). Microscale ($\leq 10^{-3}$ m) analyses address the structure, composition, and processes occurring within the fouling deposit and at the interface between the fouling deposit and the metal alloy (i.e., the substratum). At the mesoscale (10^{-3}–10 m), the influence of hydrodynamics and geometry (e.g., circular tube) was considered. At the macroscale (> 10 m), the system design and operation (e.g., hydraulic residence time, cycles of concentration) determine the bulk environmental conditions (e.g., water quality, temperature, etc.) in which the fouling and corrosion take place.

Macroscale: RCT System

The RCT system is located near Beaumont Texas, several miles from the Gulf of Mexico. Topography is flat, and the water table high. Swamps, bayous, sloughs, and estuaries are numerous. Surrounding vegetation is dominated by water oaks and southern pine. Ambient temperature ranges from 4 to 35°C with an average annual temperature of 19 to 21°C. Humidity ranges from 65-90 %.

The work site contains several plants including methanol, aniline, ammonia, and two specialty-polymers. The Methanol plant is located in the southwest corner of the site with the ammonia plant located nearby.

The cooling water source (make-up water) for Methanol plant is a canal which is fed by the Neches River and Pine Island Bayou.

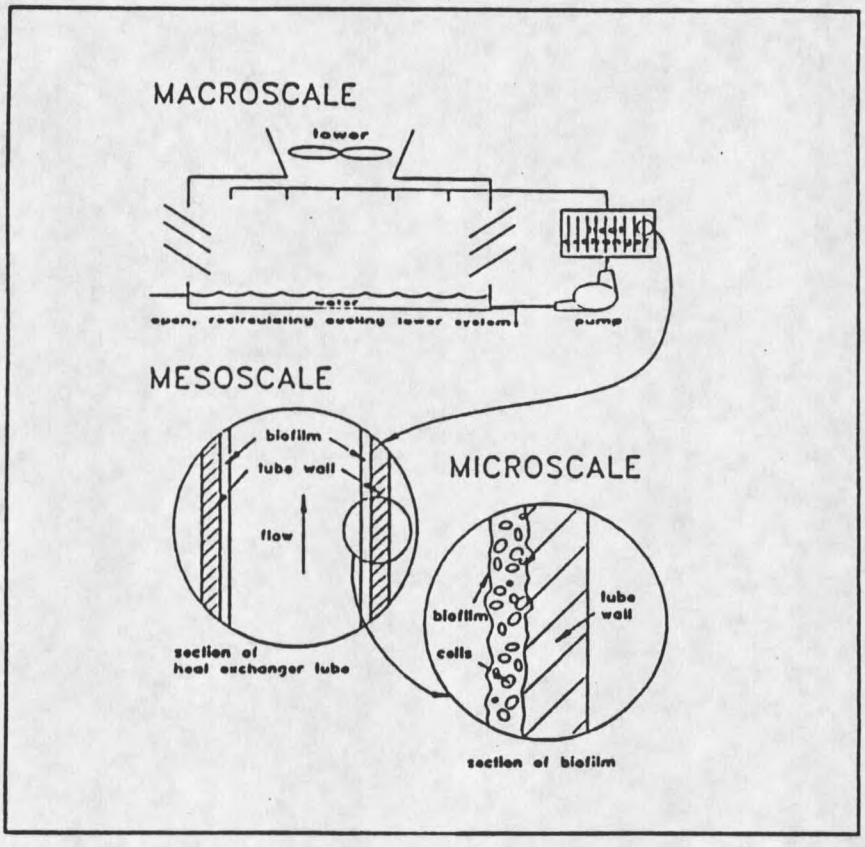

Figure 2. The relationship of engineering scale to interfacial microbial processes.

Temperature of the make up water at RCT inlet varies between 20 to 34°C. The RCT system is fed with untreated canal water. All other plants on site receive canal water that is clarified before use as make-up. Analytical results of the canal water near the plant before and after the shift to Pine Island water (Appendix D) are reported in Table 12. It is important to note that the failures occurred before the shift to Pine Island water. No large variation in canal

source water quality is obvious on a seasonal or yearly basis (Appendix D, Table 13). The water quality has improved significantly since the time of the corrosion failures.

The cooling tower system is an open, recirculating, forced-draft type with shell-and-tube condensers, including the two main crude condensers which operate in parallel (Figure 3). Several smaller condensers also operate in the system. The piping from the RCT basin to the crude condensers is cement-lined carbon steel with the bulk of the system piping made of reinforced concrete.

The system is operated with a volume, V, of water. The warm water return, Q_R, is pumped from the basin through a series of heat exchangers to the plenum at the top of the cooling tower. From the plenum, the water is distributed uniformly through an assembly of spray-nozzles over the interior of the structure which contains splash packing or fill material, constructed of slats stacked in decks and spaced in staggered rows. Water splashes from row to row, breaking into droplets, at a fixed rate. This rate is called the "water loading" rate of the tower.

The stream of air and water vapor containing entrained droplets is drawn upwards through the tower by the fans and passes through a "drift eliminator" - an arrangement of baffles that produces sudden changes in direction. Thus, water droplets are separated from the vapor stream and fall with the bulk of the water into the basin. Water vapor, Q_E, and air pass out through the fan stack to the atmosphere. A small amount of liquid water, Q_D, is blown out of the tower by wind in the form of fine droplets. This is called drift or windage loss; in a well designed tower it amounts to 0.1-0.2 per cent of the recirculation rate.

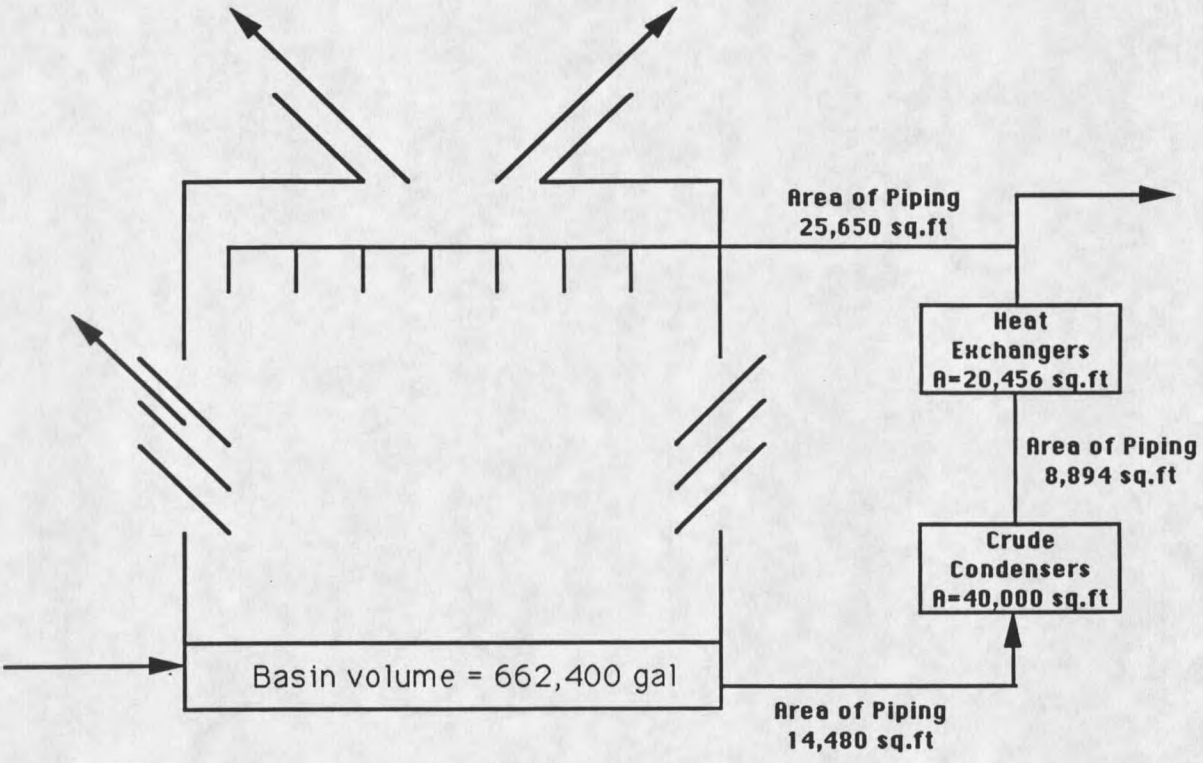

Figure 3. Schematic of RCT system at Methanol plant.

A volume of water, Q_B, called blowdown, is periodically (or continously) withdrawn from the system and a volume of fresh make-up water, Q_M, is added to the basin to maintain the total volume of

water, V, constant. The concentration of total dissolved solids in make-up water, C_M, and bulk concentration of total dissolved solids in RCT basin and recirculating water, C, are monitored regularly.

Reynolds numbers indicate that turbulent flow conditions exist in all relevant piping during operations.

The characteristic values for the RCT system under study are reported as follows:

	Description	Value	Units
Q_M	make-up water flowrate	1.07E-1	m^3/sec
Q_R	recirculating water flowrate	4.725	m^3/sec
Q_B	blowdown flowrate	2.2E-2	m^3/sec
Q_E+Q_D	loss due to evaporation and drift	8.5E-2	m^3/sec
Q_M/Q_B	cycles of concentration	2.5 - 5	
V_{CT}	volume of cooling tower basin	2.52E+3	m^3
V_{SYS}	volume of RCT system	3.04E+3	m^3
A_{C1}	surface area, crude condensers	3718	m^2
A_{C2}	surface area, other condensers	2162	m^2
A_{P1}	surface area, piping	1346	m^2
A_{P2}	surface area, piping	827	m^2
A_{P3}	surface area, piping	2384	m^2
A_{CT}	surface area, distribution system	2789	m^2
Θ_S	Mean retention time in RCT system	2.81E+4	sec
Θ_b	Mean retention time in RCT basin	498	sec

Material Balance

Material balances are an essential tool for microbial process analysis of systems such as the RCT system. Material balances can be used in industrial systems to:

1. Design relevant sampling programs
2. Locate areas of microbial activity
3. Describe the type of microbial activity
4. Quantify rates of microbial activity.

A RCT system model has been developed to study the system behavior and the effect of operating variables on biofouling and

biocorrosion in the system. The entire RCT system at the macroscale can be considered as a continuous stirred tank reactor (CSTR) because the volumetric flow rate of recirculating water in the RCT system is much higher (about 40-50 times) than the flow rate of make-up and/or blowdown. The heat exchanger and condenser units increase the surface area of the CFSTR. The model has been developed for a single limiting substrate: organic carbon (OC). The contributions of OC from different environments (e.g., make-up water, air, CT basin) have been summed as a single source for that component. Chlorine has been used as a biocide in the model system.

The following assumptions have been included in the model:

1. The make-up water added to the system has a stable microbial and chemical concentration over a period of time.
2. At steady state, detachment of cells from biofilm equals the rate of growth of cells in the biofilm.
3. Attachment of cells at the deposit surface is negligible, i.e., microbial growth in the biofilm is the dominant process leading to biofilm accumulation.

The computer model has been based on Monod equation which states that the growth of continuous cultures of single bacterial species growing on defined media could be approximated adequately by the equation for a rectangular hyperbola.

Conserved Species. A material balance can also be performed on a conserved species (non-volatile, unreactive) in the system (e.g., sodium):

rate of change of concentration of conserved species = transport rate of species in by make-up - transport rate of species out by blowdown - transport rate of species out drift

$$V \frac{dC_S}{dt} = C_M \cdot Q_M - C_B \cdot Q_B - C_D \cdot Q_D \quad \ldots\ldots\ldots (1)$$

At steady state (dC/dt=0) and assuming drift is negligible compared to blowdown rate,

$$Q_M \cdot C_M = Q_B \cdot C_B \quad \ldots\ldots\ldots (2)$$

$$Q_M/Q_B = C_B/C_M \quad \ldots\ldots\ldots (3)$$

The resulting ratio is termed the cycles of concentration and is an important parameter in assessing performance of a cooling tower in relation to water quality. For example, as concentration increases due to evaporation, solubility products for inorganic salts (e.g., $CaCO_3$, $CaSO_4$) are exceeded and inorganic deposits can form on slats and other parts of RCT system exposed to recirculating water causing decreased heat transfer rate and reduced operational life of the RCT system.

Suspended Cells. The observed accumulation of suspended cells can be expressed in words,

rate of change of viable suspended cells = transport rate of cells in with make-up water - transport rate of cells out with blowdown water - transport rate of cells out with drift + production of cells due to growth + rate of net detachment of cells from biofilm - rate of cell death by biocide action

and mathematically,

$$V\frac{dX_b}{dt} = X_{bM}.Q_M - X_b.Q_B - X_b.Q_D + \mu_{max}.\frac{C_{s1}}{K_{s1}+C_{s1}}.\frac{C_{s2}}{K_{s2}+C_{s2}}.X_b.V$$

$$+ k_d.L_f.A.X_f - k_a.X_b.V - k_b.X_b.C_b.V \quad \ldots\ (4)$$

where X_b = bulk suspended cell concentration $[ML^{-3}]$

k_d = detachment rate coefficient $[t^{-1}]$

k_a = attachment rate coefficient $[t^{-1}]$

k_b = biocide kill rate coefficient $[t^{-1}]$

X_f = biofilm cell concentration $[ML^{-3}]$ per unit biofilm volume

C_b = biocide concentration $[ML^{-3}]$

film rho = biofilm density $[ML^{-3}]$

C_s = substrate concentration $[ML^{-3}]$

L_f = biofilm thickness [L]

V = volume $[L^3]$

A = area $[L^2]$

Q = flow rate $[L^3t^{-1}]$

μ = growth rate of cells $[t^{-1}]$

Substrate. The rate of consumption of substrate in the system can be expressed in words;

rate of change of substrate = transport rate of substrate in with make-up water − transport rate of substrate out with blowdown water − transport rate of substrate out with drift − rate of substrate consumed for cell growth − substrate flux into biofilm

and mathematically;

$$V\frac{dC_{S1}}{dt} = C_{SM}.Q_M - C_S.Q_B - C_S.Q_D - \mu_{max}.\frac{C_{S1}}{K_{S1}+C_{S1}}.\frac{C_{S1}}{K_{S1}+C_{S1}}.\frac{1}{Y_{1S/X}}.\frac{1}{Y_{2S/X}}.X_b.V + J_{S1}.A \quad \ldots\ldots\ldots(5)$$

$$V\frac{dC_{S2}}{dt} = C_{SM}.Q_M - C_S.Q_B - C_S.Q_D - \mu_{max}.\frac{C_{S1}}{K_{S1}+C_{S1}}.\frac{C_{S1}}{K_{S1}+C_{S1}}.\frac{1}{Y_{1S/X}}.\frac{1}{Y_{2S/X}}.X_b.V + J_{S1}.A \quad \ldots\ldots\ldots(6)$$

where $Y_{S/X}$ = yield [M/M]

J_S = flux of substrate into biofilm [$ML^{-2}t^{-1}$]

A = area of biofilm (L^2)

Water. The evaporation rate of water, $Q_{(E+D)}$, depletes V. The make-up flow rate, Q_M, replaces that lost by evaporation and blowdown. Because of evaporation, the concentration of non volatile components in the recirculating water increases. Once this concentration (generally determined by conductivity) has reached a preset maximum value, a valve in the return line is opened allowing a certain volume of water, Q_B, to bleed off to drain. A material balance on water across the system yields the following expression:

rate of change of water = transport rate of water in by make-up − transport rate of water out by blowdown − transport rate of water out by evaporation − transport rate of water out by drift

expressing mathematically;

$$\frac{dV}{dt} = Q_M - Q_B - Q_E - Q_D \quad \ldots\ldots\ldots (7)$$

at steady state (dV/dt=0)

$$Q_M = Q_B + (Q_E + Q_D) \quad \ldots\ldots\ldots (8)$$

Mesoscale: Condensers

The focus of this research at the mesoscale was the two crude condensers. The condensers are 2.3 m in diameter, 14.3 m long and are piped in parallel. The condensers are horizontal, shell-and-tube heat exchangers with 5,000 tubes in a "U-tube" configuration. The tubes are 0.02 m OD, 16 ga (0.002 m wall thickness) and 10.7 m in straight length.

The condenser tubes were 304 SS (16 ga) during the corrosion failures. However, the crude condensers have recently been upgraded to Hastealloy C-276.

Flow velocity of cooling water in the tubes is presently maintained at 2.44-3.05 m per second (mps) except during winter months when flow velocity is reduced to approximately 1.53 mps because cooler water is available. At the time of failures, the flow velocity in the tubes was 0.9-1.53 mps.

Pressures in the system are maintained at 250 KPa on the product side (shell) and 96.5 KPa on the coolant side (tube). Therefore, any leaks result in product (methanol) leaking into the cooling water. Operating personnel at the Methanol plant indicated that some Methanol is always in the recirculating water. Methanol is a readily biodegradable substrate.

Microscale: Condenser Tubing Wall and Biofilm

The elemental composition of the SS 304 tubing used in the crude condensers is Cr=18-20%, Ni=8-10.5%, C=0.08%, Mn=2%, Si= 1.0%, P=0.045%, S=0.030 per cent. The surface of the tubing is the standard industrial finish which exhibits significant surface roughness on a microscale (30-100 μm) and is prone to occasional surface imperfections.

Differential Material Balances in the Biofilm

Substrate. A steady state differential material balance on substrate within the biofilm located in the tubing or piping can be expressed as follows:

0 =	transport rate of of substrate in radial direction	-	rate of consumption of substrate for cell growth

expressing mathematically;

$$0 = D_s.\frac{d^2C_s}{dr^2} - \mu_{max}.\frac{C_{s1}}{K_{s1}+C_{s1}}.\frac{C_{s2}}{K_{s2}+C_{s2}}.X_f.\frac{1}{Y_{1X/s}}.\frac{1}{Y_{2X/s}}.V \quad \ldots\ldots (9)$$

where L_f = biofilm thickness [L]

D_s = diffusion coefficient for substrate in water $[L^2t^{-1}]$

Biofilm Thickness. The biofilm thickness increases as cells accumulate on the surface area exposed to the recirculating water. The rate of change of biofilm volume due to the accumulation of cells can be expressed as a result of the following processes:

rate of change of biofilm volume = rate of growth of cells in the biofilm + net rate of detachment from biofilm

expressing mathematically;

$$\frac{dV_f}{dt} = \mu_{max} \cdot \frac{C_{s1}}{K_{s1}+C_{s1}} \cdot \frac{C_{s2}}{K_{s2}+C_{s2}} \cdot X_f \cdot V_f \text{ /film rho}$$

$$+ k_a \cdot X_b \cdot V \text{ /film rho} - k_d \cdot V_f \qquad \ldots\ldots (10)$$

Some typical values used in computer model are as follows (Ewout Van Der Wende):

μ_{max} = 0.40/hr
K_a = 0/hr
K_d = 0.15/hr
K_b = 0.02/hr
$Y_{X/S}$ = 0.4 gm/gm
C_b = 0.016 kg/m^3

The other values are typical of those described for RCT system characteristics and make-up water analyses.

EXPERIMENTAL APPARATUS AND METHODS

Annular Reactor

Laboratory experimentation of the observed corrosion phenomenon were conducted in miniaturized versions of RotoTorques (Figure 4). The reactor consists of two concentric cylinders, the outer fixed cylinder made of a 5E-4 m^3 glass beaker (Kimax), while the rotating inner solid cylinder was constructed of acrylic plastic. Rotational velocity was controlled by a fractional horsepower gear motor, high enough to ensure complete mixing in the reactor, and kept constant throughout the experiment. Each reactor contained four (4) removable slides (SS 304 corrosion coupons) for biofilm sampling and corrosion observation. The slides hung vertically in the annular space with both sides exposed to reactor fluid. The inner and outer sides of the slides were marked to differentiate them. The reactor had a working volume of 2E-4 m^3, and the four slides provided a total surface area of 0.0013 m^2. The reactors were covered with an acrylic plastic top. The reactor fluid was pumped through a variable speed peristaltic pump (Masterflex Co.) from the top of the reactor, and the effluent pumped out from the bottom. The residence time in the reactor could be varied by changing the speed of peristaltic pumps. The rotating inner cylinder ensured complete mixing of bulk fluid in the reactor. Advantages of the annular configuration include the following:

- due to complete mixing, no concentration gradient exists in the bulk liquid, which simplifies sampling and mathematical analysis.
- fluid shear stress at the coupon surface can be varied

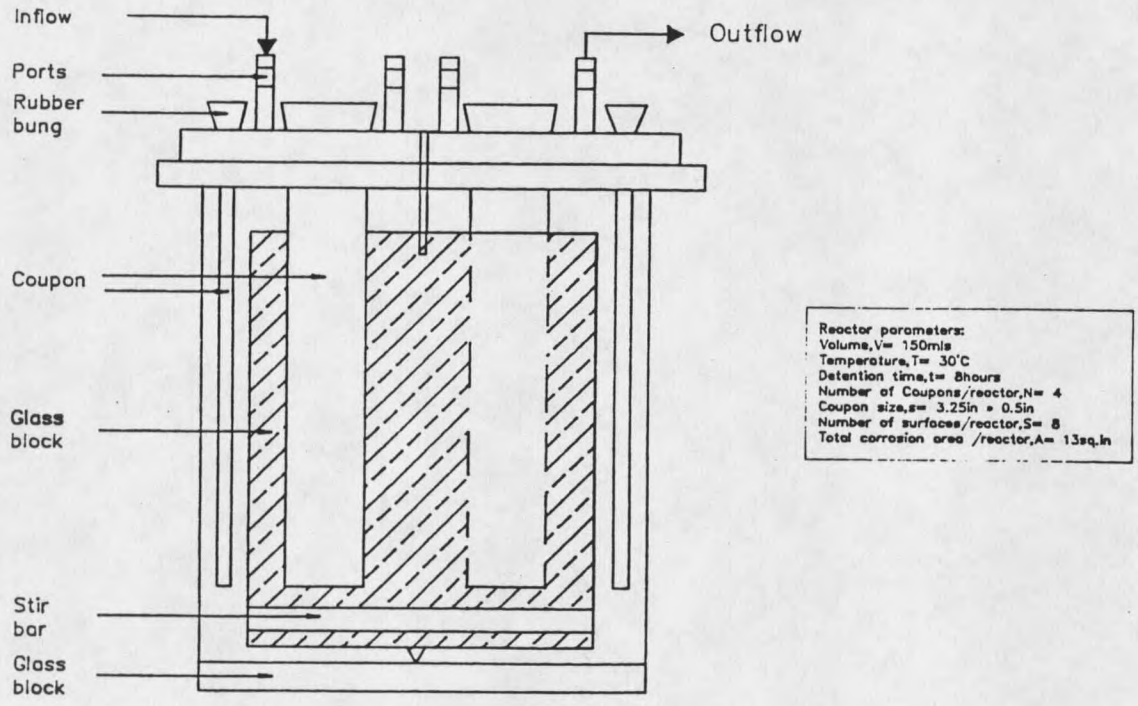

Figure 4. Detail design of laboratory reactor used for simulation of corrosion problem.

independent of reactor mean residence time.

- high surface area to volume ratio (A/V = 7000 per meter).

Coupons

The coupons were 304 (16 ga) stainless steel strips (Metal Samples, Inc., Mumford, AL), 8.26E-2 m (3.25 inch) long, 1.27E-2 m (0.5 inch) wide, and 6.35E-4 m (0.025 inch) thick, with a surface

roughness of 3-5 μm. The elemental composition of SS 304 is presented in Table 1 (analysis by Metal Samples).

Table 1. Elemental composition of the SS 304 coupons

Element	C	P	S	Mn	Cr	Si	Ni
%	0.08	0.045	0.03	2.0	18	1.0	10

Bulk Media

RCT system make-up water was used as a bulk media for biofilm growth in the reactor. The make-up water was shipped chilled in a cooler and, after being received, was immediately transferred to a refrigerator and maintained at 4°C. The make-up water was preheated prior to being pumped into the reactor. The composition of the make-up water varied slightly over the duration of experiments (Table 2).

Assuming three (3) cycles of concentration, the composition of recirculating water in the RCT system, with some exceptions, will be three times the composition of make-up water.

Experimental Start-Up

Standard cleaning and sterilization procedures were established to ensure uniform conditions throughout the experimental work.

Table 2. Average Composition of Experimental Reactor Feed as well as make-up water for RCT (Tables 3, 4, and 5, Appendix A). Units are kg/m^3 unless otherwise noted.

Physical	
pH	pH 6.34
TSS	4.26E-2
VSS	8.80E-3
Conductivity, µmho	128
Chemical	
Carbon	1.34E-2
Phosphorus*	< 1.0E-4
Iron	1.50E-3
Manganese*	< 5.0E-5
TKN*	< 1.0E-3
NO_3-N	3.0E-4
NH_4-N*	< 1.0E-4
Calcium	6.30E-3
Magnesium	1.75E-3
Microbial viable cell count (per m^3)	
SRB	1.2E+10
HPC	5.3E+10
GAB	2.6E+10

* = minimum detectable limit

Coupons

The coupons were ultrasonically cleaned twice with 100 per cent ethanol for 30 seconds each time. The coupons were air dried at room temperature, preweighed, marked with a serial number, and installed aseptically in the reactor.

Reactor

1. After an experiment, the reactor was operated in a batch mode for 900 sec (15 min) with 10 % (v/v) Chlorine bleach.
2. The reactor was disassembled and soaked in warm water for 600 sec (10 min).
3. The surface of the reactor was scrubbed with a soft bristle brush and rinsed.

4. Preceding an experiment, the reactor was autoclaved at 121°C for 900 sec and allowed to cool to room temperature inside the autoclave.
5. The reactor was soaked in 70 % ethanol for 1800 sec (30 min) and air dried.
6. The reactor was assembled.
7. The nutrient feed lines were autoclaved at 121°C for 1200 sec (20 min).

Experimental Procedure

The experimental work was performed in the laboratory and at the Methanol plant RCT system in Texas.

Laboratory Experiments

The experimental system consisted of six (6) RotoTorques (Figures 5 and 6). The reactors were covered with aluminum foil to avoid exposure to light. All reactors were run at a constant rotational speed to provide an uniform shear stress. The temperature in the system was maintained at 30°C throughout the experiments. Chlorine was fed once a day in a slug manner. The concentration of chlorine and the residence time in the reactors varied in two experiments (Figures 5 and 6). The coupons were pulled from each reactor according to a preset schedule (Figures 5 and 6). Replication was achieved by pulling at least two coupons from each reactor at the end of each preset time period. The time duration for the first experiment was 8 weeks and 12 weeks for the second.

All reactors run in parallel
Mean Hydraulic Retention Time (MHRT) = 8 hours
Flow Rate, Q = 7.5E-9 m^3/sec, Temperature, T = 30 C

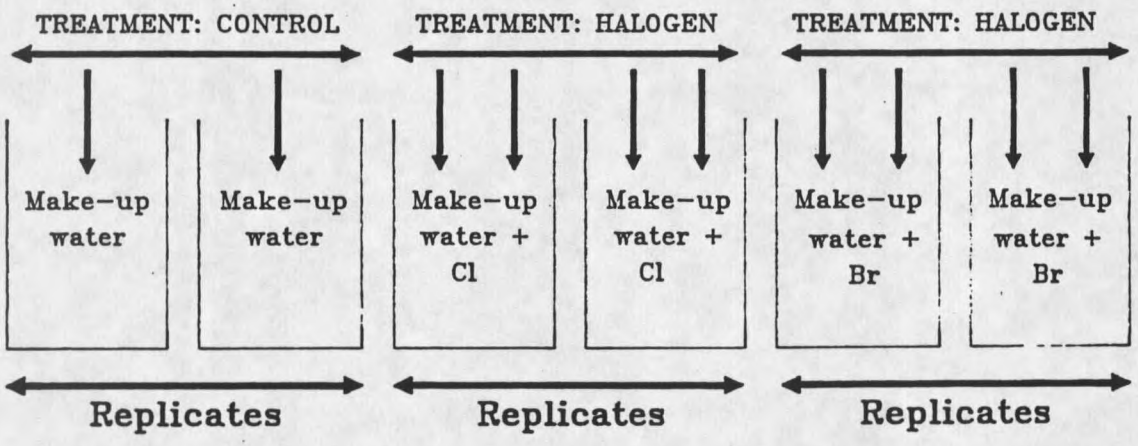

Figure 5. Experimental plan for laboratory simulation with RCT system make-up water as nutrient. One coupon was pulled from each reactor at the end of 3, 6, 9, 12 weeks respectively.

Laboratory experiments to study the SS 304 metal surface characteristics required etching the corrosion coupons in 10 % oxalic acid (Annual Book of ASTM Standards, 1984) and observing the etched surface under low power (15X) microscope on a statistically valid number of coupons. The same was done with RCT system SS 304 heat exchanger tubing

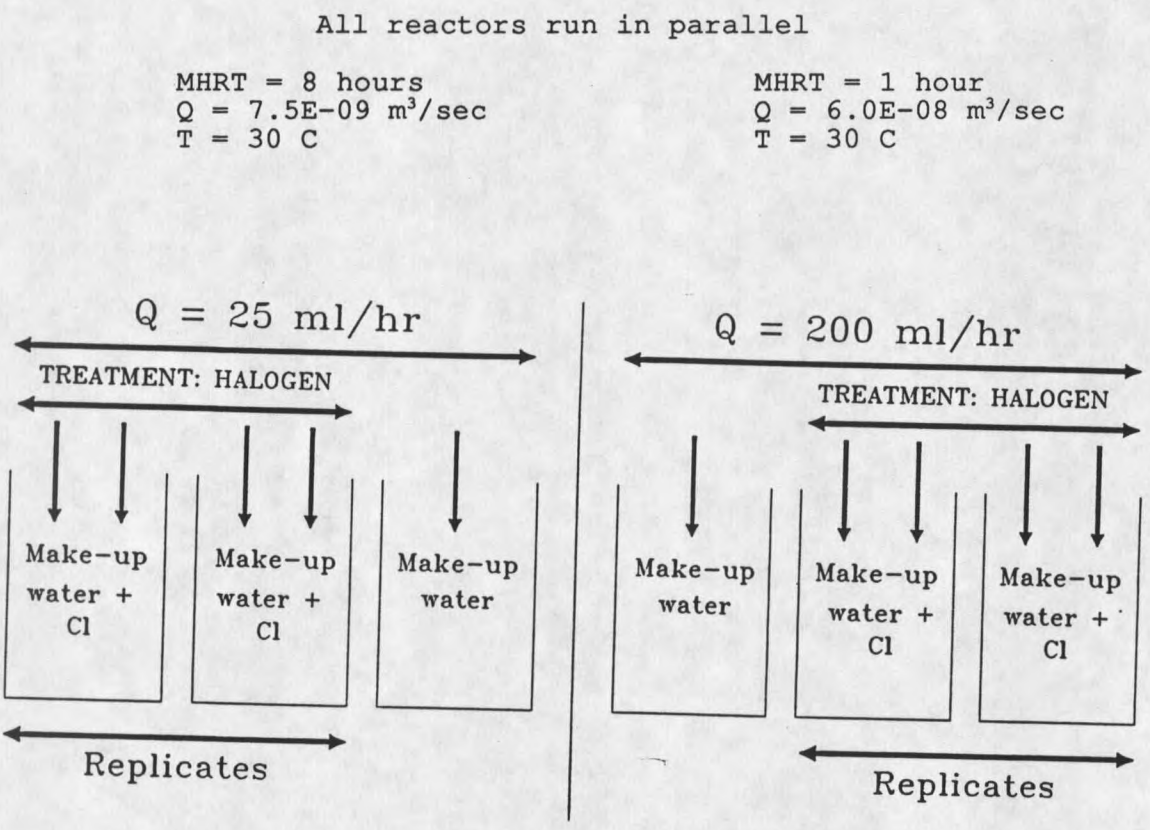

Figure 6. Experimental plan for laboratory simulation with RCT make-up water as nutrient. One coupon was pulled from each reactor at the end of week 3, and the rest at the end of week 12.

Methanol Plant Experiments

Six (6) SS 304 coupons, identical to those used in the laboratory experiments, were installed in the RCT system. Each coupon was marked with a serial and preweighed before installation. The coupons were installed in the make-up well in the absence of light in a region of well-mixed but not vigorously turbulent fluid conditions. The coupons remained in the make-up well for a period of 8 weeks.

The retrieved samples were placed in plastic vials on site,

filled with pre-sterilized RCT system make-up water, and shipped in an insulated container to Bozeman. The temperature of the sterilized make-up water was 10°C upon receipt of samples.

Water Quality

The physical analyses of the RCT system make-up water and other reactor fluids consisted of a qualitative check of color and odor. pH was measured using pH meter (Corning Scientific Instruments, Model 7) calibrated with a standard solution at 30°C. Turbidity was measured with Hach 210 turbidimeter calibrated with a standard solution of 100 NTU turbidity. Total dissolved and volatile solids were analyzed as described in the Analytical Methods section. The conductivity of the reactor fluid was measured with a conductivity meter (Wescan Co.) calibrated at 30°C.

Chemical analyses were performed to characterize the fluid for elemental composition and microbial nutrients. The analyses included total dissolved phosphorus, total organic carbon (TOC), Kjeldahl nitrogen (TKN) (digestion technique), dissolved iron, manganese, calcium (atomic absorption flame spectrophotometer), magnesium, ammonia nitrogen (NH_4-N), and nitrate nitrogen (NO_3-N).

Microbial analyses of the reactor fluid included total cell count (TCC), viable general anaerobic bacteria (GAB), viable heterotrophic plate count (HPC), and viable sulfate reducing bacteria (SRB).

Analytical Methods

General Sample Processing

The biofilm on the coupons was subjected to chemical and microbial analyses. The biofilm surfaces were sampled with a 10-section template. Each analysis was performed in duplicate. Each side of the coupon (two surfaces) was sub-divided into five (5) equal sections to quantify the spatial distribution of deposits and their chemical and microbial components over the surface. The coupon dimensions were 0.015 m x 0.085 m and each sector was 1.275E-4 m^2 in area.

Sample Processing for Chemical Analyses

Each section of the coupon surface was scraped with a sterile, plastic spatula into a 2.0E-5 m^3 sterile beaker of carbon-free water and homogenized to produce a uniform distribution of deposit constituents. The sample beaker was submerged in ice to prevent a temperature increase. The speed on the Sorvall Omni-Mixer (DuPont Instruments) homogenizer was gradually increased to maximum, and maintained there for 60 seconds.

The above procedure was repeated for all the scraped sections. The homogenizer probe was sterilized with 70% ethanol and rinsed with sterile water after scraping each section. The samples were immediately refrigerated and analyzed within 24 hours.

Total solids (TS). 15 small crucibles were acid-cleaned, rinsed with carbon-free water and air dried. 0.22 µm Whatman glass fiber filters were placed in the crucibles, transferred to a muffle

furnace, and ignited at 500°C for 1800 sec (30 min). The filters were weighed using a digital micro-balance (up to four significant figures), and transferred into a desiccator. 1.5E-5 m^3 of homogenized sample were filtered and the filters laid into crucibles which were placed in an oven for drying at 105°C for 8 hours. Filters were then weighed, the filter tare subtracted and total solids reported as kg/m^2.

Volatile solids (VS). Filters from the TS procedure were placed in aluminum crucibles, and ignited in a muffle furnace at 550°C for 40 minutes. Filters were transferred into a desiccator and allowed to cool. Filters were then weighed for VS and the data reported as kg/m^2.

Total organic carbon (TOC). The analysis was performed using a Dohrmann DC-80 Total Organic Carbon analyzer. 1.0E-6 m^3 of homogenized sample was injected into the system using a micro-syringe. Each sample was run in triplicate and data reported as kg/m^2.

Sample Processing for Microbial Analyses

The homogenization procedure produces a uniform distribution of single cells for enumeration. This is crucial when enumerating sessile bacteria (i.e., bacteria in biofilms). The scraped material was suspended in 2.0E-5 m^3 of sterile homogenization fluid (Tris buffer, pH 7.0, 0.01M; Zwittergent 3-12, 10^{-6}M; EGTA, 10^{-3}M; and Peptone, 0.01%) to prevent reattachment of bacteria to charged

particulate material after homogenization ceases. The samples were homogenized for 180 sec, refrigerated immediately, and analyzed within 24 hours after being refrigerated.

Heterotrophic plate count (HPC). The number of total viable and culturable aerobic and facultative anaerobic bacteria in samples were obtained. R_2A agar medium was allowed to cool to 46-47°C, and plates poured aseptically. Dilution tubes were prepared by autoclaving the dilution media and aseptically dispensing 9.0E-6 m^3 into sterile tubes. The dilution tubes were prepared in triplicates. The first set of tubes were inoculated with 1.0E-6 m^3 of homogenized sample. Each subsequent dilution was inoculated from the prior set of tubes by transferring 1.0E-6 m^3 of fluid. The procedure was repeated for other tubes and samples. To inoculate the agar plates, 1.0E-7 m^3 of fluid from the dilution tube was pipetted onto the agar surface. The inoculum was spread over the surface with a sterile, glass "hockey stick". The plates were inverted and incubated at 30°C. The colonies on the plates were counted on a regular schedule until no further growth was observed. The data was reported as number of colony forming units (cells)/m^2.

Sulfate reducing bacteria (SRB). The number of viable and culturable bacteria that grow anaerobically by reducing sulfate to hydrogen sulfide was determined. 9.0E-6 m^3 of hot Postgate's medium was dispensed into Hungate tubes. The tubes were prepared in triplicate for several dilutions. The filled tubes were transferred to an anaerobic chamber to drive off all residual oxygen and then were tightly capped. The tubes were autoclaved at 121°C for 900 sec,

and left to cool. Inoculation of tubes was performed by injecting 1.0E-6 m^3 of homogenized sample in the first set of tubes. Each subsequent dilution was inoculated from the prior set of tubes, the tubes being thoroughly mixed prior to the transfer of fluid. The inoculated tubes were incubated for 4 weeks at 30°C. The tubes were read for positive growth, indicated by the presence of black FeS precipitate. Cell numbers were determined using MPN tables.

General anaerobic bacteria (GAB). The number of viable and culturable general anaerobic bacteria present in a sample was determined in a manner similar to SRB analysis except that fluid thyoglycolate medium was used for inoculation tubes. Positive growth was indicated by increased turbidity in tubes. Cell numbers were determined using MPN tables.

Total cell count (TCC). The total number (viable and non-viable) of cells in a sample were determined using a Petroff-Hauser hemocytometer, a glass slide with precisely machined chambers so that cells in very small volumes can be counted using a microscope. 1.0E-6 m^3 of homogenized sample was stained in 20% acridine orange for 1800 sec. The slide was observed under the microscope at low-power (50X). The total number of cells was counted in each square and averaged over 20 squares. The procedure was repeated with Hoechst stain. The concentration of cells in the original sample was calculated using the following formula :

$$\text{cells/m}^3 = \frac{\text{average \# cells} * 10^9}{1/400 * 1/50 * \text{dilution}} \quad \ldots\ldots\ldots \quad (11)$$

The volumetric cell concentration (cells per m^3) was

multiplied by the sample volume (2.0E-5 m^3) to yield total number of cells. The total number of cells was divided by the area scraped to obtain the biofilm sample. Care was taken to use dilutions such that there were no more than 3 cells in any square (2.5E-09 m^2 i.e., 1/400 mm^2).

Microscopic examination for Mn/Fe oxidizing bacteria. A qualitative determination for the presence/absence of microorganisms that oxidize Fe and/or Mn was conducted by observing the sample under a light microscope for size, shape, and staining characteristics that are peculiar to these types of bacteria. The procedure is the same as for TCC, except that an unmarked microscopic slide is used instead of the hemocytometer. Epiflourescence light was used in parallel to visible light to differentiate between inorganic and microbial deposits.

Surface Analysis of Biofilm and Corrosion Products. The distribution of elements heavier than sodium on metal coupon surfaces and deposits was measured and mapped. The biofilm samples were transferred to an anaerobic chamber and fixed for 8 hours with 2.5% Glutaraldehyde solution (technical grade) in 0.1M sodium cacodylate buffer (pH 7.0 $\pm$ 0.2). The samples were drained and placed in 30% ethanol solution for 15 minutes to dehydrate deposits. The dehydration procedure was repeated with 50%, 70%, 90%, and 100% ethanol solutions. The samples were air dried, gold sputtered and analyzed using ISI-40 scanning electron microscope. Composition of the biofilm deposits and substratum and were determined with the scanning electron microscope (SEM) and a Princeton Gamma-Tech System

4 energy-dispersive x-ray spectrometer (EDAX).

Metallurgical Analyses

The analyses has been divided into two sections: 1) new heat exchanger tubing and new laboratory corrosion coupons, and 2) corroded heat exchanger tubing and corroded laboratory corrosion coupons.

Analyses of New SS 304 Heat Exchanger Tubing and Laboratory Corrosion Coupons. The analyses of new (unused) SS 304 tubing and laboratory coupons were performed to establish a baseline of quantitative information on the spatial distribution of elements in the metal. The analyses included general surface chemistry, metallurgical studies, and surface topography.

Sections were obtained from unused SS 304 tubing and laboratory coupons, appropriate in size for SEM (based on SEM system specifications), and cleaned as described in the electrochemical cleaning procedures. The cleaned sections were analyzed using SEM, EDAX, and x-ray mapping techniques.

General surface morphology. Surfaces of sample sections were observed with phase contrast microscopy for surface topography. Surface roughness was obtained at several locations with averages and standard deviation noted. Surfaces were scanned with SEM for metallurgical heterogeneities (defects/irregularities/inclusions).

General surface chemistry. Analyses were performed on a statistically valid number of sections and/or different tube

sections for elements including iron, manganese, sulfur, and chloride. Quantitative analysis was obtained by EDAX. EDAX and x-ray mapping was performed on the areas surrounding the irregularities.

General Metal Structure. A section of unused, cleaned tubing was etched as described in Annual Book of ASTM Standards, 1984. The etched surface was analyzed with SEM for granular structure of metal, grain boundaries, and inclusions.

Electrochemical Cleaning Procedure

The sample to be cleaned was made the cathode in a cyanide-alkaline electrolyte. Alkaline attack by the electrolyte, coupled with hydrogen generated at the surface, removes surface oxides by mechanical and chemical action.

The electrolyte used for steel samples was ENDOX 214, a powdered product containing sodium cyanide. The cleaning procedure involves mixing 2.268E-1 kg of ENDOX 214 in 1.0E-3 m^3 of water to which small amounts of Photoflo wetting agent have been added. The temperature of the solution is maintained between 70 and 150°F. The anode is an inert material (e.g., platinum, gold or SS 316). A suitable dc voltage is applied to produce a current density of 2.50E+6 $\mu A/m^2$. Cleaning is done ultrasonically for 60 sec, followed by washing in Alconox. Samples were transferred immediately to a desiccator until further analyses to avoid surface oxidation reactions. Any direct contact with the surface was avoided before or during analyses.

Sample Processing for Corrosion Analysis

The coupons were ultrasonically cleaned twice in 70% ethanol solution to remove any deposits left on the surfaces after the scraping procedure. The coupons were acid-cleaned with corrosion inhibitor to remove any corrosion products on the surface, without attacking the metal surface itself. The coupons were quickly transferred to an anaerobic chamber to prevent any oxidation reactions at the metal surface.

Corrosion Analyses. Acid-cleaned coupons were weighed using a digital micro balance (detection limit up to 1.0E-8 kg) to determine the weight loss due to corrosion. The average corrosion rate was determined by averaging the total weight loss of the entire coupon divided by total exposure time. The coupons were observed under low-power microscopy (15X) and epiflourescent light for pitting analyses. The observations included the following: (a) number of pits/m^2, (b) shape and size of pits (qualitative), and (c) depth of pits.

RESULTS

Make-up Water Analysis

The physical and chemical analyses were performed weekly on the make-up water shipped from the Methanol plant RCT system (Tables 3, 4 and 5 in Appendix A, and Figure 7). Microbial analyses were performed once a month. The results do not indicate a wide variation in the water quality. However, there is a sudden decrease in conductivity for a couple of samples obtained during experiment duration. The make-up water exhibits high turbidity, and is rich in inorganic content.

The make-up water is relatively rich in organic carbon (TOC 0.012-0.015 kg/m^3) which provides the source of energy for heterotrophic bacteria in the Methanol plant RCT system. The amount of assimilable organic carbon (AOC) was not determined. There are sufficient microorganisms in the make-up water to provide a significant inoculum for microbial growth in the recirculating water in the RCT system. The samples taken 20 days apart show practically no fluctuation in planktonic microbial cell numbers.

Nitrogen and phosphorous, important nutrients for microbial growth in the make-up water, are rather low for balanced growth. However, nitrogen can enter the plant by absorption of ammonia from a nearby ammonia plant.

Iron concentration averages around 1.5E-3 kg/m^3 and may be at least partially complexed with organic materials. Manganese concentration was around 5.0E-05 kg/m^3.

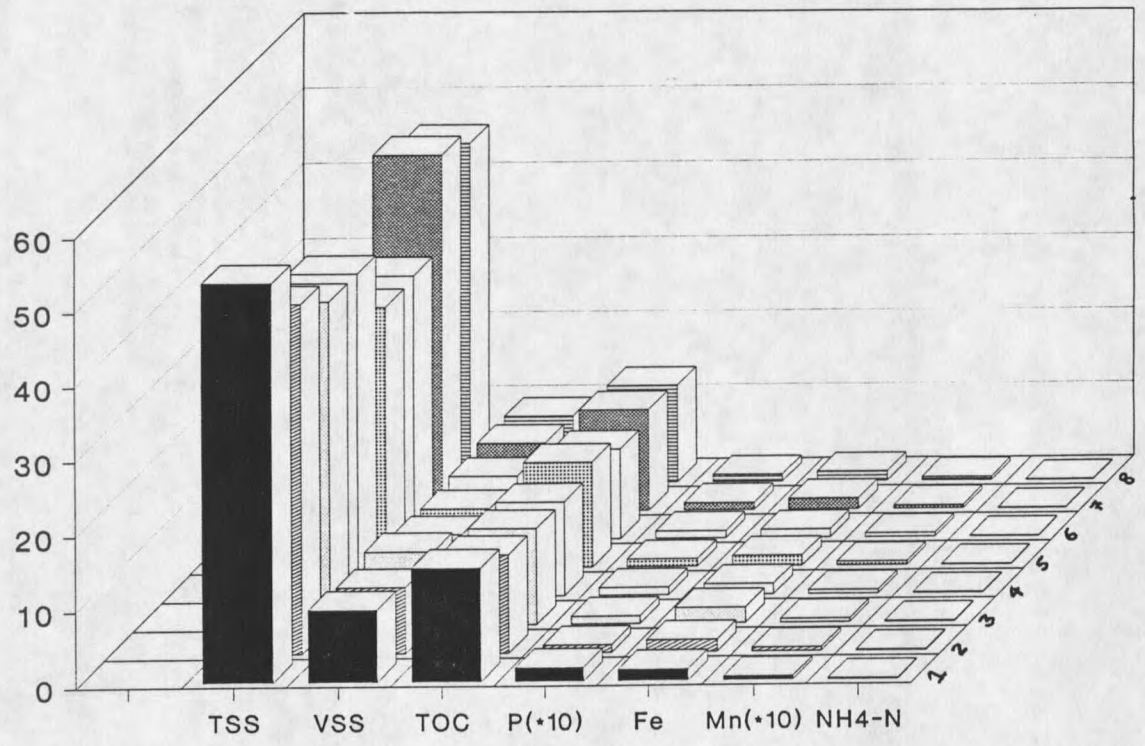

Figure 7. Results of chemical analyses performed on Methanol plant make-up water. (x10) indicates that the values shown in Figure have been magnified ten times.

Analysis of 304 SS Laboratory Coupons

SEM/EDAX analysis did not indicate the presence of any kind of inclusion in the metal surface of the SS 304 coupons (Figure 8). The micrograph highlights the metallurgical heterogeneities on the coupon surface. Fe, Cr, Ni, and Mn are characteristic of 304 stainless steel metal, and appear to be present in expected quantities as indicated by the X-ray dot map (Figure 9).

Laboratory Experiments Results

Make-up Water

SEM and EDAX analyses were conducted on coupons from laboratory bench scale reactors using RCT make-up water as the feed. SEM indicates the "patchiness" of the deposit distribution (Figure 10). The deposit patchiness occurred regardless of chlorine or no chlorine treatment (Figure 11) and was observed at all sample times through the seven weeks run. The patches of deposits appear to increase in size and number over time.

EDAX of the patchy deposits are high in Si and Al concentration which indicates that the deposit was largely inorganic.

Filamentous microorganisms may be present (Figure 11). EDAX analysis (Figure 11) did not reveal the presence of Fe and/or Mn associated with the filamentous structures, thus minimizing the possibility of Fe/Mn oxidizing bacteria.

The micrographs (Figures 10 and 11) suggest that non-chlorinated deposits are populated by greater numbers of microbial cells.

Crevice corrosion was observed on a few coupons at the interface between the rubber stopper (holding the metal coupon) and the metal surface.

Micrographs of the coupon surface after ultrasonic cleaning demonstrate scratch lines on the metal surface ruling out any significant corrosion regardless of chlorine or no chlorine treatment.

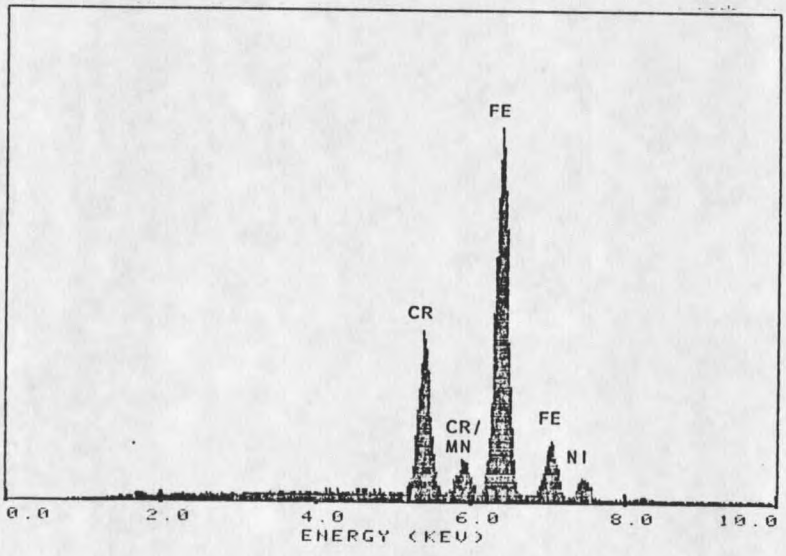

Figure 8. SEM of blank (unused) laboratory coupon surface (x100) after ultrasonic cleaning. EDAX, performed on region marked by arrow in SEM, is typical of SS 304.

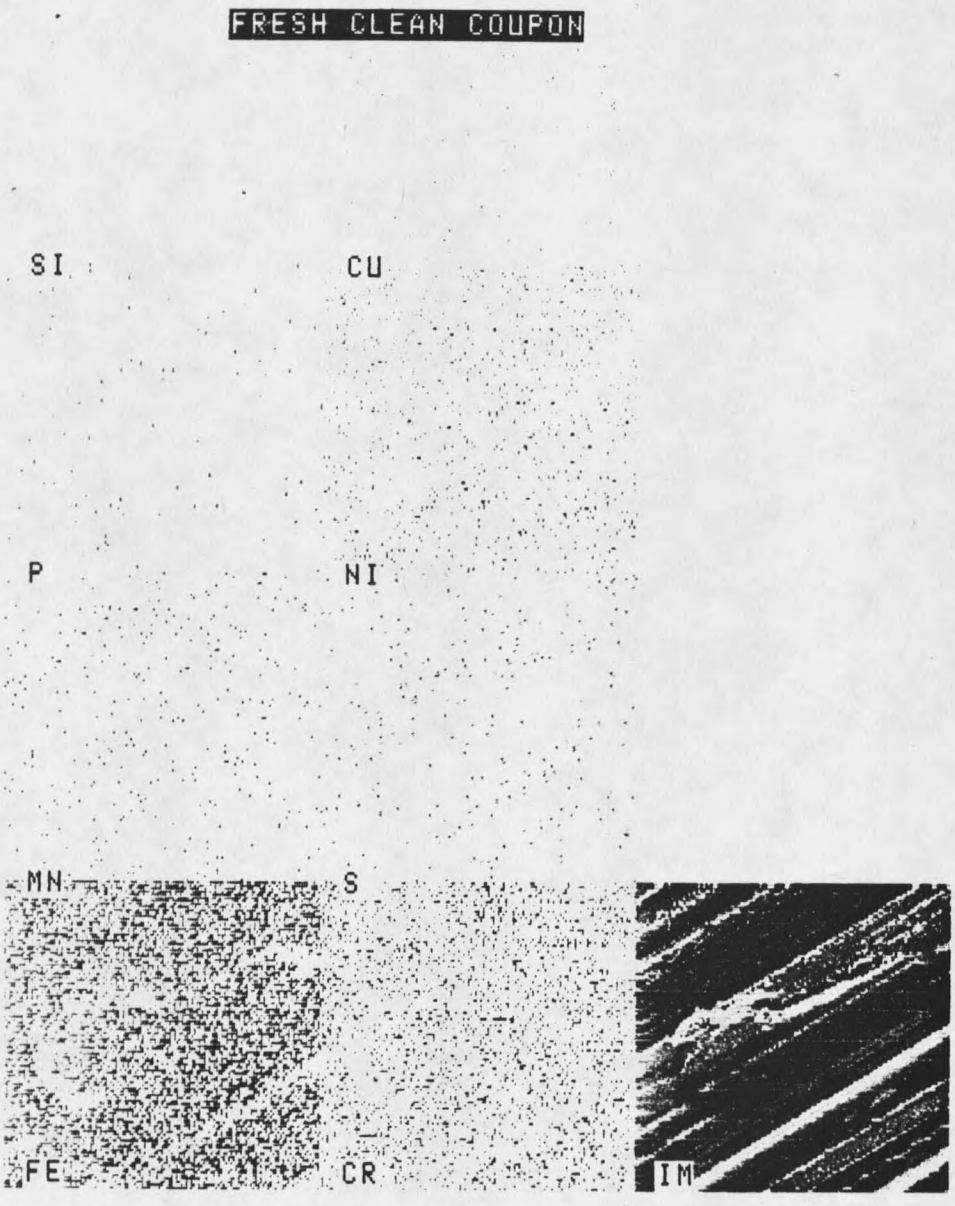

Figure 9. X-ray dot map of a blank coupon surface (x980), shown on right, after ultrasonic cleaning. The results are typical of SS 304.

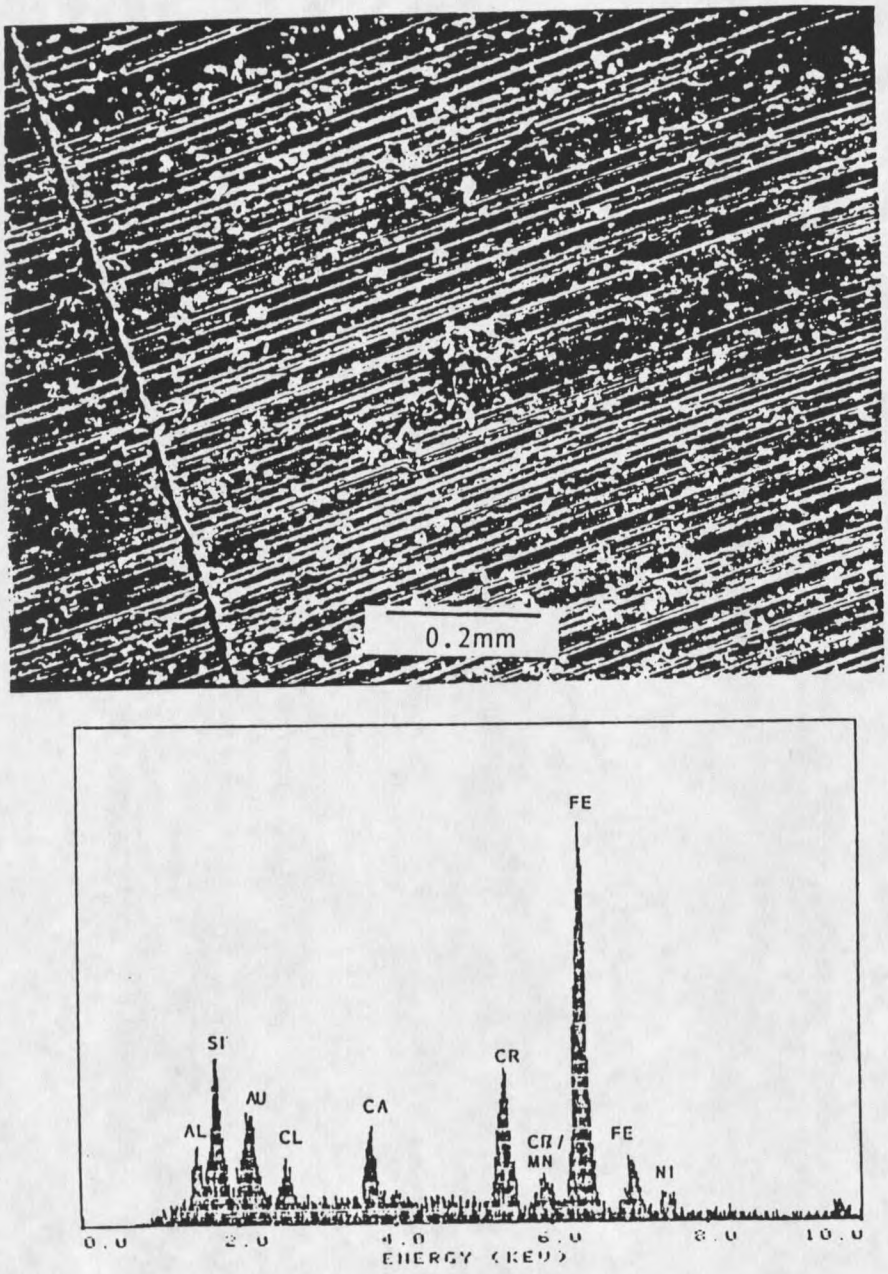

Figure 10. SEM of coupon surface (x97). The coupon was in laboratory reactor with make-up water for 7 weeks. The reactor was chlorinated for 3 weeks. EDAX highlights the inorganic nature of deposits as well as absence of highly localized chloride deposits.

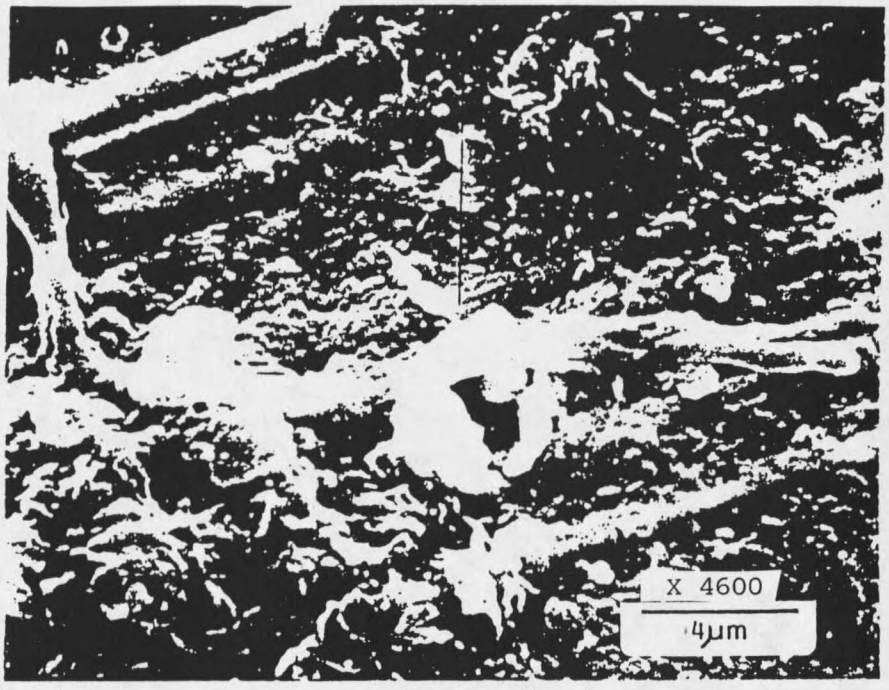

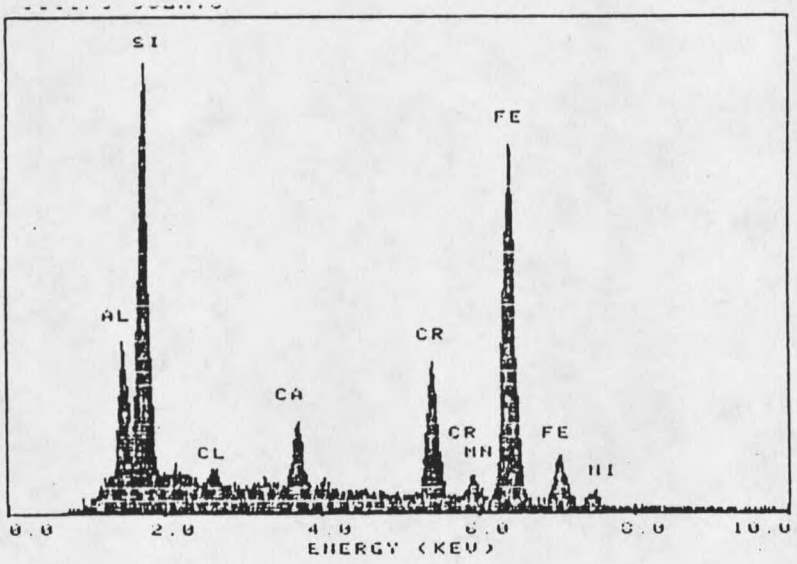

Figure 11. SEM of coupon surface (x97). The coupon was in laboratory reactor for 7 weeks, receiving no treatment during that time.

Recirculating Water Experiment

The cycles of concentration in the Methanol plant RCT system tend to concentrate the incoming make-up water by three-five times. Thus, the make-up water received from the Methanol plant was concentrated four times by addition of various elements present in the water. This concentrated make-up water simulated the recirculating water and was used as the feed for some experimental work.

Chemical Analysis. Chemical analyses of coupon deposits at different dilution rates, respectively 7.5E-9 m^3/s (25 ml/hr) and 6E-8 m^3/s (200 ml/hr) is presented below.

At low dilution rate, the total dry mass on the coupons ranged from 5E-4 kg/m^2 to 2.8E-3 kg/m^2 averaging around 1.7E-3 kg/m^2. Total dry mass appeared to be more on the bottom end of the coupons. Percent volatile mass ranged from 45% to 80% averaging around 71%. Total organic carbon (TOC) ranged from 3E-5 kg/m^2 to 9E-5 kg/m^2 averaging around 7E-5 kg/m^2 (Figure 12).

At high dilution rate, the total dry mass on the coupons ranged from 1.2E-3 kg/m^2 to 5.6E-3 kg/m^2 averaging around 2.8E-3 kg/m^2. Total dry mass appeared to be more on the bottom end of the coupon. Percent volatile mass on coupons ranged from 62% to 85% averaging around 74%. Total organic carbon (TOC) ranged from 5E-5 kg/m^2 to 3.6E-4 kg/m^2 averaging around 1.2E-4 kg/m^2 (Figure 13).

Chlorination had some effect on sessile microbial population. At either dilution rate, total dry mass, percent volatile, and TOC were lower on chlorinated coupons compared to non-chlorinated coupons (Figures 14 and 15). However, the differences in chemical

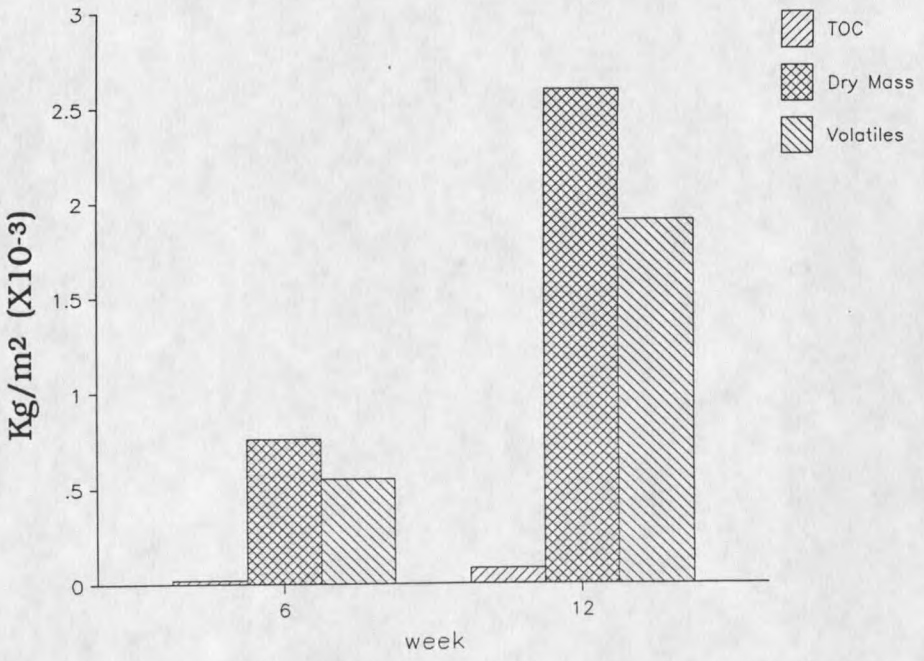

Figure 12. TOC/dry mass/volatile mass distribution on deposits at low dilution rate. No chlorine treatment was provided.

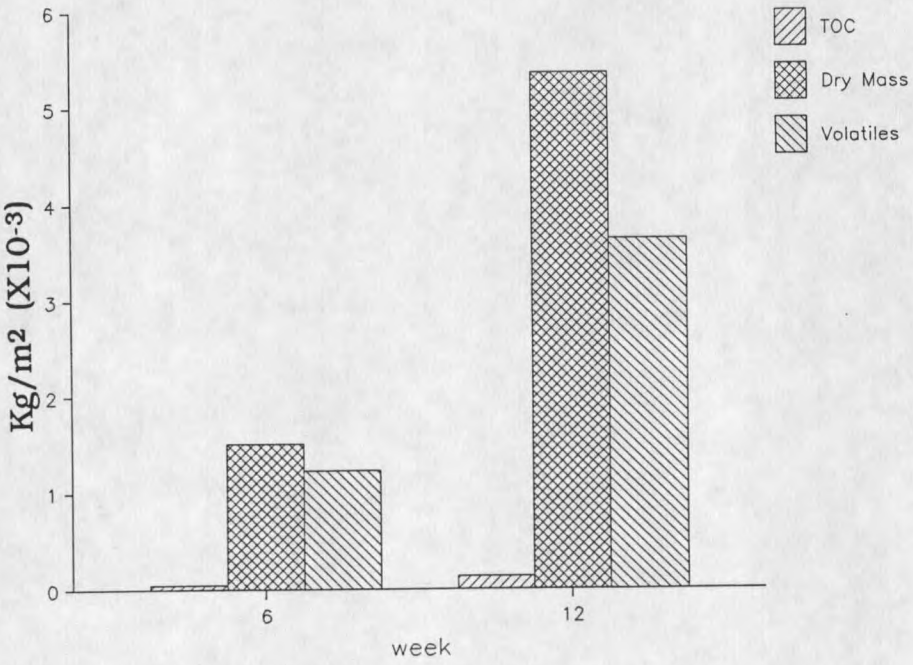

Figure 13. TOC/dry mass/volatile mass distribution on deposits at high dilution rate. No chlorine treatment was provided.

and microbial composition of deposits did not produce any differences in corrosion phenomenon.

Microbial Analyses. Dilution rates did produce some differences in general anaerobic bacteria (GAB) and aerobic (HPC) sessile population on the coupons. The GAB population appeared to vary between 2E+06 cells/m^2 at low dilution rate to 2E+08 cells/m^2 at high dilution rates, while HPC varied from 5.7E+07 cells/m^3 at low loading rate to 6.3E+09 cells/m^3 at high loading rate. With blank media (water) contribution being taken into account, this represents an average increase by a factor of 10 to 100. Sulfate reducing bacteria (SRB) population was less than 7E+04 cells/m^2, and was observed only on two of the coupons. Difficulty in accurately counting total cells precluded obtaining this data.

Chlorination had a significant effect at low dilution rate but was not very effective in controlling the sessile microbial population at high dilution rate (Figure 14 and 15).

SEM/EDAX Analyses. Dilution rates did not produce any qualitative differences among the constituents in the patchy deposits (Figures 16 and 17). EDAX of the deposits indicates largely inorganic composition (Figure 18). Non-chlorinated surfaces appear to be populated by greater numbers of microbial cells as compared to chlorinated surfaces (Figures 19 and 20). SEM and x-ray dot map of a cross-section of biofilm (Figure 21) indicate insignificant amounts of Fe/Mn at the biofilm-substratum interface.

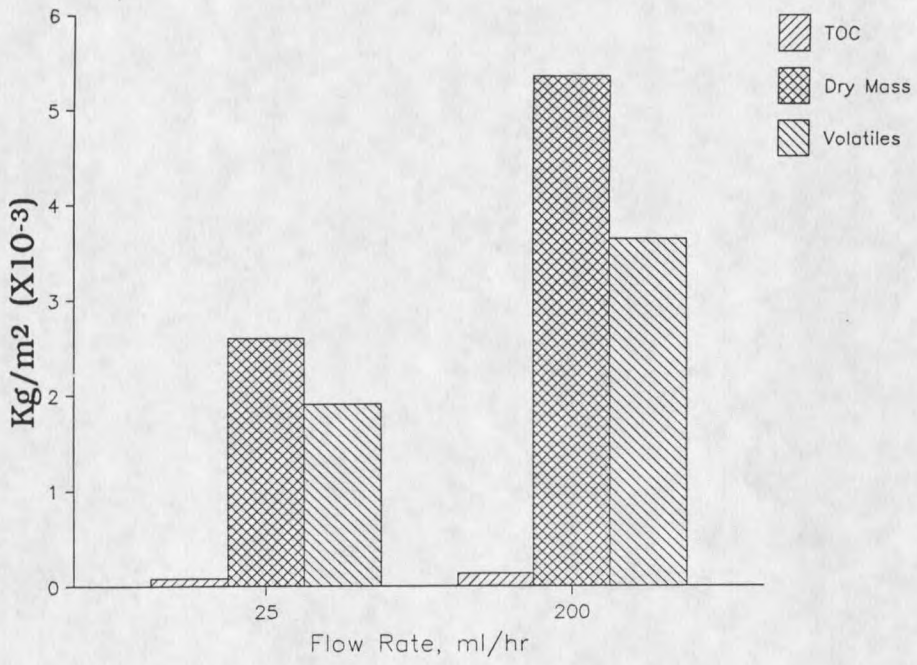

Figure 14. TOC/dry mass/volatile mass distribution on deposits at different dilution rates at the end of 12 weeks. No chlorine treatment was provided.

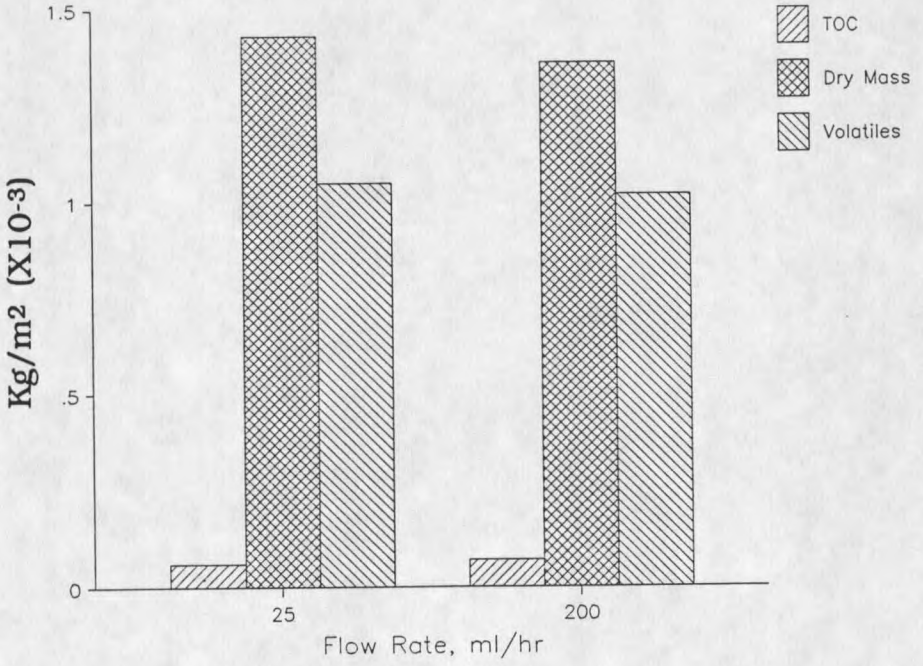

Figure 15. TOC/dry mass/volatile mass distribution on deposits at different dilution rates with chlorine treatment. The coupons were in the reactor for 12 weeks.

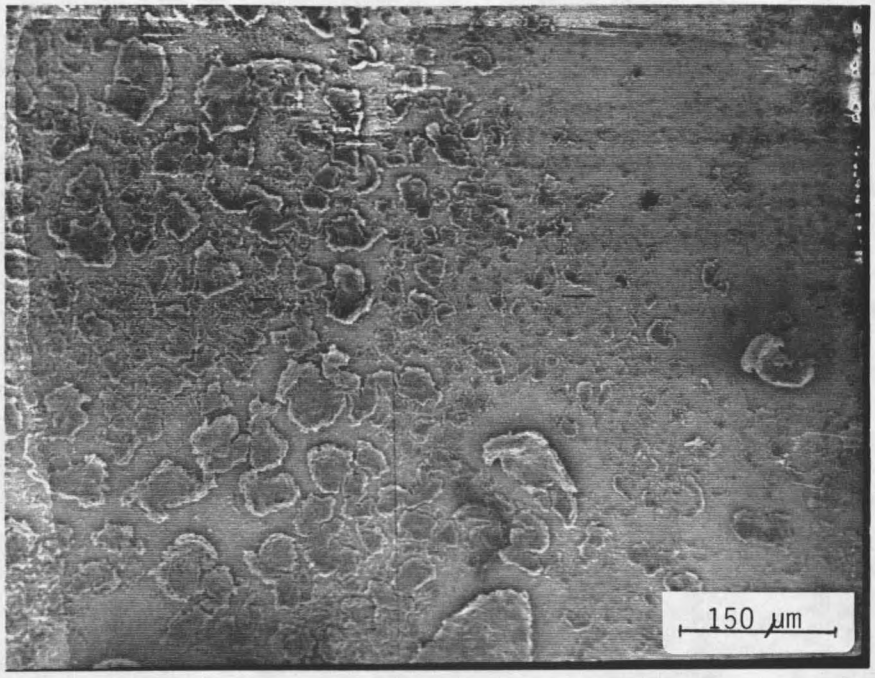

Figure 16. SEM of coupon surface (x600) exposed to recirculating water strength bulk reactor media at low dilution rate. No chlorine treatment was provided during that time.

Corrosion Analysis. The coupon surface beneath deposits after ultrasonic cleaning still exhibits scratch lines (Figure 22) indicating the absence of significant corrosion at either dilution rate. Similar results were obtained for chlorinated and non-chlorinated laboratory experiments.

Field Experiment Results

The coupons recovered from the RCT system were coated on both sides with a fine, patchy, dark brown deposit with no detectable odor. In transit from Texas, the deposits had sloughed off from one side of each of two coupons and were in the bottom of the sampling

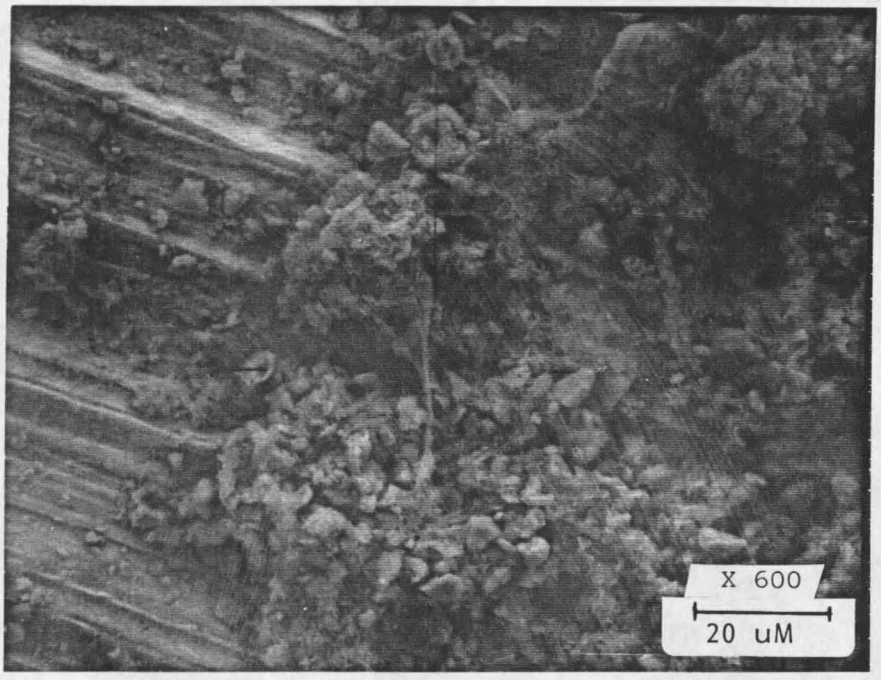

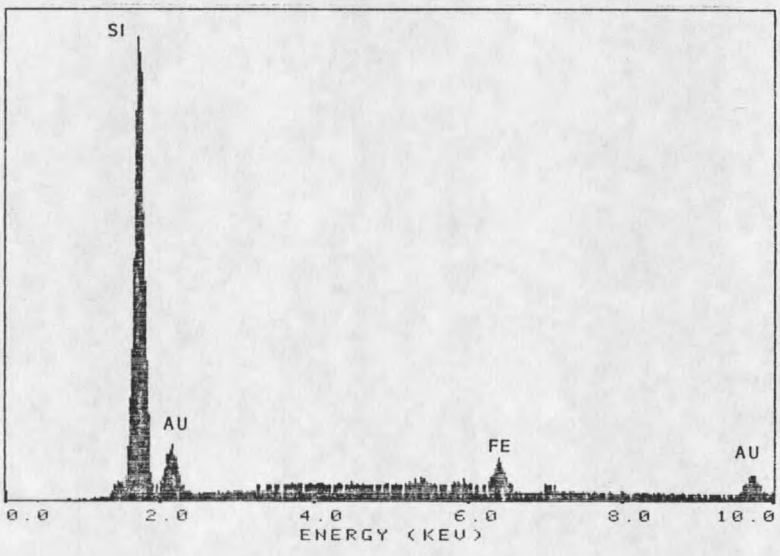

Figure 17. SEM of coupon surface (x600) exposed to recirculating water strength bulk reactor media at high dilution rate. No treatment was provided. Comparison with Figure 20 indicates differences in deposit characteristics, presumably due to absence of biocide treatment.

vial. The deposits on the rest of the coupons were intact.

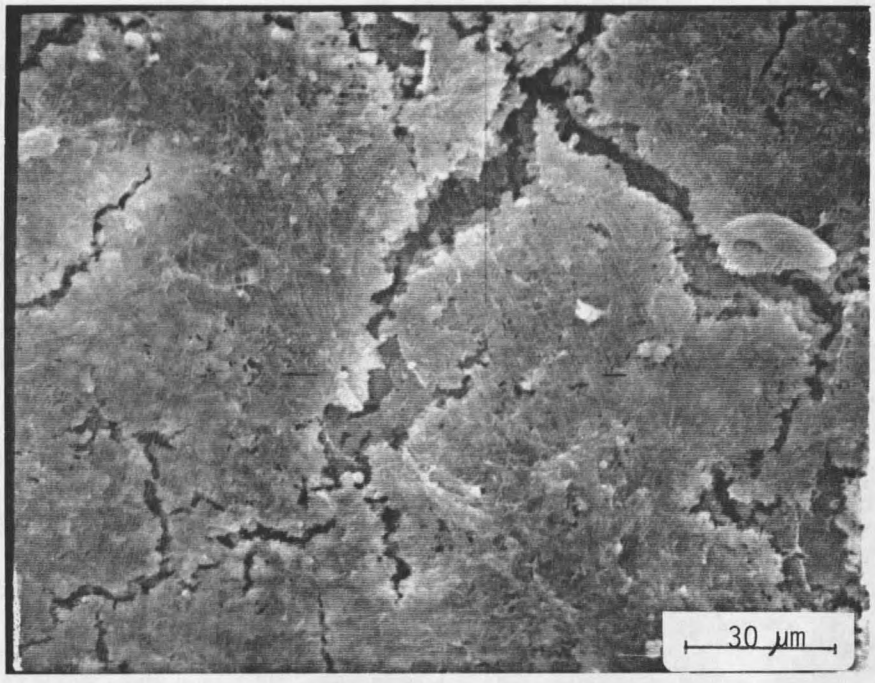

Figure 18. SEM of coupon surface (x600) exposed to recirculating water strength bulk reactor media at low dilution rate, receiving chlorine treatment during that time.

Chemical Analysis

The results of sector analysis of chemical constituents of deposits on coupons installed in the RCT system make-up well water are presented in Table 8 and Figure 22.

Total dry mass on the sectors of the two coupons ranged from 7.3E-3 kg/m^2 to 2.0E-2 kg/m^2 averaging around 1.1E-2 kg/m^2. The area of each sector is 1.275E-4 m^2. Total dry mass was more on one side

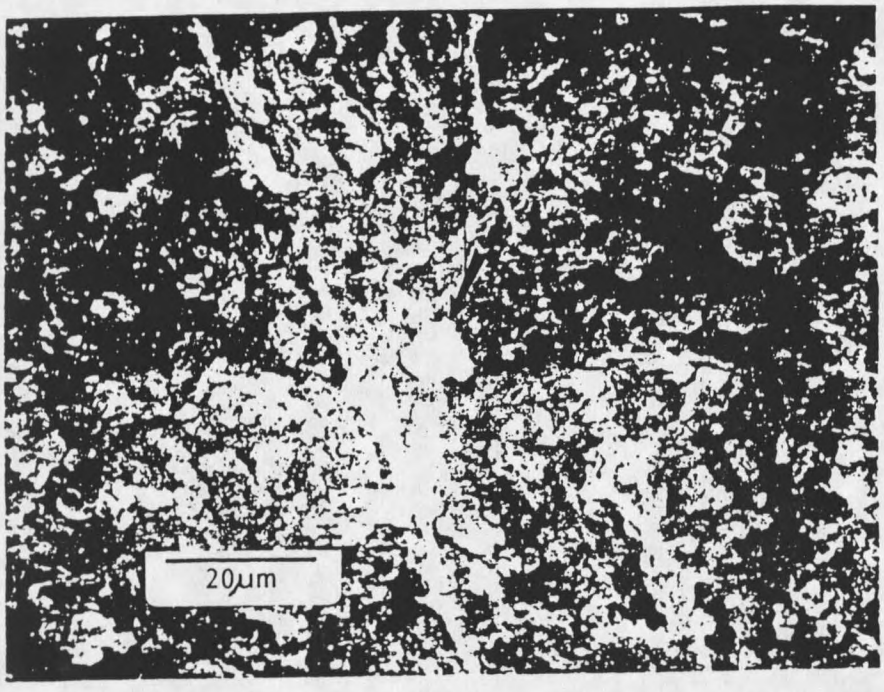

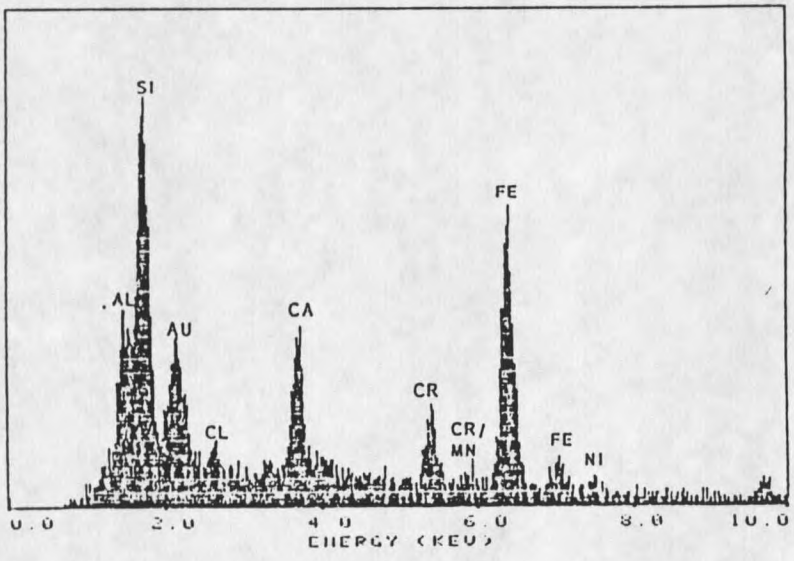

Figure 19. SEM of a coupon surface (x870) exposed to recirculating water strength bulk reactor media at high dilution rate with chlorine treatment. EDAX, performed on area shown by arrow in SEM highlights the inorganic nature of deposits. Visual observation did not indicated the presence of microbial organisms in deposits. Comparison with Figure 10 shows deposit's physical similarity with make-up water and recirculating water simulations.

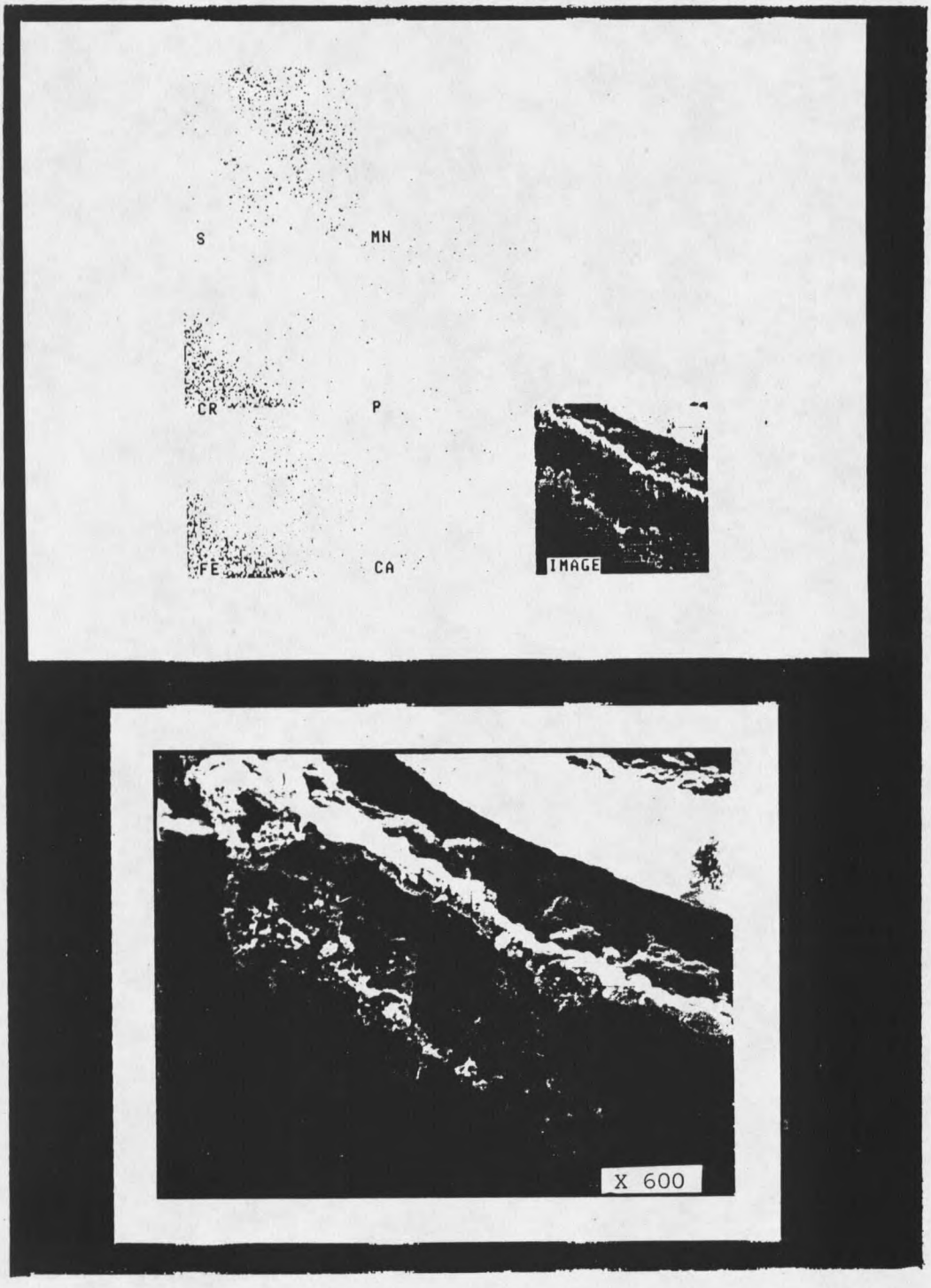

Figure 20. SEM and x-ray dot map of a cross-section (x600) of a deposit on coupon surface. The micrograph indicates insignificant amounts of Fe/Mn at the biofilm-substratum interface.

of the coupon. However, due to lack of information on the orientation of coupons, it is not possible to determine the reason(s) for this behaviour. Percent volatile mass on sectors of the coupons ranged from 50% to 94% with an average of 67% on one coupon and 59% on the other. Total organic carbon (TOC) ranged from 2.1E-4 kg/m^2 to 3.5E-4 kg/m^2 with an average of 2.8E-4 kg/m^2.

Microbial Analyses

General anaerobic bacteria (GAB) and aerobic bacteria (HPC) populations did not indicate any significant variation (less than 1.0E+07 cells/m^2) between the coupons analyzed. GAB ranged from 8.0E+05 cells/m^2 to 7.15E+07 cells/m^2, while HPC varied from 5.35E+06 cells/m^2 to 4.7E+09 cells/m^2 from sector to sector. With blank media (make-up water) contribution being taken into account, an average growth of two orders of magnitude was observed. Sulfate reducing bacteria (SRB) were detected in low numbers (less than 1.0E+7 cells/m^2), and only on a couple of sectors. Difficulty in accurately counting total cells precluded obtaining this data.

Microscopic examination of biofilm did not reveal any structure resembling filamentous bacteria (Fe/Mn oxidizing bacteria).

SEM/EDAX Analysis

The deposits on the coupon surface were patchy in all cases (Figures 23 and 24). EDAX (Figure 23) and x-ray dot map analyses of the deposits shows high silicon levels indicating that the deposits were largely inorganic (Figure 25). The x-ray dot map shows the spatial distribution of inorganic deposits with silicon (Si) and

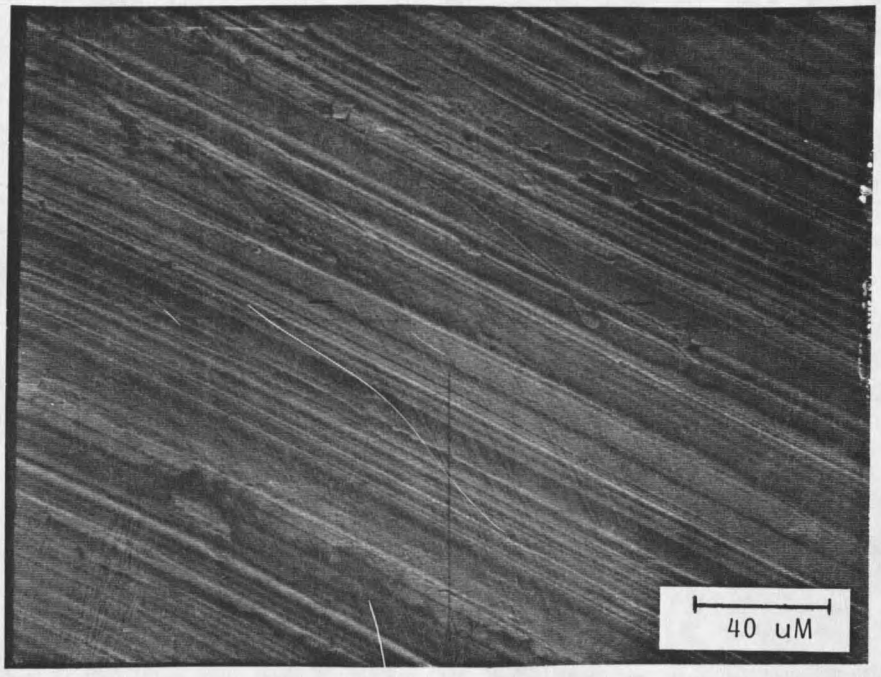

Figure 21. SEM of coupon surface (x390) beneath the deposit after ultrasonic cleaning. Note the scratch lines on the surface, indicating absence of corrosion phenomenon.

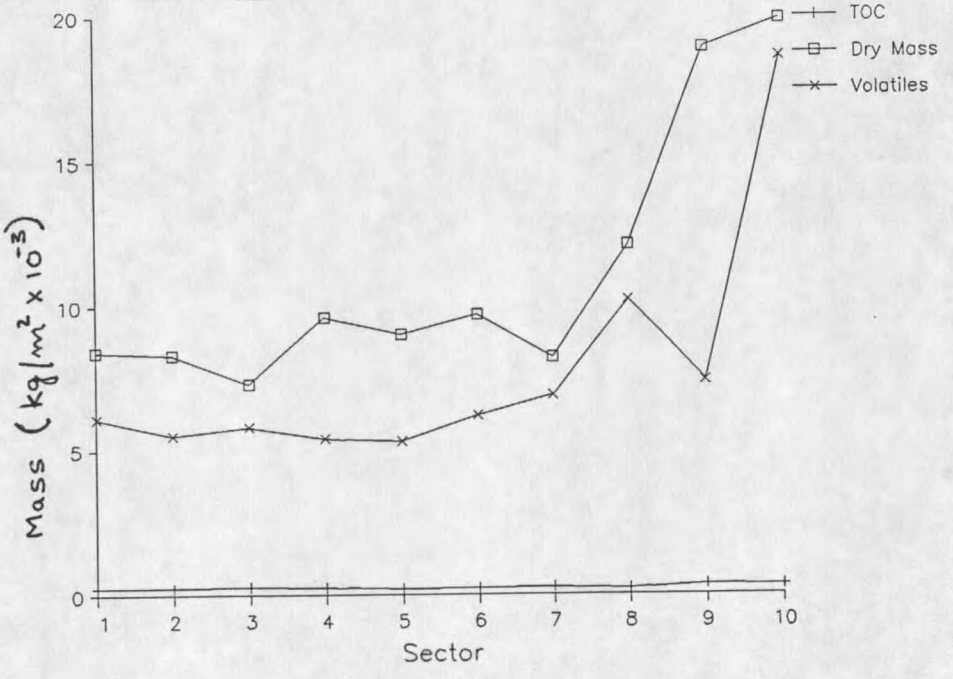

Figure 22. TOC/dry mass/volatile mass distribution on deposits from field simulation.

aluminum (Al) dominating. Each dot shows a particular element's position on the surface (IM). However, this is not an absolute measure as weak signals (e.g., S, Mn) can yield misleading results. The image (IM) is a composite x-ray dot picture of the elemental distribution on the surface.

Evidence of cells in the biofilm was collected (Figure 26) but no bacterial identification was conducted.

The coupon surface exhibited scratch lines after ultrasonic cleaning with no pitting obvious on the coupon surfaces (Figure 27).

Certain non-conductive deposits were observed on the coupon surface after ultrasonic cleaning. The deposits appear as dark spots on micrographs. The middle section of the deposits (appearing white) appears to be composed of non-ionic elements which charge the electron beam (Figure 28).

Corrosion Analyses

Visual, light microscopic, and SEM analyses of the used coupon surfaces did not reveal any pitting.

Analysis of RCT system 304 SS Heat Exchanger Tubing

SEM and EDAX analyses were performed on the pit deposit in 304 stainless steel heat exchanger tubing obtained from another DuPont plant in Texas which had suffered similar problems (Figure 1, p.2). The deposit was primarily inorganic. Neither chlorine nor sulfur was detected in the pits.

Surface metallurgical heterogeneities are evident on unused samples of 304 stainless steel heat exchanger tubing used during

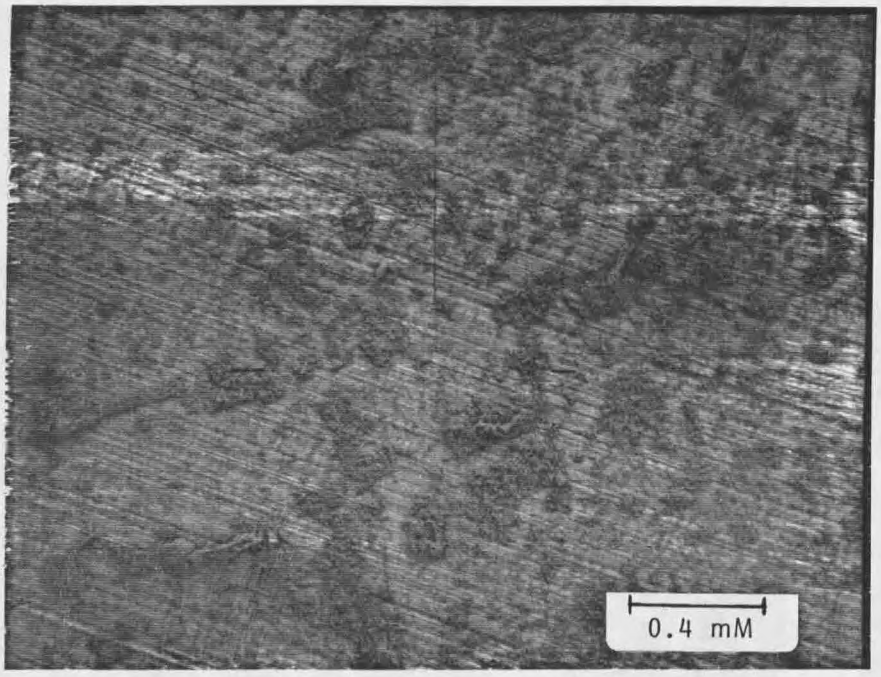

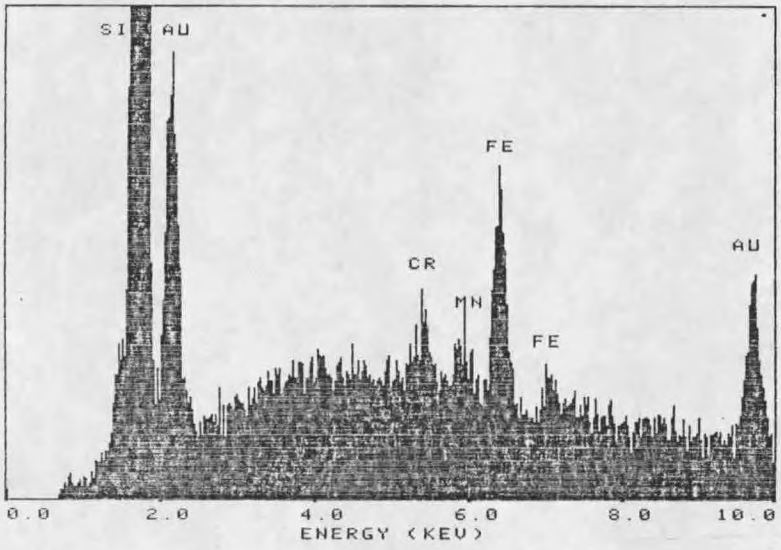

Figure 23. SEM of surface (x40) of a coupon which was in the RCT system make-up water system for 8 weeks. EDAX, performed on the whole surface shown in the micrograph, indicates the inorganic nature of deposits. See Figures 20 and 23 for physical and chemical similarity of results obtained from laboratory and field experiments.

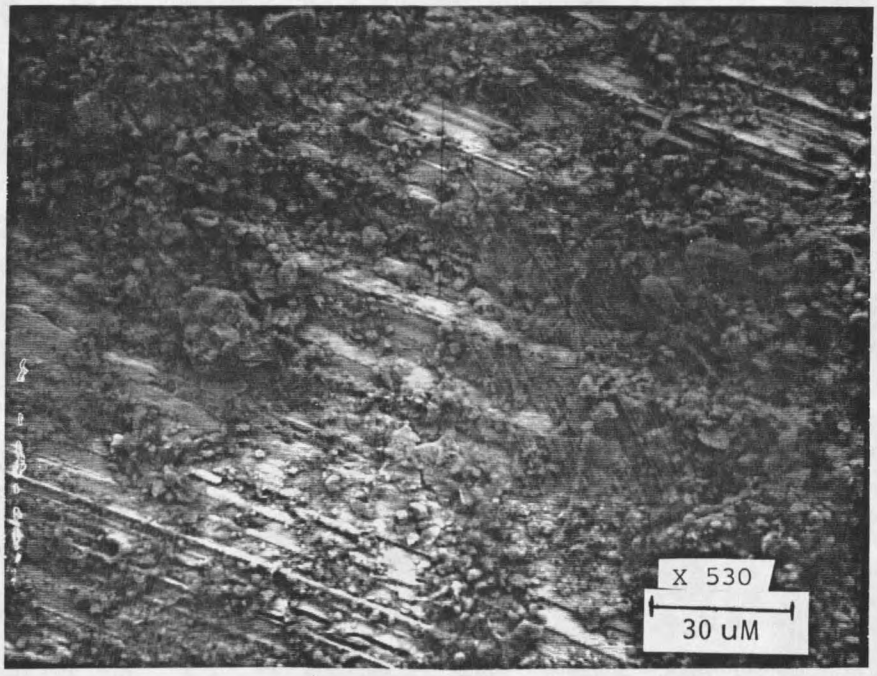

Figure 24. SEM of surface (x530) of a coupon which was in the RCT system make-up water system for 8 weeks.

corrosion failures in the RCT system (Figure 29). The heat exchanger tubing surface exhibits significantly more roughness (greater than 30 μm) as compared to the coupons (2-3 μm) used in laboratory experiments.

The EDAX analysis indicates localized spots of concentrated chromium and sulfur quantitatively higher than the rest of the base metal (Figure 30). X-ray dot map on the sample (Figure 31) indicates areas of high chromium and sulfur concentration overlapping at some spots, suggesting a chromium sulfide inclusion, as shown by dark spots (marked with arrow in Figure 29).

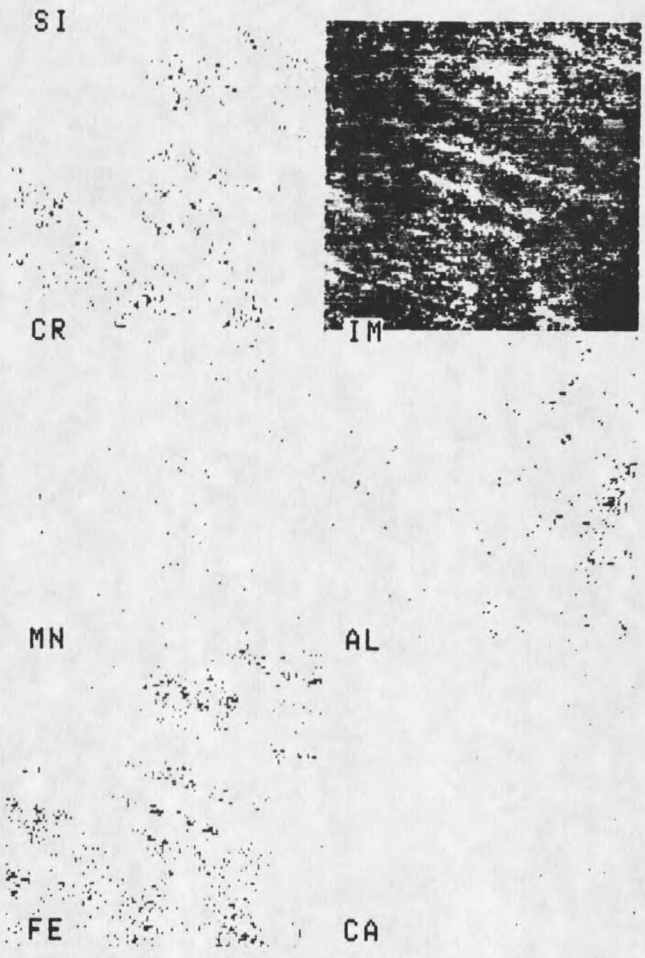

Figure 25. X-ray dot map of surface (x530) of a coupon which was in RCT system make-up water for 8 weeks. X-ray analysis, performed on the whole surface shown in Figure 26, highlights the absence of Fe/Mn, hypothesized to associated with corrosion phenomenon.

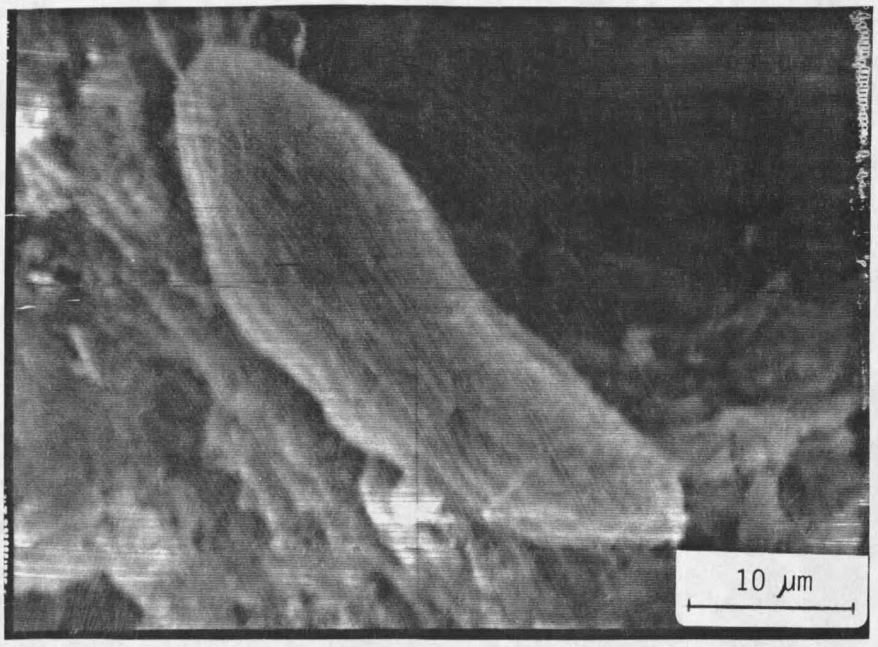

Figure 26. SEM of surface (x2000) of a coupon which was in the RCT system make-up water system for 8 weeks. The micrograph shows physical characteristics of a cell in biofilm on the coupon surface. Cell identification was not performed.

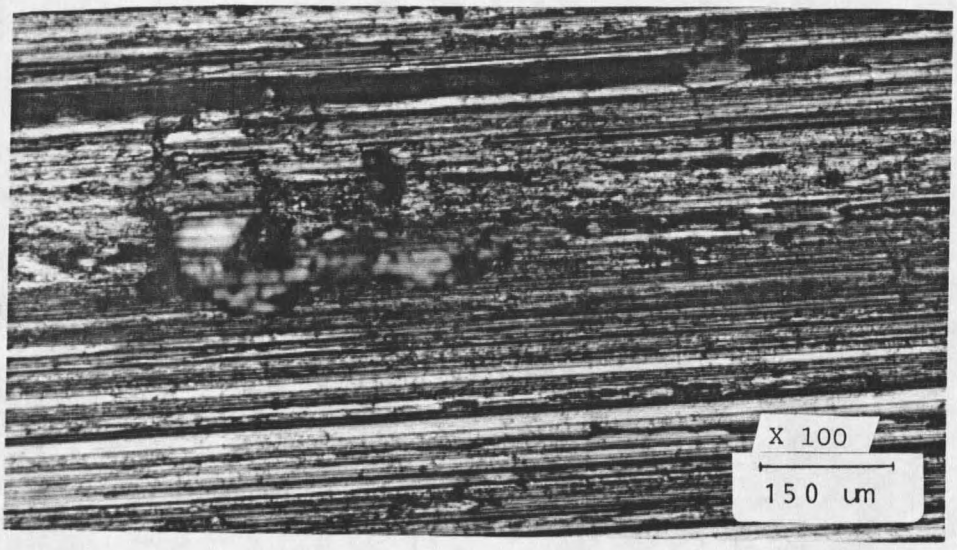

Figure 27. Photograph of a coupon surface (x100) after ultrasonic cleaning. The coupon which was in RCT system make-up water for 8 weeks. The photograph highlights the scratch lines on the surface, indicating absence of corrosion phenomenon.

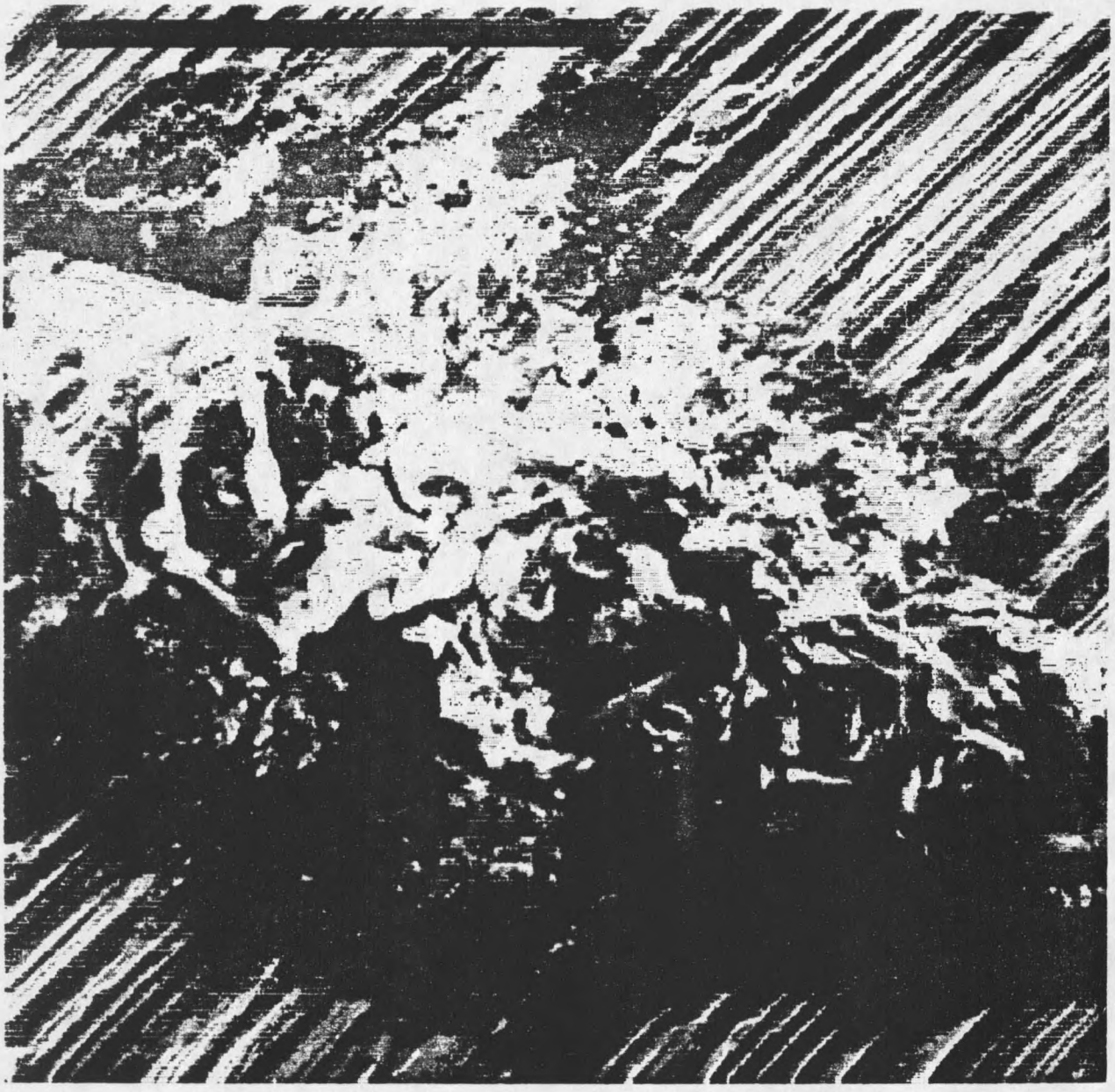

Figure 28. X-ray digitized image of non-conductive deposits on surface (x490).

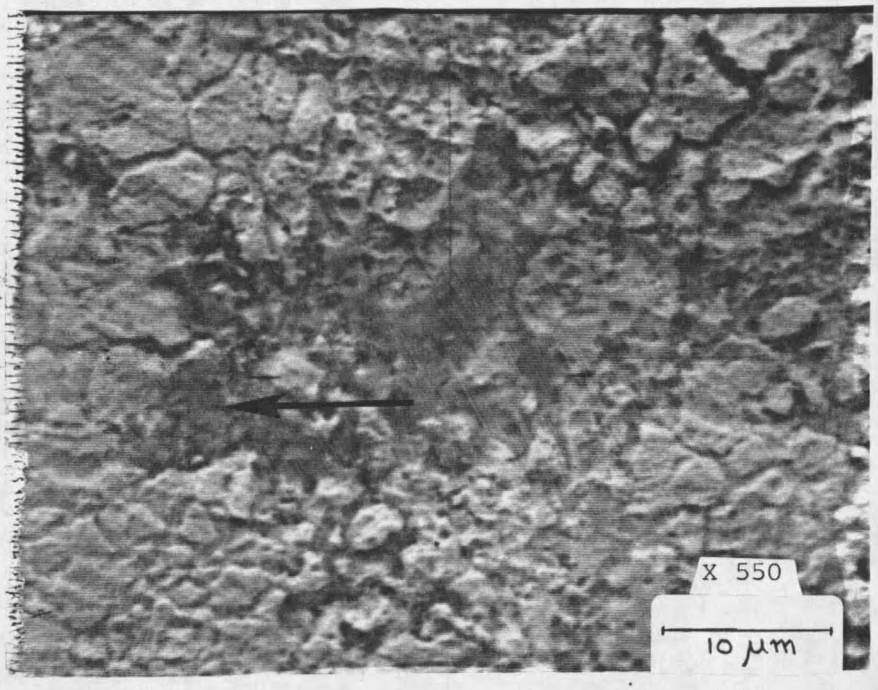

Figure 29. SEM of sulfide inclusions (x550) in the RCT system heat exchanger tubing. See Figure 32 for x-ray dot map of the region.

Statistical Analyses of Results

Analysis of deposits obtained from field tests on duplicate coupons permitted evaluation of variance (1) between coupons, (2) between sides of the same coupon, and (3) within the same coupon (i.e., patchiness phenomena).

Paired t-tests were used to compare differences between coupons. No statistically significant differences were found between coupons for dry mass, % volatile, TOC, HPC, GAB, and SRB on a per unit area basis. Thus, for obtaining representative samples of surface deposits single coupons may provide sufficient area. The

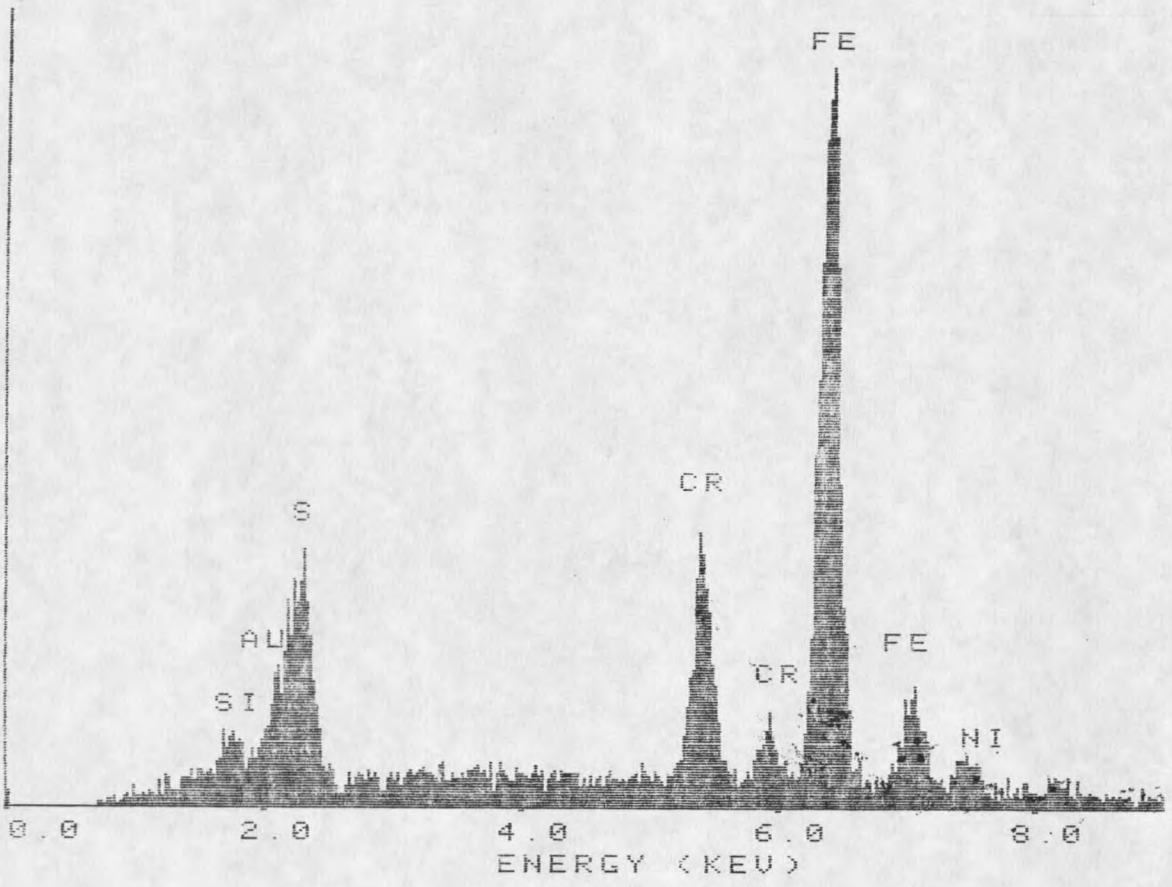

Figure 30. Energy Dispersive X-ray Analysis (EDAX) of sulfide inclusion (x550) in Methanol plant heat exchanger tubing.

area of each coupon was 1.3E-3 m^2. Paired t-tests showed that different sides of the same coupon do vary with respect to dry mass only. Differences did not appear with other variables.

Regression analysis (REGA) and analysis of variance (ANOVA) on

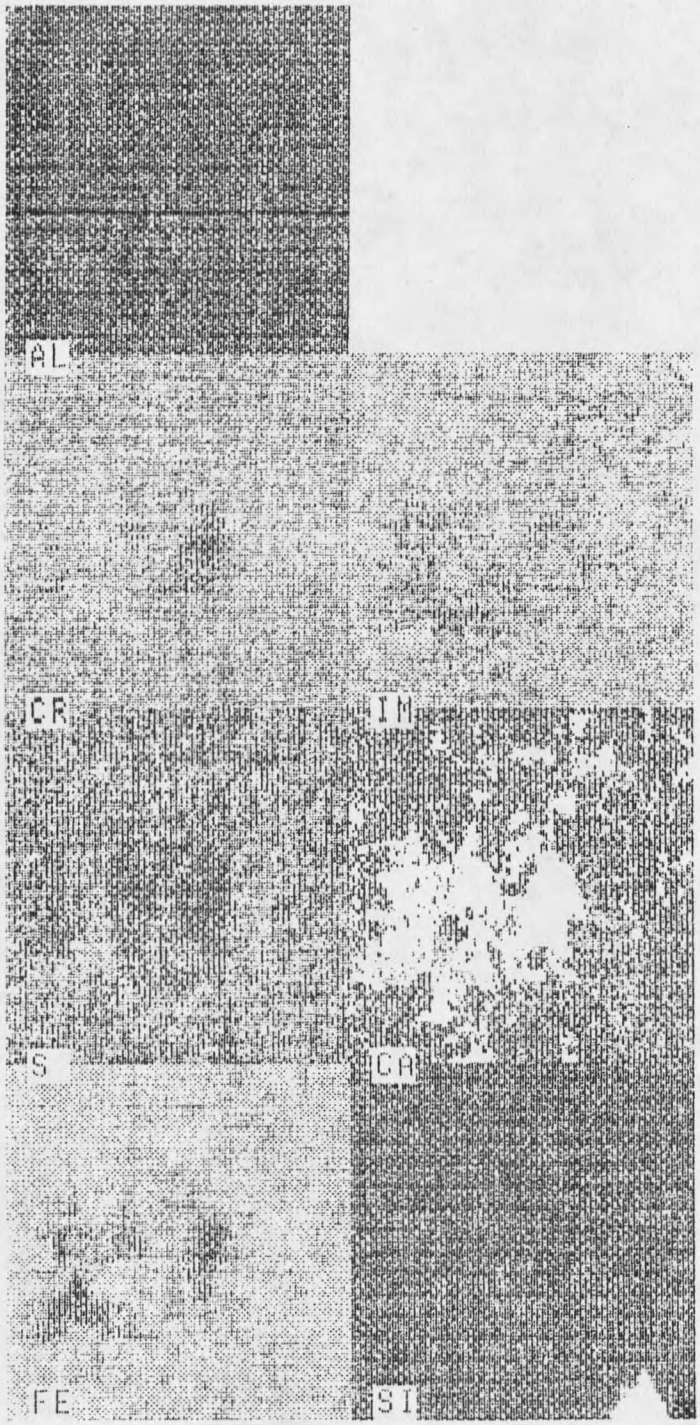

Figure 31. X-ray dot map of a sulfide inclusions (x2000) in RCT system heat exchanger tubing.

different sectors of the coupons indicated a third order, non-linear relationship between different variables analyzed, suggesting a random distribution of chemical and microbial deposits on coupon surfaces. The results do not support to the patchiness phenomenon hypothesis at the sector area level. However, there is a possibility of observing patchiness phenomenon at a smaller scale.

RCT System Modelling Results

The laboratory experiments were conducted with the make-up water shipped from the Methanol plant. However, the corrosion failures occurred in contact with the recirculating water, which is three to five times more concentrated than the make-up water. To study the effect of recirculating water on the RCT system, and to correlate the make-up water results with that obtained from recirculating water, a computer model of the RCT system was developed based on equations (1) to (10) described in Description of the Industrial System section. The equations describe the material balances in the Methanol plant RCT system. The following assumptions were included in the model:

1. The make-up water added to the system has a stable microbial and chemical concentration.
2. Detachment of cells from biofilm equals the rate of growth of cells in the biofilm.
3. Attachment of cells to the deposit surface is negligible. This assumption means that microbial growth was the dominant process leading to the accumulation of biofilm.

The model developed and the computer simulations performed

were used in (1) evaluating the effectiveness of laboratory experiments attempted, and (2) predicting the behavior of RCT system under different operating conditions (e.g., different dilution rate, biocide dosage, and varying retention time of the system).

The results obtained from computer simulation under field operating conditions (Figure 31) are similar to those obtained from

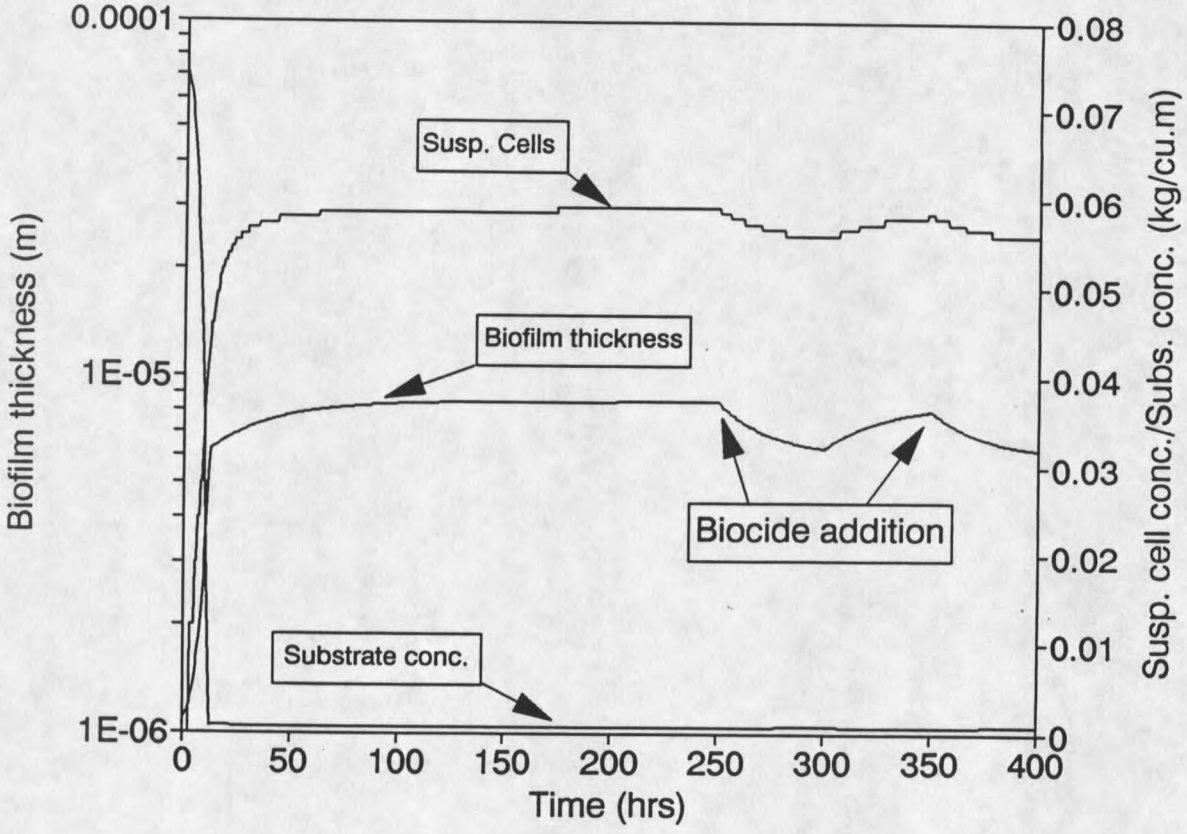

Figure 32. Prediction of suspended cell population, biofilm thickness and substrate consumption in the Methanol plant RCT system by computer simulation technique with make-up water as feed.

laboratory experiments. In both cases, the results show a growth of two orders of magnitude for suspended aerobic cells, and 25-30 μm thick biofilm. Chlorination was not a very effective method for controlling the microbial activity in the RCT system. Biofilm cells were less affected than planktonic cells by chlorination.

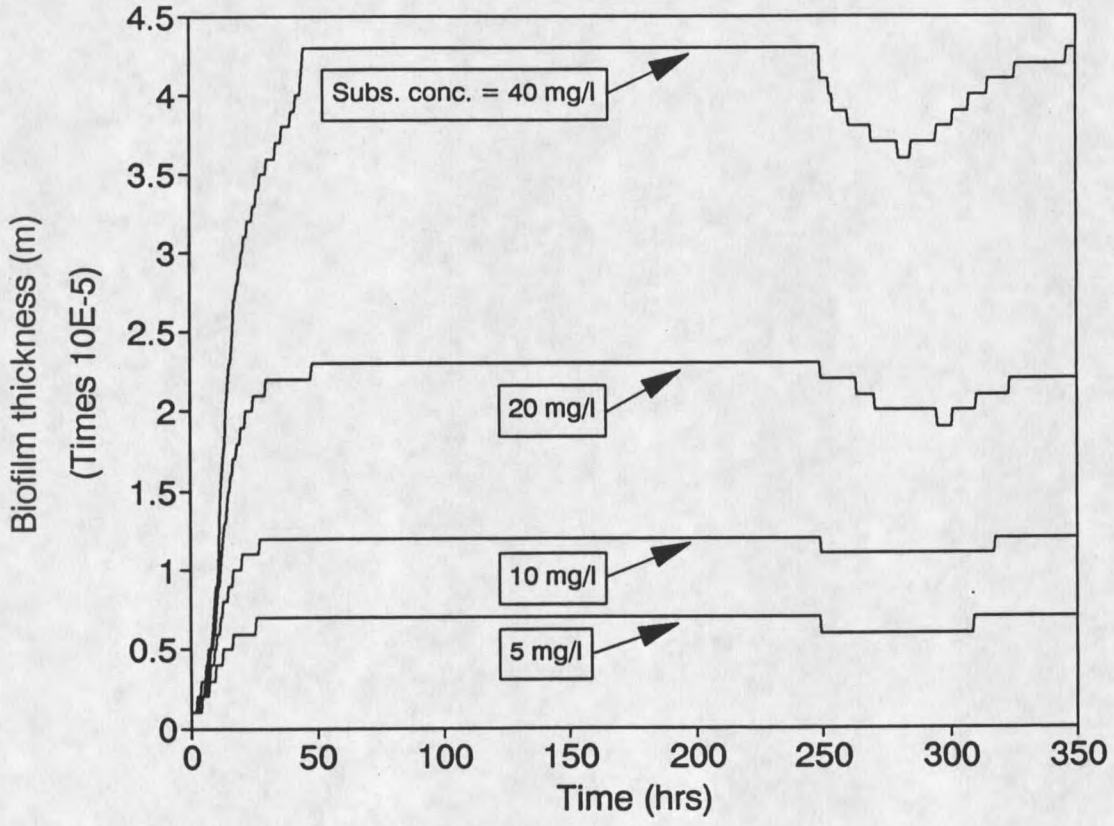

Figure 33. Computer simulation results for biofilm thickness versus time for different substrate concentrations.

Effect of Operating Variables on RCT System

Cycles of Concentration. Cycles of concentration in the RCT system are directly related to dilution rate in the laboratory experimental system. As described in earlier sections, increased dilution rate increased the deposit accumulation on coupons substantially. However, major constituents of the deposit were inorganic in nature. The suspended cell population increased by three orders of magnitude. The effect of increased dilution rate in the experimental system has been described in earlier sections (pp xx). Increasing the cycles of concentration in the RCT system had a similar effect (Table 16 and Figures 33 and 34). Change in cycles of concentration from 1 to 5 caused the suspended cell population to increase by two orders of magnitude (10^{12} to 10^{14} cells/m^3) and the biofilm thickness increased by approximately 25 μm.

Biocide Concentration. Increasing biocide concentration had a significant effect on the suspended cell concentration. Increasing the biocide concentration from 1.0E-2 to 3.0E-2 kg/m^3 increased the number of cells killed by a factor of 4 (Table 17 and Figures 35 and 36). However biofilm cells were not much affected by this increase.

Inlet Substrate Concentration. Increasing the substrate concentration also had a deteriorating effect on the system (Tables 18 and 19 and Figures 37 and 38). Increase in substrate concentration from 5E-3 to 4E-2 kg/m^3 increased the suspended cell population by more than two orders of magnitude (10^{12} to $5x10^{14}$ cells/m^3) and the biofilm thickness by 30 μm.

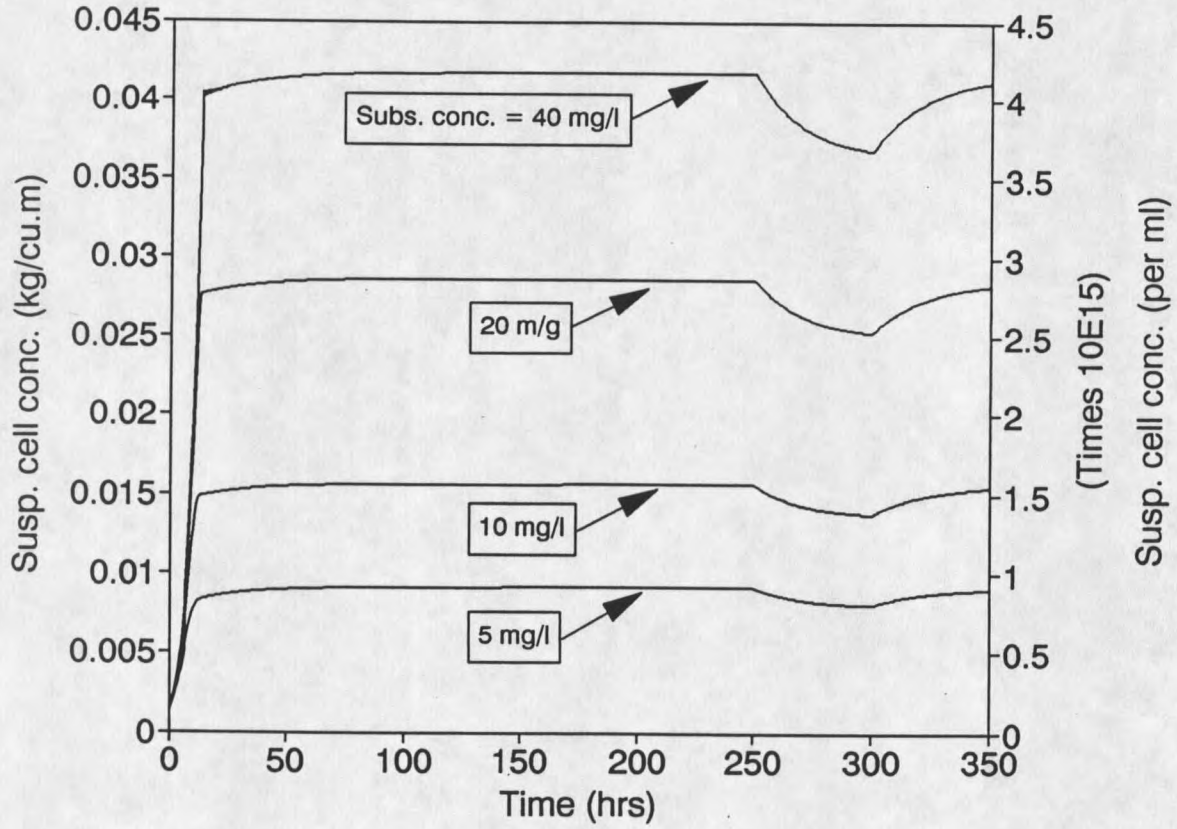

Figure 34. Computer simulation results for suspended cell concentration versus time for different substrate concentrations.

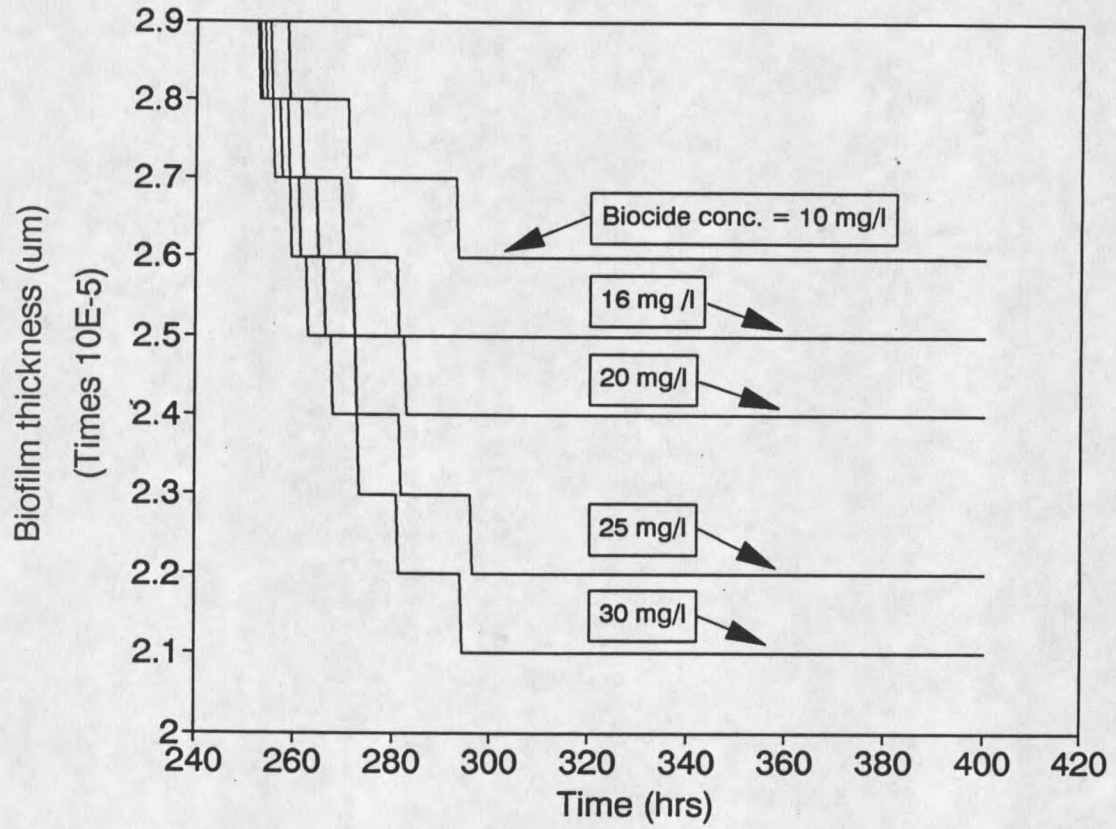

Figure 35. Computer simulation results for biofilm thickness versus time for different biocide concentrations.

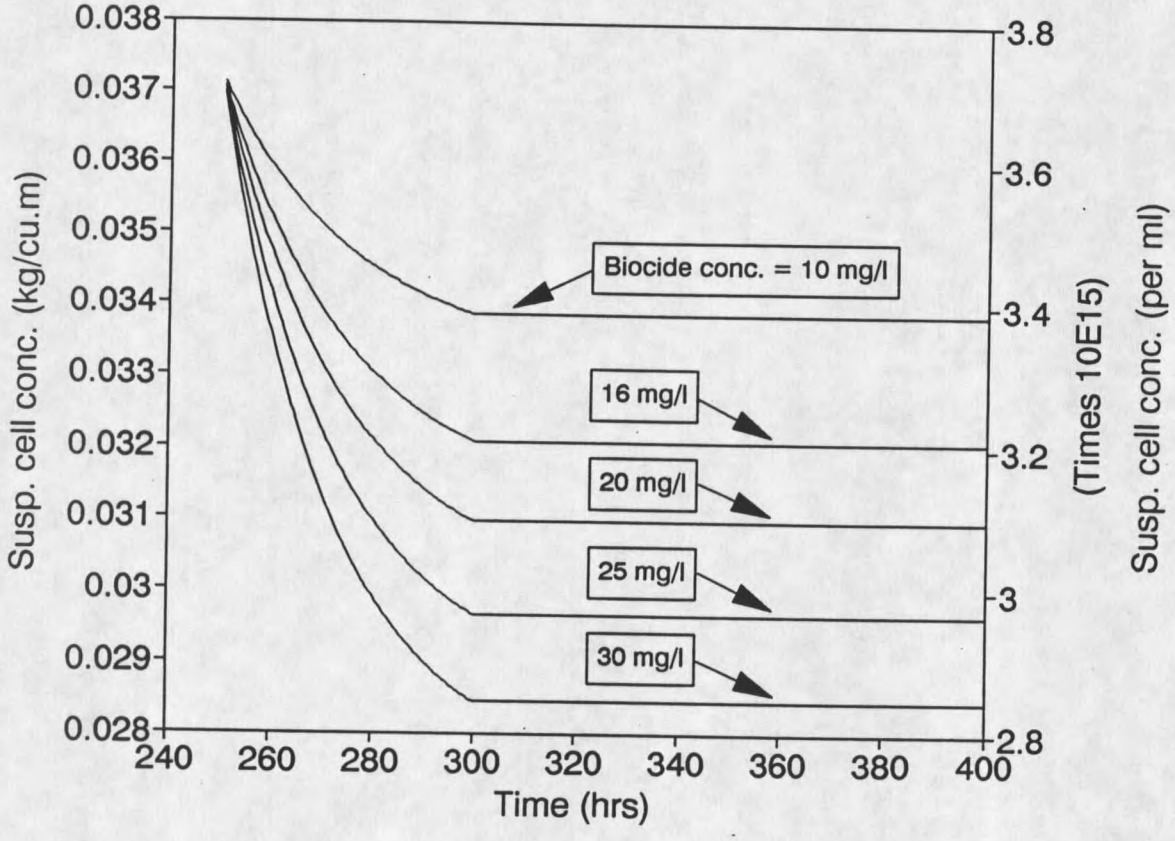

Figure 36. Computer simulation results for suspended cell concentration versus time for different biocide concentrations.

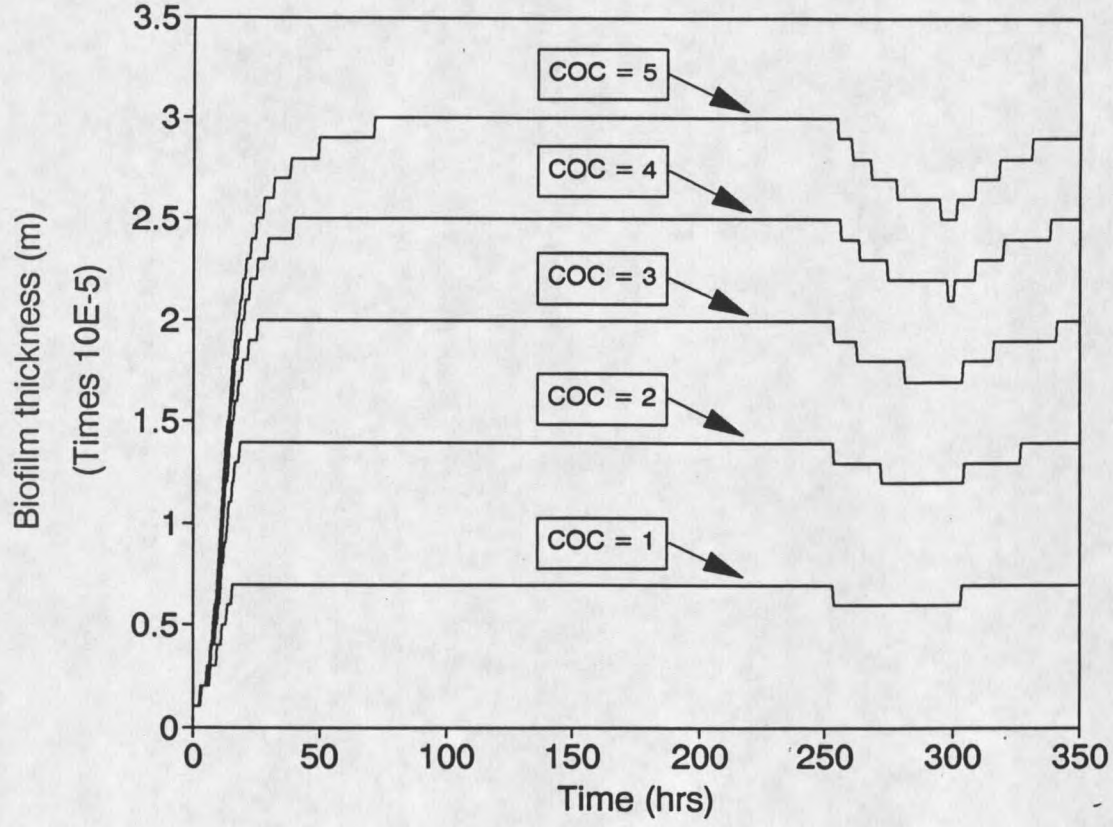

Figure 37. Computer simulation results for biofilm thickness versus time for different cycles of concentration.

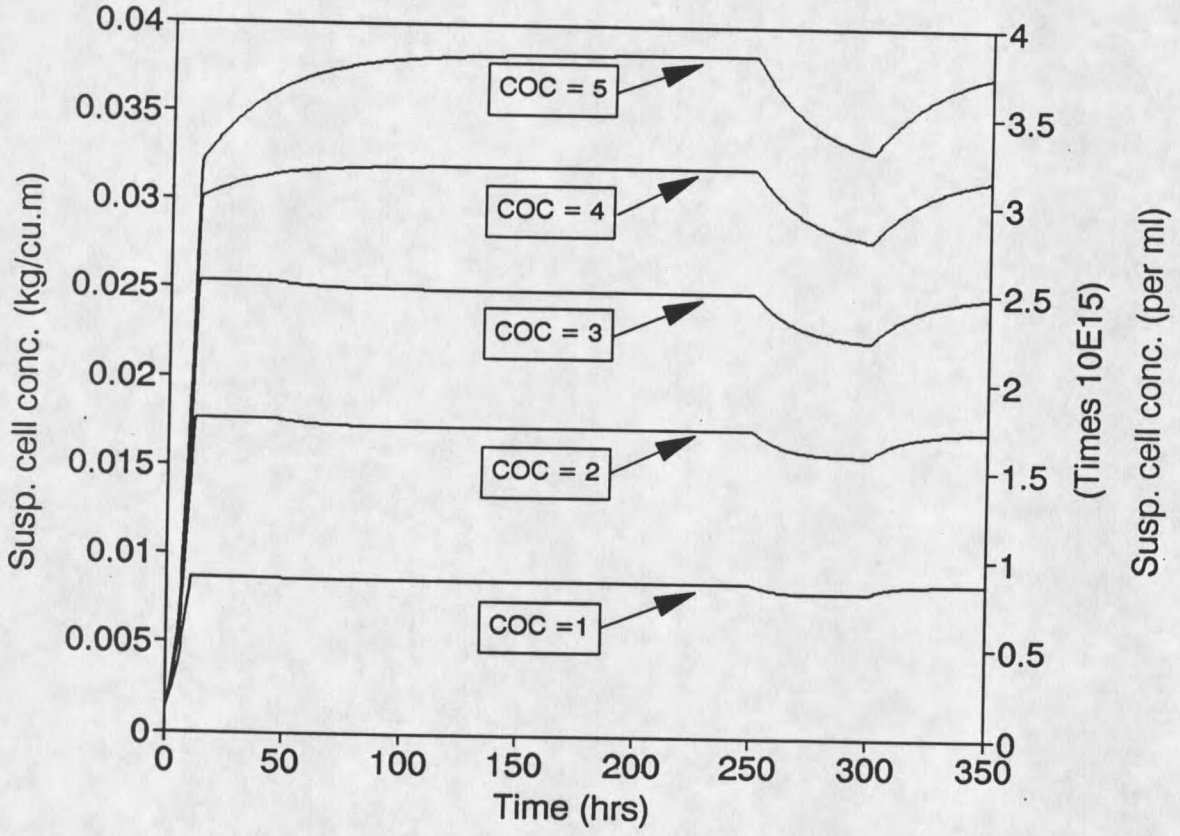

Figure 38. Computer simulation results for suspended cell concentration versus time for different cycles of concentration.

DISCUSSION OF RESULTS

Water Quality Results

Nitrogen and phosphorus, important nutrients for microbial growth in the make-up water, are rather low. Balanced microbial growth generally occurs for carbon-to-nitrogen (C/N) and carbon-to-phosphorus (C/P) ratios less than or equal to 6 and 60, respectively. If we presume that the TOC measured is all assimilable (AOC) and the only source is make-up water, then microbial growth in the system is nitrogen or phosphorus limited since $C/N \geq 10$ and $C/P \geq 120$. When the make-up water enters the cooling tower, TOC, N, and P are concentrated 2.5-5 times (cycles of concentration) making the water richer for microbial growth. Since organic carbon and nutrients also enter the RCT from other sources besides the make-up water, the calculated levels are to be considered minimum levels. Personal communication with plant operators indicates that methanol from process leaks is always present in the recirculating water. In addition, if any chemical additives (e.g., corrosion or scale inhibitor) contains assilimable nitrogen or phosphorus, then the microbial activity will be further enhanced.

Ammonia may also enter the recirculating water from the ammonia plant vapors when the wind direction is favorable. The ammonia can cause a significant spurt in microbial activity in the system (nitrification/denitrification). Observation of large deposits of insect remains in the basin solids suggests another source of OC and microbial nutrients.

There are enough microorganisms in the make-up water to

provide a significant inoculum for microbial growth in the recirculating water in the RCT system. Although no identification was done, microscopic examination indicates the absence of filamentous microorganisms (Fe/Mn utilizing and/or oxidizing bacteria). SRB are present in relatively low numbers, and will probably not play a major role since the system is well aerated. However, if organic loading increases, anaerobic biofilm layers will form and prominent SRB activity will be observed.

The high turbidity and color are presumed due to suspended solids (3E-2 to 5E-2 kg/m^3) and tannic or humic acid complexed with iron which are characterized by a dirty yellow appearance. Tannic and humic acid are relatively refractory to biodegradation so may not represent a high assimilable organic carbon (AOC). The suspended solids can enhance microbial fouling by settling on the condenser surfaces and providing sites for adsorption of cells. In such cases, the biofilm "thickness" may exceed 25-40 μm as predicted by computer simulations.

Laboratory Experiments Results

Chemical and Microbial Analyses

The sector analysis of the coupon surfaces permitted analysis of spatial distribution of chemical and microbial constituents of the deposits. The analysis indicated that the deposits were distributed randomly on the sectors of the coupon surfaces used for the experimental work. The area of the sectors however was not small enough to detect minor patchiness phenomena, if any.

Although dry mass, TOC and sessile microbial population on

coupon surface increased with increasing substrate loading rate, the differences were not significant to perturb the system. This indicates that increasing the substrate loading rate increases the loading rate of inorganic constituents, but does not affect the growth rate of microorganisms significantly.

SEM/EDAX Analysis

Laboratory experiments attempted with RCT system make-up and recirculating water indicated no evidence of pitting on 304 SS coupons.

SEM and EDAX analysis showed that the deposits were mainly composed of inorganic particulate material, especially Si and Al, which are the major constituents of suspended solids in natural flowing systems, and probably originated from the make-up water added to the RCT system. The rest of the peaks represent the base content of the alloy. Occasional Au peaks result from the gold sputtering required for some specimens.

Microscopic examination of the deposit patches did not indicate any conclusive evidence of filamentous (Fe/Mn utilizing and/or oxidizing) bacteria hypothesized by several persons as a possible cause of the corrosion failures. EDAX and x-ray dot mapping analyses failed to indicate localized concentrated spots of Iron (Fe) and/or Manganese (Mn) associated with these bacteria.

Deposits accumulated in make-up water and recirculating water contained no inorganic constituents in the bottom layer (in contact with the solid substratum). Sulfur, implicated in corrosion on stainless steel surfaces, was present only in the upper layers of the deposits. Thus, sulfur did not come in direct contact with the

base alloy. The bottom layer probably consisted of cells and EPS and may have prevented initiation of corrosion. Mn, another element hypothesized to influence corrosion of stainless steel surfaces, was not present in the deposit.

Absence of SRB in RCT make-up water indicates that the Methanol plant RCT system was well aerated, as expected. Thus SRB, hypothesized to be a major cause in the failure of stainless steel surfaces, could not produce conditions conducive to initiate pitting corrosion in the system although there is no conclusive evidence of the absence of anaerobic conditions at the deposit-substratum interface.

Chlorine, used as a biocide, did not prove effective in controlling sessile bacterial populations. Though the reactors treated with chlorine did not show many planktonic cells in the effluent stream during chlorine addition period, coupons analyzed for sessile bacteria from those reactors showed results similar to those from non-chlorinated reactors. This behavior is in agreement with other studies done in similar industrial water systems (Marshall and Walker, 1990).

Field Experiment Results

The recirculating cooling water at the Methanol plant RCT system could not be used for laboratory experiments because it was receiving a high dosage biocide treatment which prevented "typical" microbial growth in the laboratory system. Thus, make-up water was the only water suitable for laboratory experiments. Parallel field tests were conducted in the make-up water line of the Methanol plant

RCT system to determine if the laboratory experiments mimicked the real system, i.e., the make-up water of the RCT.

Chemical and microbial analyses of coupons installed in the RCT system make-up water well indicated results similar to those obtained from laboratory experiments. Dry mass was slightly higher compared to that obtained in laboratory experiments (Tables 6 and 8) which could be attributed to higher suspended solids concentration in the make-up water as compared to that in laboratory experiment. Sessile bacterial counts were similar to those obtained in laboratory experiment (Tables 7 and 9).

SEM and EDAX analyses did not indicate any evidence of SRB or filamentous bacteria in deposit. Also, no pitting was observed on the coupon surfaces. The detailed examination of deposit and surface beneath the deposit merely reproduced results obtained in the laboratory experiment.

The coupons were installed in the make-up water well and not in recirculating water line where the corrosion failures occurred. Recirculating water is concentrated 2.5-5 times the make-up water. Presence of more dissolved and suspended particulate material, especially microbial nutrients, could have had an accelerating affect on the growth of biofilm, scale deposition, and possibly the corrosion phenomena.

The results obtained from the coupons installed in the make-up water line supported those obtained from laboratory experiments with similar water. Thus laboratory experiments can provide an effective tool for analyzing and solving biofouling and biocorrosion problems in complex industrial systems.

RCT System Modelling Results

The results obtained from computer simulations echo those obtained from laboratory and field experiments. Computer simulation indicate limited microbial growth under present operating conditions. Planktonic cells show an increase of two orders of magnitude (10^{12} to 10^{14} cells/m^3), while a 25-30 μm biofilm develops on the surfaces of the RCT system.

However, increased substrate (energy source for bacteria) concentration has a significant effect on planktonic and sessile microbial population in the system. Increased substrate concentration also makes the system less susceptible to chlorination. Thus, biofouling and other related phenomena increase in rate and extent. At the time of the corrosion failures, the make-up water added to the system might have had a higher dissolved concentration of microbial nutrients. The computer simulations indicate that, at the time of failures, the microbial activity in the system was out of control and might have contributed towards the corrosion phenomenon.

Increasing the cycles of concentration has a similar effect on the microbial population in the RCT system. However, increased cycles of concentration also means increased inorganic scaling potential and an increased accumulation of other corrosive material in the system. This could result in an initiation and/or enhancement of other types of corrosion phenomena.

Increasing biocide dosage did not produce any significant changes in the sessile microbial population in the RCT system. Consequently, increased biocide dosage will probably only produce

additional free chloride ions in the system, which may contribute to increased stainless steel corrosion.

Analyses of Coupon and Tubing Metal Surface

Microscopic and SEM analyses of 304 stainless steel coupons used in the laboratory experiments indicate metallurgical heterogeneities (manufacturing defects) on the metal surface but no defects in chemical composition (inclusions) of the alloy. The surface roughness of laboratory coupons was approximately 2-3 μm, an order of magnitude less than the standard industrial finish (30-50 μm) specified by ASME for industrial stainless steel tubing surfaces. Roughness can influence the settling of suspended solids on the alloy surface. The rougher surface will have a greater tendency to accumulate particles, in part due to the following reasons: (1) increased convective mass transport near the substratum, (2) more surface area for adsorption, and (3) protection from shear forces for cells, resulting in lower desorption rates (Characklis and Marshall, 1989).

On the other hand, SEM and EDAX analysis of 304 stainless steel heat exchanger tubing from RCT system revealed localized concentrated spots of chromium and sulfur, indicating chromium sulfide inclusions. According to published literature, chromium sulfide inclusions are not uncommon in low manganese stainless steels. The sulfide inclusions, in chloride environments, have been hypothesized to be the initiation sites for pitting corrosion (Wranglen, 1973) (Figures 39-41). According to this theory, chlorine added to the system reacts with water producing hypochlorous acid

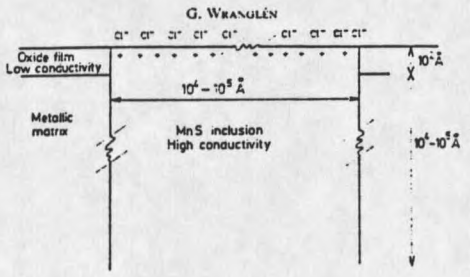

Figure 39. Schematic illustration of MnS inclusion in SS, showing dimensions. Preferential adsorption of chloride ions occurs on the sulfide inclusion due to its higher electron conductivity, giving stronger electrostatic image forces than on the surrounding oxide film.

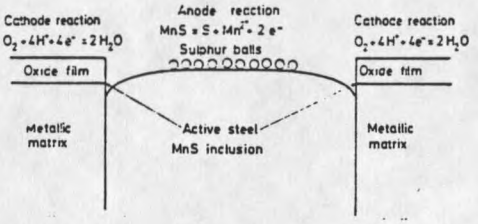

Figure 40. First stage of initiation of pitting on SS: dissolution of the sulfide inclusion under the separation of elementary sulfur and the exposure of active, not oxide-coated steel along the periphery.

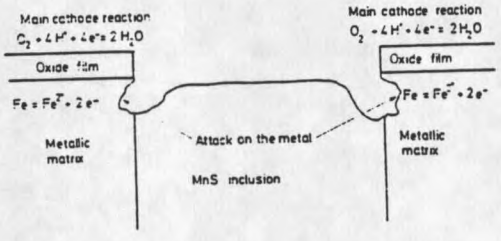

Figure 41. Continued anodic attack on sulfide inclusion in SS under oxidation to H_2SO_3 and H_2SO_4, which cause chemical dissolution of the sulfide. Incipient attack on the metal close to the inclusion.

(HOCl) and chloride ions. The chloride ions formed are preferentially adsorbed on sulfide inclusions. The adsorbed chloride ion provides a stronger electrostatic charge at the adsorbed sites than on the surrounding oxide film. The preferentially adsorbed chloride ions facilitate the anodic dissolution of sulfide inclusions, oxidizing them to primary sulfur:

$$CrS = Cr^{3+} + S + 3e^-$$

$$O_2 + 4H^+ + 4e^- = 2H_2O$$

$$Cr^{3+} + H_2O = H^+ + CrOH^{2+}$$

The overall reaction is as follows:

$$CrS + 4H_2O = Cr^{2+} + SO_4^{2-} + 8H^+ + 8e^-$$

The attack is aggravated by low pH conditions, causing dissolution of metal ions. Oxidation of sulfide inclusions to sulfurous and sulfuric acid carries the attack forward until all sulfide from the inclusion is removed, leaving a pit behind.

The reports describing the failures in the RCT system indicate high concentration of chloride ions in pit deposits. One initial hypothesis implicated filamentous microorganisms in the formation of concentrated Fe/Mn-chloride deposits but this does not seem probable based on available evidence.

Chlorine added to the system as a biocide, possibly in excess of system demand, produced chloride ions in the system. The free chloride ions would have been transported to the tubing surface, where they may have reacted with sulfide inclusions resulting in pit corrosion. Presence of microbiological slime might have helped in entrapment and transportation of chloride ions to the tubing surface, thus aggravating the corrosion attack. The microbial slime

may have also reduced local pH depending on biodegradable OC in the system.

SUMMARY

The purpose of this study was to investigate microbially influenced corrosion (MIC) of stainless steel 304 heat exchanger tubing in an open, recirculating, cooling tower system of a methanol plant.

The recirculating cooling water presently in the RCT could not be used for laboratory experimentation because it was receiving a high dosage biocide treatment. To determine if the laboratory experiments simulated the biofilm accumulation in the RCT, field experiments were conducted by immersing corrosion coupons, identical to those in the laboratory experiments, in the make-up water line of the RCT. The rate of deposit accumulation and deposit composition in the laboratory and field make-up water experiments compared exceptionally well.

Observable pitting corrosion did not occur in the laboratory or field experiments. Possible reasons for these observations are as follows: (1) corrosion coupons and heat exchanger tubing are significantly different in terms of physical and chemical characteristics, (2) the recirculating water could not be simulated accurately because no data was available on its nutrient status or biocide treatment (i.e., dosage) during the failures, and (3) make-up water available to this project was not the same source water used during the corrosion failures.

Recommendations for Further Work

Additional research is necessary before real cause or corrosion can be determined. The research should focus on the following:

1. Influence of fluid velocity in heat exchange tubes must be determined. Low fluid velocity increases the net rate of accumulation of fouling deposit. Presently, fluid velocity in the heat exchange tubes is 8-10 fps in summer and approximately 5 fps in winter when cooler water is available. During the corrosion failures, fluid velocity was approximately 3-5 fps. In addition, the failures are also related to "downtime" when the tubes were "laid up" wet.
2. Coupons exhibit considerably less roughness (3-5 μm) than heat exchange tubing (>30 μm). Greater surface roughness presents a suitable environment for settling inorganic solids, microorganisms, or other particulate material. Thus, fouling deposit accumulation in the heat exchange tubing would be faster than on corrosion coupons.
3. The corrosion coupons contained no visible inclusions while the heat exchange tubing did. Inclusions are known to accelarate pitting corrosion of stainless steels, especially in the presence of high chloride concentration. Biofilm or other deposits could influence the transport of ferrous chloride salts out of the inclusion areas thus accelerating pitting corrosion initiated at the inclusion sites.
4. There is no indication of organic carbon (OC) content of recirculating water during failures. The only available data

is from laboratory analyses of make-up water during period of the laboratory research. Recirculating OC can be calculated from make-up water OC and the cycles of concentration if no other sources of OC are available. However, personal communications with plant operators indicate that methanol from process leaks is always present in the recirculating water.

5. There is no indication of the biocide dosage during the corrosion failures. In addition, a bromine biocide (Bromicide) was introduced prior to the failures. Bromicide enters the water in colloidal form or, in unusual cases, enters in the form of larger particulates. There is some indication that solid Bromicide accumulated in RCT areas of low flow. At low flows, solids may have also accumulated in the heat exchanger tubes as well.

6. There is no indication of the dosage of other treatment chemicals during the failures which may have added nutrients (e.g., nitrogen and/or phosphorus) necessary for microbial growth.

LITERATURE CITED

LITERATURE CITED

Agrawal, V., R.S. Cahoon, and W.G. Characklis (1989), Analysis of 304 Stainless Steel Tubing, A Report, Montana State University, Bozeman.

Agrawal, V., R.S. Cahoon, and W.G. Characklis (1990), Montana State University, Bozeman.

Annual Book of ASTM Standards (1984), G46-76, G1-81, G16-71, G4-68, ASTM.

Bailey, J.E. and D.F. Ollis (1986), 2 nd edition, Biochemical Engineering Fundamentals.

Booth, G. (1971), Microbiological Corrosion, Mills and Boon, London, England.

Cahoon, R.S., W.G. Characklis, and V. Agrawal (1989), Investigation of Microbially Influenced Corrosion of Condenser Tubing in the Methanol Plant at Beaumont Works, A Report, Montana State University, Bozeman.

Castleberry, J.R. (1969), Trends in Cooling Tower Construction. Material Protection, 8(3), p.67-70.

Characklis W.G. (1980), Biofilm Development and Destruction. Electric Power Res. Inst., RP912-1, Palo Alto, CA.

Characklis, W.G. and K.C. Marshall (1990), (ed.), Biofilms, A Wiley Interscience Publication.

Cooling Water Treatment Manual (1981), NACE Publications.

Costerton J.W., G.G. Geesey, and P.A. Jones (1987), Bacterial Biofilms in Relation to Internal Corrosion Monitoring and Biocide Strategies. Corrosion/87, Paper 54.

Fontana, M.G. and N.D. Greene (1978), 2 nd edition, Corrosion Engineering.

Fontana, M.G. and R.W. Staehle (1972), Advances in Corrosion Science and Technology, Vol.2.

Hobbie J.G., R.J. Daley, and S. Jasper (1977), . Applied and Environmental Microbiology, Vol.33, p.1225.

Kelly, B.J. (1965), Microorganisms in Hydrocarbon Contaminated Cooling Water System. Material Protection, 4(7), p.62-67.

Kobrin, G. (1999), . Material Protection, Vol.15, No.7, p.38.

Kodama, J. and J.R. Ambrose (1977), Effect of Molybdate Ion on the Repassivation Kinetics of Iron in Solutions Containing Chloride

Ions. Corrosion, Vol.33, No.5, May 1977.

Lee, W. (1990), Corrosion of Mild Steel under an Anaerobic Biofilm, A Ph.D Thesis, Chemistry Department, Montana State University, Bozeman.

McCoy, J.W. (1974), The Chemical Treatment of Cooling Tower.

Metals Handbook (1972), Vol.7, 8 th edition.

Miller, J.D.A. (1981), Metals. In: Rose A.H. (ed.), Microbial Biodeterioration, Academic press. New York.

Mittleman, M.W. and G.G. Geesey (1987), Biological Fouling of Industrial Waste Systems: A problem Solving Approach.

Norman, G., W.G. Characklis, and J.D. Bryers (1977), Control of Microbial Fouling in Circular Tubes with Chlorine. Dev. Ind. Microbiol. 18: 581-590.

Park, J.Y. and S. Danyluk (1977), An Intergranular Fracture Technique for Grain Boundary Segregation Studies of Austenitic Stainless Steel. Corrosion, Vol.33, No.8, August 1977.

Pope, D.H., R.J. Soracco, and E.W. Wilde (1982), Studies on Biologically Induced Corrosion in Heat Exchanger Systems at Savannah River Plant, Aiken, SC. Corrosion/82, Paper 24.

Puckorius, P.R. (1983), Massive Utility Condenser Failure Caused by Sulfide Producing Bacteria. Corrosion/83, Paper 248.

Snoeyink, V.L. and D. Jenkins (1980), Water Chemistry.

Source Book on Stainless Steel (1977), American Society of Metals.

Standard Methods for the Examination of Water and Wastewater (1981), 15 th edition, Washington, American Public Health Association.

Stoeker J.G. (1983), Guide for the Investigation of Microbiologically Induced Corrosion. Corrosion/83, Paper 245.

Tatnall R.E. (1981), Fundamentals of Bacteria Induced Corrosion. Corrosion/81, Paper 129.

Tatnall R.E. (1981), Case Histories: Bacteria Induced Corrosion. Corrosion/81, Paper 130.

Uhlig, H.H. (1962), Corrosion and Corrosion Control.

Ventura, G., E. Traverso, and A. Mollica (1999), Effect of NaClO Biocide Addition in Natural Sea Water on Stainless Steel Corrosion Resistance.

Videla, H.A. (1986), Mechanism of MIC. Proceedings of Argentina-USA Workshop on Biodeterioration (CONICET-NSF).
Videla H.A. (ed.), Published by Aquatec Quimica S.A., Sao Paulo,

Brasil.

Wranglen, G. (1972), An Introduction to Corrosion and Protection of Metals, A John Wiley & Sons, Inc., Publications.

Wranglen, G. (1973), Pitting and Sulfide Inclusions in Steels, J. Corrosion Science

APPENDICES

APPENDIX A

RCT SYSTEM MAKE-UP WATER QUALITY ANALYSIS

APPENDIX A

RCT SYSTEM MAKE-UP WATER QUALITY ANALYSIS

Table 3. Raw water quality data: Sample description and physical analyses

Sample #	Source	pH	TSS (kgm^{-3})	VSS (kgm^{-3})	Conductivity
1	PNR	5.55	4.39E-2	9.2E-3	NMD
2	LNVA	5.70	3.15E-2	8.4E-3	NMD
3	LNVA	7.20	5.33E-2	9.5E-3	160
4	LNVA	6.35	4.67E-2	8.7E-3	150
5	LNVA	6.79	4.33E-2	9.7E-3	150
6	LNVA	6.28	4.33E-2	8.2E-3	150
7	LNVA	6.50	3.50E-2	7.9E-3	80
8	LNVA	6.31	3.55E-2	8.5E-3	60
9	LNVA	6.22	4.78E-2	9.1E-3	130
10	LNVA	6.50	4.56E-2	9.0E-3	140
Average		6.34	4.26E-2	8.8E-3	128
S.D.		0.48	6.70	6.0E-4	37

Table 4. Raw water quality data: chemical analyses

		kgm^{-3}							
No.	TOC	P*	Fe	Mn*	TKN*	NO_3-N	NH_4-N*	Ca	Mg
1	14.7	NMD	NMD	NMD	NMD	NMD	NMD	NMD	NMD
2	13.5	NMD	NMD	NMD	NMD	NMD	NMD	NMD	NMD
3	15.0	0.1	1.5	.05	1.0	0.2	NMD	NMD	NMD
4	13.0	0.1	1.6	.05	1.0	0.3	NMD	NMD	NMD
5	12.7	0.1	2.0	.05	1.0	0.3	NMD	NMD	NMD
6	12.5	0.1	1.5	.05	1.0	0.3	NMD	NMD	NMD
7	14.0	0.1	1.4	.05	NMD	NMD	0.1	4.6	1.1
8	12.0	0.1	1.1	.05	NMD	NMD	0.1	6.3	1.2
9	13.5	0.1	1.5	.05	NMD	NMD	0.1	7.2	2.3
10	13.0	0.1	1.3	.05	NMD	NMD	0.1	7.0	2.4
Avg	13.4	0.1	1.5	.05	1.0	0.3	0.1	6.3	1.8
S.D.	0.90	0.0	0.26	0.0	0.0	0.05	0.0	1.2	0.7

Table 5. Raw water quality data: microbial analyses

Sample #	per m^3			
	HPC	GAB	SRB	TCC
1	5.2E10	2.4E10	1.1E8	3.8E13
2	5.3E10	2.6E10	1.2E8	3.0E13

APPENDIX B

EXPERIMENTAL DATA

APPENDIX B

EXPERIMENTAL DATA

Table 6. Coupon biofilm chemical analysis: Laboratory system with recirculating water strength bulk reactor media

	kg/m²				
No.	TOC	Dry mass	Volatile	% volatile	% TOC
Blank	-----	4E-6	4E-6	100.0	5.92
Week 6					
Sct 1	1.04E-4	2.79E-3	2.48E-3	89.2	3.76
Sct 2	2E-5	8.1E-4	6.3E-4	78.0	2.98
Sct 3	3E-5	9.3E-4	5.9E-4	63.5	3.12
Sct 4	1E-5	4.6E-4	3.1E-4	67.1	1.91
Sct 5	2.6E-5	8.9E-4	6.4E-4	72.3	2.87
Sct 6	1.7E-5	9.4E-4	7.1E-4	76.27	1.78
Avg	3.4E-5	1.14E-3	8.9E-4	74.39	2.74
S.D.	3.2E-5	7.57E-4	7.2E-4	8.29	0.69
Week 12					
Sct 1	3.6E-4	6.60E-3	4.13E-3	62.58	5.46
Sct 2	9E-5	2.0E-3	1.31E-3	65.50	4.33
Sct 3	8E-5	1.37E-3	1.05E-3	76.64	5.70
Sct 4	5E-5	1.16E-3	0.87E-3	75.0	4.21
Sct 5	1.1E-4	4.11E-3	3.15E-3	76.64	2.57
Sct 6	8E-5	2.43E-3	1.63E-3	67.08	3.12
Sct 7	7E-5	2.77E-3	2.18E-3	78.7	2.65
Sct 8	4E-5	1.20E-3	1.02E-3	85.0	3.39
Sct 9	7E-5	1.83E-3	1.43E-3	78.14	3.75
Sct 10	1.4E-4	2.35E-3	1.79E-3	76.17	5.81
Sct 11	3E-5	0.73E-3	0.59E-3	80.82	4.37
Sct 12	3E-5	0.51E-3	0.23E-3	45.1	4.86
Avg	9.6E-5	2.26E-3	1.61E-3	72.28	4.19
S.D.	8.5E-2	1.62E-3	1.06E-3	10.32	1.08

Table 7. Coupon biofilm microbial analysis: Laboratory System with recirculating water strength bulk reactor media

	per m^2			
Sample #	GAB	SRB	HPC	TCC
Blank	3.5E7	NDT	1.570E6	NSV
Week 6				
Sct 1	1.882E6	NDT	5.490E7	NSV
Sct 2	1.882E6	NDT	5.490E7	NSV
Sct 3	3.373E6	NDT	2.353E8	NSV
Sct 4	2.352E6	6.27E4	5.490E7	NSV
Sct 5	1.882E6	NDT	1.569E8	NSV
Sct 6	3.373E6	6.27E4	1.569E8	NSV
Average	2.457E6	2.09E4	1.190E8	
S.D.	0.668E6	2.96E4	6.919E7	
Week 12				
Sct 1	1.6E8	NDT	4.706E8	NSV
Sct 2	1.6E8	6.27E4	4.706E8	NSV
Sct 3	1.6E8	NDT	7.056E8	NSV
Sct 4	1.6E8	NDT	6.275E8	NSV
Sct 5	1.6E8	NDT	5.490E9	NSV
Sct 6	1.6E8	NDT	1.569E8	NSV
Sct 7	1.6E8	6.27E4	6.275E9	NSV
Sct 8	1.6E8	NDT	2.353E8	NSV
Sct 9	1.6E8	NDT	5.490E7	NSV
Sct 10	1.6E8	NDT	1.020E9	NSV
Sct 11	1.6E8	NDT	2.745E9	NSV
Sct 12	1.6E8	6.27E4	1.569E9	NSV
Average	1.6E8	1.57E4	1.205E9	---
S.D.	0.0	2.72E4	1.683E9	---

Table 8. Biofilm chemical analysis: RCT system

		kg/m² (x 1E-3)			
No.	TOC	Dry mass	Volatile	% volatile	% TOC
Blank	0.15	2.80	0.96	34.28	5.36
Sct 1	0.26	8.40	6.10	72.61	3.10
Sct 2	0.24	8.30	5.50	66.27	2.89
Sct 3	0.27	7.30	5.80	79.45	3.70
Sct 4	0.25	9.60	5.40	56.25	2.61
Sct 5	0.21	9.00	5.30	58.89	2.33
Sct 6	0.23	9.70	6.20	63.92	2.37
Sct 7	0.26	8.20	6.90	84.15	3.17
Sct 8	0.21	12.1	10.2	84.29	1.74
Sct 9	0.35	18.9	7.40	39.15	1.85
Sct 10	0.32	19.9	18.6	93.47	1.61
Sct 11	0.25	8.20	6.20	75.60	3.05
Sct 12	0.34	10.1	6.40	63.36	3.37
Sct 13	0.32	12.8	6.40	50.0	2.50
Sct 14	0.45	12.0	6.20	51.67	3.75
Sct 15	0.26	11.6	6.20	53.45	2.24
Avg	0.28	11.1	7.25	66.17	2.68
S.D.	0.06	3.60	3.24	14.68	0.01

Table 9. Biofilm microbial analysis: RCT system

	per m^2			
Sample #	GAB	SRB	HPC	TCC
Blank	6.745E5	NDT	1.570E6	NSV
Sct 1	2.352E6	NDT	4.706E8	NSV
Sct 2	7.216E7	6.27E4	4.706E8	NSV
Sct 3	2.352E7	NDT	7.056E8	NSV
Sct 4	1.459E7	NDT	6.275E8	NSV
Sct 5	7.215E7	NDT	5.490E9	NSV
Sct 6	1.458E7	NDT	1.569E8	NSV
Sct 7	7.215E7	6.27E4	6.275E8	NSV
Sct 8	1.459E6	NDT	2.353E8	NSV
Sct 9	3.765E6	NDT	5.490E7	NSV
Sct 10	3.765E7	NDT	1.020E9	NSV
Sct 11	1.882E7	NDT	2.745E9	NSV
Sct 12	1.882E6	NDT	9.412E8	NSV
Sct 13	1.882E7	NDT	1.569E8	NSV
Sct 14	1.882E7	6.27E4	4.706E9	NSV
Sct 15	3.373E6	6.27E4	1.569E9	NSV
Average	1.942E7	1.67E4	1.379E9	---
S.D.	2.708E7	2.77E4	1.764E9	---

APPENDIX C

MEDIA FOR GROWTH OF BACTERIA CULTURE

APPENDIX C

MEDIA FOR GROWTH OF BACTERIA CULTURE

Table 10. Postgate's B media for SRB

Compound	Amount added ($kgx10^{-3}$) per 1E-3 m^3 of tap water
KH_2PO_4	0.5
NH_4Cl	1.0
$CaSO_4$	1.0
$MgSO_4.7H_2O$	2.0
$FeSO_4.7H_2O$	0.5
Na Lactate	3.5
Na Acetate	3.5
Yeast Extract	1.0
Vitamin C	0.1
Thioglycollic Acid (added after autoclaving)	0.1 ml

Table 11. Fluid Thioglycollate media for HPC

Compound	Amount added (kg) per 1E-3 m^3 of tap water
Yeast Extract	5.0
Casitone	15
Dextrose	5.5
NaCl	2.5
L-Cystine	0.5
Na Thioglycollate	0.5
Resazurin	0.001

APPENDIX D

RCT SYSTEM MAKE-UP WATER HISTORICAL DATA

APPENDIX D

RCT SYSTEM MAKE-UP WATER HISTORICAL DATA

Table 12. Raw data: LNVA water quality

Element	78-81 (avg)	82 10/15	83 6/01	84 2/27	84 5/04	85 11/15 -
			kgm^{-3} (x 10^{-3})			
Ca	6.9	7.8	8.8	11.2	7.1	7.7
Mg	3.3	3.6	1.9	3.0	3.1	3.2
Hardness	29	34	30	40	31	33
Na	NA	22	8.0	19.3	15.2	19
SO_4	21	14	10	34	19	23
Cl	19	26	30	37	22	25
SiO_2	10.3	21.6	28.6	34	18	18
Cond.	130	130	160	200	153	173
pH	6.8	7.5	3.5	7.1	7.2	7.2
Fe	1.66	2.7	3.3	2.9	1.3	1.2
Cu*	0.05	0.05	0.05	0.05	0.05	0.05
Al	NA	3.1	NA	4.5	NA	1.5
TOC	NA	16.3	56	10	16	29
TOC	NA	4.0	NA	8.0	3.0	5.0

LNVA = Lower Neches Valley Authority

Table 13. RCT system make-up water quality

Month	Year	pH	kgm^{-3} ($\times 10^{-3}$) Ca Hardness	Total Hardness	Total Alk
08/20	86	6.8	16	22	22
09/05	86	5.9	25	34	28
09/24	86	6.3	24	29	45
10/17	86	6.8	23	35	25
10/27	86	5.9	18	24	21
12/16	86	6.9	35	48	14
04/23	87	7.5	29	38	NA
06/26	87	7.3	26	38	NA
07/24	87	6.7	64	88	21
08/21	87	6.7	22	30	21
09/17	87	7.2	34	40	36
10/02	87	6.8	23	34	30
10/22	87	6.6	24	36	22
11/13	87	6.4	46	64	12
12/18	87	6.7	22	34	20
01/15	88	6.7	18	NA	NA
02/16	88	6.4	26	NA	NA
03/18	88	6.3	14	NA	NA
02/22	89	6.8	20	32	18
03/02	89	6.8	20	30	20

Table 13 continued

		kgm^{-3} (x 10^{-3})			
Date	Year	Si	Fe	Cu	Conductivity
08/20	86	NA	0.12	0.11	170
09/05	86	6.4	0.17	0.28	165
09/24	86	NA	0.20	0.13	175
10/17	86	NA	0.12	0.15	140
10/27	86	NA	0.06	0.08	130
12/16	86	NA	0.34	0.11	120
04/23	87	NA	0.45	0.07	170
06/26	87	NA	0.55	0.05	110
07/24	87	NA	0.30	0.03	120
08/21	87	NA	0.30	0.03	130
09/17	87	NA	0.45	0.08	290
10/02	87	NA	0.28	0.06	140
10/22	87	NA	0.30	0.02	140
11/13	87	NA	0.35	0.02	180
12/18	87	NA	0.40	0.40	190
01/15	88	NA	NA	NA	120
02/16	88	NA	NA	NA	120
03/18	88	NA	0.74	0.05	105
02/22	89	NA	1.52	0.05	141
03/02	89	NA	1.50	0.05	130

APPENDIX E

RCT SYSTEM RECIRCULATING WATER DATA

APPENDIX E

RCT SYSTEM RECIRCULATING WATER DATA

Table 14. RCT system recirculating water data

			kgm^{-3} (x 10^{-3})		
Date	pH	Cycles of concentration	Ca Hardness	Total Hardness	Total Alk
08/20/86	7.9	2.4	38	56	48
09/05/86	7.7	2.6	65	84	54
09/24/86	6.9	2.1	51	68	32
10/17/86	7.2	3.0	68	89	53
10/27/86	6.5	2.8	51	65	36
12/16/86	7.1	1.8	64	80	31
04/23/87	7.2	3.6	105	129	NA
06/26/87	6.9	2.8	95	116	45
07/24/87	7.3	0.7	46	67	11
08/21/87	7.3	4.1	90	118	82
09/17/87	7.8	3.4	114	135	106
10/02/87	7.3	3.1	72	105	66
10/22/87	6.9	2.8	68	98	56
11/13/87	7.1	2.5	76	90	80
12/18/87	7.1	2.0	43	72	38
01/15/88	6.9	4.0	72	NA	NA
02/16/88	7.1	4.0	104	NA	NA
03/18/88	7.1	3.8	NA	NA	NA
02/22/89	8.0	2.25	47	72	105
03/02/89	8.4	4.33	88	130	166

Table 14 continued

Date	Halogen	Si	Fe	Cu	Conductivity
	kgm^{-3} (x 10^{-3})				
08/20/86	0.1	NA	0.20	0.08	415
09/05/86	0.3	NA	0.19	0.19	460
09/24/86	0.25	16	0.31	0.21	440
10/17/86	0.1	NA	0.27	0.18	400
10/27/86	0.0	NA	0.14	0.21	310
12/16/86	0.2	NA	0.43	0.13	240
04/23/87	0.18	NA	0.70	0.09	480
06/26/87	0.02	NA	0.80	0.07	340
07/24/87	0.25	NA	0.55	0.05	360
08/21/87	0.15	NA	0.55	0.05	500
09/17/87	0.34	NA	0.80	0.10	720
10/02/87	0.27	NA	0.36	0.07	420
10/22/87	0.24	NA	0.35	0.02	400
11/13/87	0.24	NA	0.56	0.02	480
12/18/87	0.08	NA	0.65	0.40	440
01/15/88	0.27	NA	NA	NA	420
02/16/88	0.3	NA	0.50	NA	640
03/18/88	0.17	NA	1.25	0.05	400
02/22/89	0.8	NA	4.04	0.05	773
03/02/89	0.6	NA	6.90	0.05	1278

APPENDIX F

SEM/EDAX ANALYSIS OF FAILED TUBING BY DUPONT

APPENDIX F

SEM/EDAX ANALYSIS OF FAILED TUBING BY DUPONT

Table 15. Raw data: Deposit analysis on failed Dupont tubing

Element	percent		
	Location 1	Location 2	Location 3
Zn as ZnO	58.0	0.1	0.3
Cu as Cuo	NDT	24.7	0.2
Ni as NiO	NDT	0.8	NDT
Fe as Fe_2O_3	7.0	3.9	63.0
Mn as MnO_2	NDT	0.2	0.4
Cr as Cr_2O_3	NDT	NDT	0.2
Sn as SnO_2	NDT	NDT	NDT
Ti as TiO_2	NDT	0.7	0.1
Al as Al_2O_3	1.0	8.7	1.5
Ca as CaO	2.0	1.0	0.7
Mg as MgO	1.0	0.6	0.4
Sr as SrO	NDT	NDT	NDT
Ba as BaO	NDT	NDT	NDT
Na as Na_2O	NDT	NDT	NDT
K as K_2O	NDT	0.5	NDT
Cl as NaCl	NDT	NDT	NDT
Sulfate as SO_3	NDT	0.3	0.5
P as P_2O_3	10.0	1.7	8.6
Si as SiO_2	3.0	33.9	5.4
Pb as PbO	NDT	NDT	NDT
Organics, H_2O (corrected)	16.0	20.3	15.7
Undetermined	2.0	2.0	1.8
Total	100.0	100.0	100.0

Location 1: Carbon steel exchanger outlet pipe
Location 2: Top lube oil cooler - north end
Location 3: Carbon steel exchanger water box outlet
Reported by D. Hughes on 08/12/89

APPENDIX G

DATA GENERATED FROM COMPUTER SIMULATION

APPENDIX G

DATA GENERATED FROM COMPUTER SIMULATION

Table 16. Effect of cycles of concentration

	Before Biocide		After Biocide	
Cycles of Concentration	X_b (kg/m^3)	X_f (μm)	X_b (kg/m^3)	X_f (μm)
Initial	0.001	1	----	--
1	0.007	6	0.005	5
2	0.015	12	0.012	10
3	0.08	19	0.07	15
4	0.20	25	0.16	20
5	0.39	31	0.33	25

biocide concentration = 1.6E-2 Kgm^{-3}

Table 17. Effect of biocide concentration

	Before Biocide		After Biocide	
Biocide Concentration (Kgm^{-3} x 1E-3)	X_b (kg/m^3)	X_f (μm)	X_b (kg/m^3)	X_f (μm)
Initial	0.001	1	----	--
10	0.37	30	0.34	26
2	0.37	30	0.30	24
3	0.37	30	0.26	23
4	0.37	30	0.21	22
5	0.37	30	0.16	20

cycles of concentration = 4.0

Table 18. Effect of inlet substrate concentration

Substrate Concentration (Kgm^{-3} x 1E-3)	Before Biocide X_b (kg/m^3)	Before Biocide X_f (μm)	After Biocide X_b (kg/m^3)	After Biocide X_f (μm)
Initial	0.001	1	----	--
0.005	0.005	4	0.004	4
0.01	0.029	7	0.02	6
0.02	0.075	12	0.06	10
0.03	0.22	18	0.19	15
0.04	0.3	23	0.25	19

cycles of concentration = 2.0
biocide concentration = 1.6E-2 Kgm^{-3}

Table 19. Effect of inlet substrate concentration

Substrate Concentration (Kgm^{-3} x 1E-3)	Before Biocide X_b (kg/m^3)	Before Biocide X_f (μm)	After Biocide X_b (kg/m^3)	After Biocide X_f (μm)
Initial	0.001	1	----	--
0.005	0.01	8	0.009	7
0.01	0.057	14	0.05	11
0.02	0.20	25	0.12	20
0.03	0.44	34	0.30	29
0.04	0.60	40	0.46	35

biocide concentration = 1.6E-2 Kgm^{-3}
cycles of concentration = 4.0

APPENDIX H

OBSERVATIONS BY PLANT PERSONNEL

APPENDIX H

OBSERVATION BY PLANT PERSONNEL

Preliminary observations and cursory analysis has led DuPont and Conoco to conclude that the corrosion problem is caused by MIC. This conclusion is based on the following observations by DuPont and Conoco personnel:

- Heavy, foul-smelling deposits in water boxes and thin, gray, gelatinous deposits on cooling-water side surfaces of tubing.
- Patchy, discrete, reddish-brown tubercles (or stains) over pits in tubes as noted by visual inspection. Some tubercles adhere very tightly to surface. "Biological" deposits (based on visual observation by Don Hughes, Contract Consultant, Water Treatment) were flushed from condensers.
- Examination of pits indicates a relatively small "mouth" on the surface, opening to a large sub-surface cavity or tunnel. EDAX indicates relatively high concentration of Fe, Mn and Cl in pits and tunnels.
- "Eddy current" analysis (measure of surface roughness) of inner tubing walls show severity of pitting decreases with increasing wall temperature. At present, it is not clear whether eddy current testing was conducted on fouled tubes, cleaned tubes, or both.
- Sulfide and septic smell was detected in RCT basin sludge; sludge was 2-4 feet deep and "biological active" when last cleaned in 1988 (Don Hughes).
- Corrosion product accumulates in mounds or tubercles.
- Pitting is more pronounced in cooler areas of condenser.

- The source of bacteria in the RCT system was probably the supply water.
- "Mothballing" the plant in 1985 (see Chronology/Milestones) permitted bacterial growth in stagnant areas which may have initiated the problem.

Based on these observations, some DuPont personnel hypothesize that the cause may be iron-and/or manganese-utilizing and/or oxidizing bacteria which results in concentrated ferric/manganic chloride in deposits.

Plant Treatment Chronology

- 70 Methanol plant started-up. Plant equipped with air-cooled condensers.
- [??] Condensers changed to water-cooled. Condenser tube material 90-10 Cu-Ni. No problematic fouling or corrosion observed. Neches River coolant source; Biocide = daily slug of Cl_2; bimonthly Tributylinoxide (non-oxidizing). Sulfuric acid to maintain pH at 6.8-72 Caustic addition during Cl_2 treatment. Chromate/Zn corrosion inhibitor at 4/6 mgl^{-1} added. Frequency and duration of treatment is not known by us at present.
- 3/77 Tolytriazole (3-4 mgl^{-1}, frequency and duration not known by us at present) for Cu corrosion control. Same biocide treatment. pH changed to 7.0-7.6 for better action of tolytriazole. Polyacrylate (2 mgl^{-1}, frequency and duration unknown by us at present) for mud, silt dispersal.
- 1/82 Cl_2 treatment stopped. "BromiCide" started; slug dose

once/day, (70-100 lbs). During summer, slug feed sodium hypochlorite for 3-5 days every three weeks for algal control on RCT decks.

- 82 304 stainless steel condenser tubes replace copper-nickel. No apparent problem of fouling or corrosion in Cu-Ni exchangers.
- 84 Methanol plant mothballed. System flushed with canal water and "laid-up wet" for 12 months.
- 85 Methanol plant recommissioned. Deposits flushed from condensers. Copious deposits in pumps, water boxes. Evidence of leaking of condenser tubes. Eddy current analysis indicated deposits and pitting. Plugged leaking tubes.

Pine Island water begins to flow intermittently to source canal. Isothiazolone (biocide) added occasionally (concentration, frequency, and duration unknown to us at this time). BromiCide residual continuously maintained throughout system.

- 87 Installed new 304 stainless steel tube condensers.
- 3/88 Product found in coolant (i.e. perforative failure of tubing). System shut down and inspected: heavy deposit, pitting as described earlier. Plugged all tubes with pit depths greater than 80 per cent (70% of all tubes). Install on line cleaning (Amertap).